

*Numerical investigations of unsteady  
solid-liquid Non-Newtonian flows over  
stretching surfaces*



By

*Madiha Bibi*

**Department of Mathematics  
Quaid-I-Azam University  
Islamabad, Pakistan  
2021**

*Numerical investigations of unsteady  
solid-liquid Non-Newtonian flows over  
stretching surfaces*



By

*Madiha Bibi*

Supervised By

*Prof. Dr. Muhammad Yousaf Malik*

**Department of Mathematics  
Quaid-I-Azam University  
Islamabad, Pakistan  
2021**

*Numerical investigations of unsteady  
solid-liquid Non-Newtonian flows over  
stretching surfaces*



By

*Madiha Bibi*

A THESIS SUBMITTED IN THE PARTIAL FULFILLMENT OF THE  
REQUIREMENT FOR THE DEGREE OF  
**DOCTOR OF PHILOSOPHY**

IN

*MATHEMATICS*

Supervised By

*Prof. Dr. Muhammad Yousaf Malik*

**Department of Mathematics**

**Quaid-I-Azam University**

**Islamabad, Pakistan**

**2021**

## Author's Declaration

I Madiha Bibi hereby state that my PhD thesis titled Numerical investigations of unsteady solid-liquid Non-Newtonian flows over stretching surfaces is my own work and has not been submitted previously by me for taking any degree from the Quaid-i-Azam University Islamabad, Pakistan or anywhere else in the country/world. At any time if my statement is found to be incorrect even after my graduate the university has the right to withdraw my PhD degree.



Name of Student: Madiha Bibi

Date: 29-04-2021

## **Plagiarism Undertaking**

I solemnly declare that research work presented in the thesis titled "**Numerical investigations of unsteady solid-liquid Non-Newtonian flows over stretching surfaces**" is solely my research work with no significant contribution from any other person. Small contribution/help wherever taken has been duly acknowledged and that complete thesis has been written by me. I understand the zero tolerance policy of the HEC and **Quaid-i-Azam University** towards plagiarism. Therefore, I as an Author of the above titled thesis declare that no portion of my thesis has been plagiarized and any material used as reference is properly referred/cited.

I undertake that if I am found guilty of any formal plagiarism in the above titled thesis even afterward of PhD degree, the University reserves the rights to withdraw/revoke my PhD degree and that HEC and the University has the right to publish my name on the HEC/University Website on which names of students are placed who submitted plagiarized thesis.



Student/Author Signature:

Name: **Madiha Bibi**

# Numerical investigations of unsteady solid-liquid Non-Newtonian flows over stretching surfaces

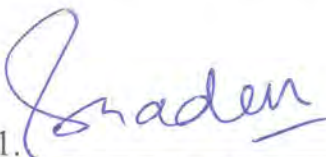
By

**Madiha Bibi**


CERTIFICATE

A DISSERTATION SUBMITTED IN THE PARTIAL FULFILLMENT OF THE  
REQUIREMENTS FOR THE DEGREE OF THE DOCTOR OF PHILOSOPHY

**We accept this dissertation as conforming to the required standard.**

1. 

**Prof. Dr. Sohail Nadeem**  
(Chairman)

2. 

**Prof. Dr. Muhammad Yousaf Malik**  
(Supervisor)

3. 

**Dr. Muhammad Mushtaq**

Assistant Professor

Department of Mathematics COMSATS  
University, Park Road, Chak Shahzad,  
Islamabad.

(External Examiner)

4. 

**Dr. Tanvir Akbar Kiani**

Assistant Professor

Department of Mathematics COMSATS  
University, Park Road, Chak Shahzad,  
Islamabad


(External Examiner)

**Department of Mathematics**  
**Quaid-I-Azam University**  
**Islamabad, Pakistan**  
**2021**

## Certificate of Approval

This is to certify that the research work presented in this thesis entitled **Numerical investigations of unsteady solid-liquid Non-Newtonian flows over stretching surfaces** was conducted by **Ms. Madiha Bibi** under the kind supervision of **Prof. Dr. Muhammad Yousaf Malik**. No part of this thesis has been submitted anywhere else for any other degree. This thesis is submitted to the Department of Mathematics, Quaid-i-Azam University, Islamabad in partial fulfillment of the requirements for the degree of Doctor of Philosophy in field of Mathematics from Department of Mathematics, Quaid-i-Azam University Islamabad, Pakistan.

Student Name: **Madiha Bibi**

Signature: 

External committee:

a) **External Examiner 1:**

Name: **Dr. Muhammad Mushtaq**

Office Address: Department of Mathematics COMSATS University, Park Road Chak Shahzad, Islamabad.


Signature: 

b) **External Examiner 2:**

Name: **Dr. Tanvir Akbar Kiani**

Designation: Assistant Professor

Office Address: Department of Mathematics, COMSATS University, Park Road Chak Shahzad, Islamabad.

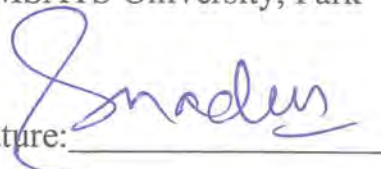
Signature: 

c) **Internal Examiner**

Name: **Prof. Dr. Muhammad Yousaf Malik**

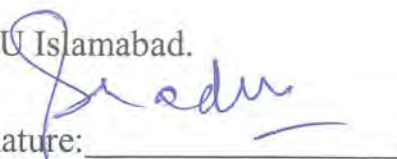
Designation: Professor

Office Address: Department of Mathematics, QAU Islamabad.

Signature: 

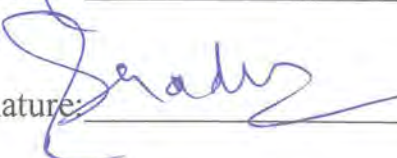
**Supervisor Name:**

Prof. Dr. Muhammad Yousaf Malik

Signature: 

**Name of Dean/ HOD**

**Prof. Dr. Sohail Nadeem**

Signature: 

## ***Acknowledgement***

I am very thankful to Almighty Allah (S.W.T) for his everlasting blessings, love, and care. Bundle of thanks to Almighty Allah (S.W.T) for giving me the strength, wisdom, and confidence to complete this work. After Almighty Allah (S.W.T), I pay my sincere gratitude to Holy Prophet Muhammad (S.A.W) for his gaudiness towards the seeking knowledge.

I am also thankful to my kind supervisor Prof. Muhammad Yousaf Malik for his beloved and caring attitude and providing me the excellent atmosphere to accomplish this work His exert gaudiness, constructive criticism and continuous encouragement helped me in all time during my research and writing this thesis. I would also like to thank my teachers who taught me able to overcome all the challenges, particularly Prof. Tasawar Hayat, Prof. Muhammad Ayub, Prof. Sohail Nadeem, Prof. Masood Khan, Prof. Babar Majeed Mirza, Prof. Khalid Saifullah.

I pay special thanks and respect to Dr. Ahmed Zeeshan for helping me out from start to completion of this work. It will not be false to say that without his guidance I cannot complete this small contribution in research. Once again, I am thankful to him for his help and guidance in every matter.

I would not imagine completing my acknowledgement without saying thanks to my parents. Every successful daughter has a supportive father at her back, who gives courage to move in society confidently. I am thankful to my Abu ji to trust me and support me to stand where I am today. I do not have words to say thanks to my Ammi ji. My each and every day is incomplete without her. My brothers and sister also have important role in my success.

Last, but not least, I would like to say thanks to my friends, Zeenat-un-Nisa, Dr. Nuzhat Irshad, Syed Irum Habib, Sara Ellahi, Dr. Maryam Subhani, Dr. Sadia Rashid, and Dr. Tanzeela Hayat, for their friendship, support, and love. I am pleased to acknowledge my lab fellows Dr. Arif Hussain, Dr. Khalil-ur-Rehman, Dr. Mair, Dr. Imad, Dr. Usman Ali. This is injustice to completing this portion without saying thanks to our program coordinators, ever helping Zahoor Lala and Sajid bhai.

Madiha Bibi



# Preface

This study is for the understanding of the time dependent solid-liquid flows of non-Newtonian fluids. The solid particles are supposed to be micro or nano sized. Dust particles effect the flow of fluid according to concentration. Fluid-particle interaction is also important for the flow of matter and heat as well. Impact of dust particles is valuable on viscous flows in petroleum industry specifically in the purification of crude oil. Also useful in medical equipment and engineering industry as pure liquids may not give the required results such as thermal conductivity can be enhanced by in cooperating nano and micro particles. In this research, the study the unsteady dusty flow is done by considering different types of base fluids in two as well as in three dimensions. The equations for both fluid and particle phase are modelled separately using conservation of mass, momentum and heat transfer. These equations are then transformed into the set of nonlinear ordinary differential equations by using the similarity transformations. The numerical solutions of transformed equations are obtained via shooting mechanism with fifth order R-K Fehlberg technique, bvp4c package in MATLAB. In order to check the accuracy of the solution methods, comparison is made with the previous results. Also, different observations are made using graph and tables for all the problems under consideration.

# Contents

0.1	<b>Nomenclature</b> . . . . .	2
<b>1</b>	<b>Introduction</b>	<b>5</b>
1.1	Solid-Liquid flow Models . . . . .	12
1.1.1	Two-Phase Dusty flow Model . . . . .	12
1.1.2	Buongiorno Nano-fluid Model . . . . .	14
1.2	Methods of finding solutions . . . . .	14
1.3	Body forces . . . . .	14
1.3.1	MHD . . . . .	14
1.3.2	Thermal Radiation . . . . .	15
1.3.3	Heat generation/absorption . . . . .	15
1.4	Constitutive equations . . . . .	15
1.4.1	Williamson Fluid . . . . .	15
1.4.2	tangent hyperbolic Fluid . . . . .	16
<b>2</b>	<b>Numerical analysis of unsteady Magneto-biphase Williamson fluid flow with time dependent magnetic field</b>	<b>17</b>
2.1	Mathematical formulation . . . . .	18
2.2	Numerical procedure of solution . . . . .	20
2.3	Outcomes and discussions . . . . .	21
2.4	Concluding remarks . . . . .	32
<b>3</b>	<b>Numerical investigation of unsteady solid-liquid flow of tangent hyperbolic fluid with variable thermal conductivity and convective boundary</b>	<b>34</b>
3.1	Mathematical formulation . . . . .	34
3.2	Numerical procedure of solution . . . . .	36
3.3	Outcomes and discussions . . . . .	38

3.4	Concluding remarks . . . . .	48
<b>4</b>	<b>Numerical analysis of unsteady flow of three dimensional Williamson fluid-particle suspension with MHD and non-linear thermal radiations</b>	<b>50</b>
4.1	Mathematical formulation . . . . .	50
4.2	Numerical procedure of solution . . . . .	54
4.3	Outcomes and discussions . . . . .	56
4.4	Concluding remarks . . . . .	66
<b>5</b>	<b>Numerically analysis of unsteady flow of three dimensional tangent hyperbolic fluid-particle suspension with MHD, viscous dissipation and joule heating with convective boundary conditions</b>	<b>70</b>
5.1	Mathematical formulation . . . . .	71
5.2	Numerical procedure of solution . . . . .	74
5.3	Outcomes and discussions . . . . .	77
5.4	Concluding remarks . . . . .	88
<b>6</b>	<b>Numerical study of unsteady Williamson fluid flow and heat transfer in the presence of MHD through a permeable stretching surface</b>	<b>93</b>
6.1	Mathematical formulation . . . . .	94
6.1.1	Skin friction coefficient, local Nusselt number and local Sherwood number . . . . .	96
6.2	Numerical procedure of solution . . . . .	97
6.3	Outcomes and discussions . . . . .	105
6.4	Concluding remarks . . . . .	108

## 0.1 Nomenclature

---

$t$	Time coordinate [T](sec)
$(x, y, z)$	Spatial coordinate [L](m)
$u, v, w$	Velocity components of liquid phase [L/T](m/sec)
$u_P, v_P, w_P$	Components of velocity of solid phase [L/T](m/sec)
$T$	Temperature of liquid phase
$T_P$	Temperature of solid phase
$Ec^*, Ec_x, Ec_y$	Viscous dissipation parameters
$C$	Volume fraction of dust particles
$C_n$	Concentration of nano-particles
$S$	Drag Coefficient
$f', g'$	Non-dimensional velocity of liquid phase
$F', G'$	Non-dimensional velocity of solid phase
$We, We_x, We_y$	Weissenberg numbers
$M$	Magnetic parameter
$Pr$	Prandtl number
$s$	Mass transfer parameter
$\lambda$	Stretching ratio parameter
$Re, Re_x, Re_y$	Reynolds numbers
$A_1$	First Rivlin-Ericksen tensor
$B(t)$	Unsteady magnetic field
$B_o$	Magnitude of magnetic field
$A$	Unsteadiness parameter
$n$	Power law index
$A^*, B^*$	Heat source/sink parameter
$R, \beta_T$	Fluid-particle interaction parameter for velocity and temperature profile
$V_o$	Uniform suction/injection velocity
$a, b$	Free stream parameters [1/T](1/sec)
$c$	Balancing parameter
$k$	Thermal conductivity

$p$	Pressure [ $ML/T^2$ ]
$\tau$	Extra stress tensor
$\mu$	Dynamic viscosity
$\mu_0$	Zero shear rate viscosity
$\zeta$	Biot number
$\mu_\infty$	Infinite shear rate viscosity
$\dot{\gamma}$	Shear rate
$\eta$	Variable of local similarity
$\psi$	Stream function for fluid phase [ $L^2/T$ ]
$\psi_P$	Stream function for solid phase [ $L^2/T$ ]
$\alpha_\infty$	Thermal conductivity at infinity
$\nu$	Kinematic viscosity
$\theta$	Non-dimensional temperature of fluid phase
$\theta_P$	Non-dimensional temperature of solid phase
$\alpha'$	Time dependent thermal diffusivity
$\rho$	Density of fluid phase
$\rho_P$	Density of solid phase
$U_w, V_w$	Stretching velocities
$V_s$	Mass fluid velocity
$T_w$	Surface/Wall temperature
$q_w$	Wall heat flux
$q_r$	Radiative heat flux
$\tau_w$	Wall shear stress
$c_p$	Specific heat capacity of fluid
$c_m$	Specific heat capacity of dust particles
$\gamma$	Ratio of heat capacities
$\tau_T$	Thermal equilibrium time
$T_\infty$	Ambient temperature
$C_{fx}, C_{fy}$	Skin friction coefficient
$Nu_x$	Nusselt number
$h_f$	coefficient Heat transfer
$\varepsilon$	Material dependent parameter
$\sigma$	Electrical conductivity
$\sigma^*$	Stefan-Boltzmann constant

$T_0$	Reference temperature
$Q_0$	Time dependent non-uniform heat source/sink
$\alpha$	Ratio of densities
$\Gamma$	Time material constant
$D_T$	Coefficient of thermophoresis diffusion
$D_B$	Coefficient of Brownian diffusion
$Nb$	Parameter for Brownian motion
$Nt$	Parameter for Thermophoresis

# Chapter 1

## Introduction

Two general topologies of multiphase flow can be usefully identified at the outset, namely disperse flows and separated flows. By disperse flows we mean those consisting of finite particles, drops or bubbles (the disperse phase) distributed in a connected volume of the continuous phase. On the other hand separated flows consist of two or more continuous streams of different fluids separated by interfaces [1].

In order to control multiphase processes, understanding of mechanisms involved is also essential. Suspensions of particles are global, with examples in biological systems in blood, household goods such as paints and industrial processing such as waste slurries. They are encountered in an extraordinarily broad array of industrial, engineering, environmental, chemical and biological problems, encompassing within it diverse subfields such as aerosol dynamics, sedimentation of sand particles in rivers, the evaporation and combustion of drops, the movement of blood cells in capillaries, the motion of catalyst particles in chemical reactors, and fluidization of solids fuels in reacting bed systems, colloidal dispersions, fluidized beds, and cohesive granular flows. Many of these flows are of great importance in energy and environmental engineering fields. To list just a few examples, key particulate suspension flow problems in the combustion area include ash transport, deposition, filtration and capture from combustion processes, heterogeneous combustion of pulverized coal, fluidized bed combustion with hot cohesive materials, flame synthesis and spray coating of nano-particles and gasification and combustion of biofuel particles, and even in-space electrostatic propulsion based on a micro and nano-particle thruster.

Main focus of the current study is of two phase flows. There are varieties of two phase flows depending on combinations of two phases as well as their interaction on the interface structures. Two-phase mixtures are characterized by the existence of one or several

interfaces and discontinuities at the interface. It is easy to classify behavior of two-phase mixtures according to the combinations of two phases, since in standard conditions we have only three states of matters namely: solid, liquid, and gas phases [2]. Following are the combination of three phases but the main focus will be on first one:

- Liquid- solid mixture
- Gas-solid mixture
- Gas-liquid mixture

The focus in this thesis is on liquid-solid mixture with either nano sized particles or dust size particles. Dusty flow is subclass of two-phase flow, that is liquid-solid flow. Dusty fluid is considered as heterogeneous mixture in which solid particles are suspended naturally or artificially. Avoiding digress although solid-particles volume fraction is presupposed to be very small that is the collision between individual particles may be neglected. Impact of dust particles is valuable on viscous flows in petroleum industry specifically in the purification of crude oil. Also in medical equipments and engineering industry as pure liquids may not give the required results such as thermal conductivity can be enhanced by in cooperating nano and micro particles. Parenthetically other important applications of such particles in boundary layer flows included soil erosion by natural winds, lunar ash flows, combustion, dust entrainment in a cloud during nuclear explosions, fluidization and centrifugal separation etc. The existence of impurities in any state of matter is really very natural and following that rule of nature many scientists and researchers introduced the new inventions and area of study. The front runner of the dusty flows was Saffmann [3]. He concluded that if the dust is fine enough then addition of dust wreck the gas flow while coarser the dust stabilizes the gas flow. After him Soo [4] investigated the dynamics of multiphase flows. Then Marble [5], Liu [6], Michael and Miller [7] analyzed the dynamics of gases specifically in detail. Almost everyone is familiar with multiphase flow, like rising mixture of dust and smoke from the chimneys of factories, foaming bear in a glass. These are daily life examples, but how it works can be analyzed mathematically. Solid-liquid flow can be considered on a large scale like sand flow with water in seas with the third phase that is air bubbles. Theoretically these problems can be solved by considering the different approaches of modeling by taking the "principles" of rational mechanics in account like equipresence, phase separation, objectivity and well-posedness etc. Numerical



techniques offered earlier by Harlow and Amsden [8] to solve the multiphase flow problems. Thermal properties of two-phase flow was earlier proposed by Bishop [9]. Boundary layer flow of two-phase fluid was introduced by Singleton [10] in his Ph.D dissertation. Now the current focus is fluid-particle flow, as it has incredible importance in medical studies, industry and nuclear technology etc. In Ultrasound, CT scan and MRI machines etc, work as to measure the granular flows and fluid-particle flows given in reference [11]. There are many strong reasons of study of fluid dynamics at macro and nano-level as well. At macro level mathematicians and engineers try to investigate the flows without defined boundaries but the case of nano or micro level is really very interesting. We can detect the presence of a micro-organisms or any impurity in water or in any other liquid. Micro-organism could be considered as solid particles, like viruses are nano-sized (20 to about 100 nanometers in size) and bacteria are mostly micro-sized (about 0.5 to 3 micrometers). Such type of study moves towards two phase or multiphase flows. Drew [12] derived a set of coupled equations Orr-Sommerfield, which were helpful to govern the infinitesimal distribution of dust particles in fluid. Then Mekheimer et al. [13] used the same concept of equations gave results for peristaltic flow in a channel. Somehow in last thirty years eminence researchers did good job for exploring the fluid-particle flow for newtonian and non-Newtonian, steady and unsteady case as well [14]-[16]. The concur findings was that momentum of fluid and solid fragments dwindle with the elevation in particles density and fluid-particle interaction. In last decade of twentieth century Kumar and Sarnma [17] presented work for fluid-particle suspension flow due to stretching. He perceive that velocity profile of fluid and particle decreases with the increase in particle loading and fluid particle interaction. Valentini and Maiellaro [18] studied the non-linear stability for dusty flows. Recently Sandeep and Sulochana [19] has studied dusty nanofluid flow due to stretching. He concluded that fluid and particle phase interaction enhances the temperature of dusty fluid and depreciate the friction factor. Sandeep et al.[20]and Kumar et al.[21] also presented observations about the unsteady dusty flow due to exponential stretching.

Vast classification of non Newtonian fluids are based upon their characteristics and the physical factors. Time dependent fluids class is one of the major classes. Heat and mass flow is effected with the change in time that's why the study of unsteady flows have great importance in industry. In historical point of view a classical paper was given by Stewartson [22], in which he has given the concept of unsteady laminar boundary layer for the very first time. Perepelitza [23] investigated the unsteady heat transfer and gave the experi-

mental results that stabilized heat transfer was at Reynolds numbers of  $(0.8 - 6.8) \times 10^4$  for  $5mm \times 40mm$ ,  $10mm \times 40mm$ , and  $20mm \times 40mm$  channels. Recently Bachok et al. [24] compared the time dependent boundary layer for two different solutions. Rees et al. [25] investigated the time dependent flow for the Bingham fluid in the porous medium, they concluded that the fluid stayed stagnant at early times because the resulting buoyancy forces were too weak to overcome the yield threshold.

Wide range of Non-Newtonian fluids are used in industry for the various purposes according to their nature, either shear thickening or thinning etc. Here, we are considering a shear thinning fluid that is Williamson fluid which was probably a neglected fluid by the researchers but recently studied and analyzed rapidly. It is from the literature that front runner of Williamson fluid was Williamson [26]. Bibi et al. [27] unfolded the Williamson fluid flow in 2-D where the cause of flow is stretching. The study of Williamson fluid in three dimensions is studied by the Malik et al. [28]. They concluded that Williamson parameter reduces the momentum transport. Hayat et al. [29] perceive that concentration profile decreases due to increased chemical reactions. Zehra et al. [30] have discussed the Poiseuille and Couette flow that is pressure dependent viscosity for Williamson fluid flow. While Bilal et al. [31] temperature dependent conductivity for three dimensional Williamson fluid flow caused by bidirectional non-linear stretching surface. Other latest investigations about steady Williamson fluid are in the following references [32]-[39]. Recently Kumar et al [40] analyzed the Williamson fluid flow in three dimensions with chemical reactions. Mair et al. [41] additionally studied the variable diffusion and conductivity for 3-D rotating flows.

Currently the Williamson non-Newtonian fluid is also taken as base fluid for Nano-fluid. Nano particles are used to enhance the heat flow rate. The word "nanofluid" was firstly used by Choi et al. [42] allude to the scattering of nano-particles in the base fluid for the enhancement of thermal conductivities. He had unwrapped a field of study which has great importance in industry because nanofluids plays a magical role as coolants for many industrial and automotive purposes. Nandy et al. [43] investigated the effect of nano particles in presence of MHD. Latest numerical model for the cooling performance of exhaust gas recirculation (EGR) cooler by using nanofluids is given by Shabgard et al. [44].

The use of fluids having non-Newtonian nature found in engineering and industrial processes, like food mixing, mercury amalgams, and lubrications. This study is also for the non-Newtonian tangent hyperbolic considered as base fluid which obeys the power law

model and it is also shear thinning fluid. Boundary layer flow of tangent hyperbolic fluid flow under consideration of two many conditions and effects is discussed in handy publications recently. In the last going decade the boundary layer flow as well as the peristaltic flow considered in the following literature. Akbar et al. [34] discussed the stretching problem for 2D, Malik et al. [45] proposed the numerical scheme for the flow over stretching cylinder, and Bibi et al. [46] investigate the dusty stretching flow. Salahuddin et al. [47],[48] have addressed the MHD tangent hyperbolic flow for stagnation point and heat generation absorption. Thermo-physical properties are analyzed for tangent hyperbolic fluid flow by Khalil et al.[49]. He detected that local Nusselt number grows due to enhancement of Prandtl number and curvature parameter but lessen due to stratification factor. As the time-dependency is one of the accountable issues of contemporary disquisition. A perfectly phenomenal discourse have to be mentioned in which Kumar et al. [50] analyzed the time dependent squeezed flow of magnetized tangent hyperbolic fluid flow while considering the variable thermal conductivity. He concluded that increment of power law index reduces the momentum and temperature boundary layer. More literature about non-Newtonian tangent hyperbolic fluid and Maxwell fluid is given in the references [51]-[53].

Study of flowing bodies between confined boundaries and infinite boundaries are two main distinguished areas of interest for the researchers. In this study the boundary layer flow for two and three dimensions both are under consideration and the flow is because of stretching of a sheet. As boundary layer flows gained much importance and attention as per industrial requirement, for example metal and polymer extrusion, metal wires, plastic sheets and films production etc. From literature review it is well known that front runner researchers of boundary layer flows due to stretching were Sakiadis[54], Crane[55], Grubka and Bobba[56]. They have started study for two dimensions but afterwards as the research area growing vast then the study of flows shifted towards the three dimensions. Although its tough to handle 3-D but in reality flows exist in three dimensions. So taking in account the importance of three dimensional flow Wang [57] took initiative to analyze the 3-D flow over a flat stretching surface. Recently Arif et al. [58] evaluate the two dimensional stretching flow for a viscoelastic natured fluid. Here three dimensional flow is discussed with time dependency. As the time dependency is a major factor which we cannot neglect in real life problems. Surma Devi et al. [59] studied the three-dimensional flows due to stretching for unsteady case. Mahanthesh et al. [60] scrutinized the unsteady three-dimensional MHD flow for non-Newtonian Eyring-Powell fluid under the effect of

thermal radiations. Ariel played a remarkable role in this research area mentioned in the following reference [61]-[63]. The latest consultations about non-Newtonian three dimensional flows are mentioned in following references [64]-[67].

Ishak et al. [68] contemplate the boundary layer of mass and heat flow of nano fluid past over a porous shrinking sheet. Numerical solution of MHD stretching flow with fluid-particle suspension was found by Giressha et al [69]. A stability analysis of stretching flow through permeable surface was given by Yasin et al. [70] numerically. Momentum and thermal boundary layer for porous cylinder was reported by Sia et al [71].

Noteworthy effect is under consideration that is MHD. Study of dynamics of fluid and particles under the effect of magnetic field lies in MHD having striking importance in industry, medical diagnostics, and nuclear power generation. MHD (magnetohydrodynamic) technology had a start form the first MHD experiment by Michael Faraday at the River Thames. In commercial point of view, basically this technology is used in the power plants. Malghan [72] wrote the history of MHD from first experiment up to that date with several evidences. Chiou et al [73] studied in mid of 90's that the magnetic effect is moderate if Prandtl number of fluid is low and magnetic effect increases with the increase in Eckert number. Exact and numerical solution for the out-turn of MHD and permeability for the concentration boundary-layer is given by Aly et al [74]. He observed that magnetic force and permeability reduces the nano-particle concentration. Vajravelu and Nayfeh [75] added the magnetic field effect while study of fluid-particle interaction and select the porous sheet for flow. And gave the results of fluid-particle MHD flow over a permeable stretching sheet. These results have strong agreement with present results will be discussed afterwards in same disquisition. Unsteady MHD flow for dusty fluid due to oscillating plates was analyzed by Debnath and Ghosh [76]. They concluded that if time-periods are small then automatically frequency will be high and fluid velocity will be retarded by the particles. Recently effect of MHD for different fluids is scrutinized by researchers, e.g, effect on Sisko, tangent hyperbolic, Casson, Carreau and Carreau Yasuda by Hussain et al. [77], Hayat et al. [78], Reddy et al. [79], Khan et al. [81] and Salahuddin et al. [80] respectively.

The energy conservation is very important and most under discussion area all over the world. That efforts in absorption technologies perform a distinct role in global energy and environmental issues. Some of the absorption technologies are absorption heat pump (AHP), generator absorber heat exchange (GAX), compression-absorption heat pump (CAHP), Open-cycle absorption heat pump (OAHP), etc. There are many residential

and commercial applications of absorption heating systems because of huge amount of energy consumption. For example Direct-fired absorption chiller/heater works on absorption pump theory, Latent heat recovery of vapor works on OAPH, Hybrid CAHP heating systems, District heating systems, thermal energy storage and transportation, etc are civil applications. Absorption-assisted drying, Absorption-assisted evaporation, Absorption-assisted distillation, etc are industrial applications. Internal heat generation with multi-boiling effects on cylindrical bodies are discussed by Rybchinskaya et al. [82]. Uniform and non-uniform heat generation results for cylindrical, rectangular and longitudinal surfaces examined by H.C.Unal [83, 84]. The effect of heat generation on unsteady flow with mixed convection and magnetic force examined numerically by Mahapatra et al. [85]. Recently boundary layer flow problem with effect of thermal conductivity and heat generation solved numerically and to remove the highly non-linearity of momentum and heat equation, differential transformation method (DTM) is used by Mohsen Torabi et al. [86]. As we know thermal conductivity is a material property and varies with the change in temperature. It depends on material, if fluid is electrically conducting then temperature flow is increased. Study of variable thermal conductivity is important in electrolytes which have important part in preparation of D.C. batteries. Chaim [87] studied that variable thermal conductivity vary linearly with temperature.

Study of heat flow with convection is prodigious due to huge industry requirement. Convection can be qualified in terms of being natural, forced, gravitational, granular, or thermomagnetic. Consequential implementation of convection is in gas turbines, nuclear reactors, geothermal energy extraction and material dying etc. There are other additions of heat source or sink and variable thermal conductivity effects while determining the temperature of the fluid and particles in cooperation of convection. Yao et al. [88] delineate the heat flow due to stretching including convective boundary conditions. Boundary layer flow of dusty fluids due to heat generation or absorption is given by Gireesha et al. [89]. Hussain et al. [90] reviewed the MHD influence on tangent hyperbolic fluid flow due to stretching with convective boundary conditions. Ahmed et al. [91] proclaim the unsteady stretching flow for power-law fluid considering convective conditions. Manjunatha and Gireesha [92] found the outcome of thermal conductivity on heat flow. Malik et al [93] have discussed the variable thermal conductivity for williamson fluid flow. They concluded that evocation of variable thermal conductivity raise the temperature profile of fluid. Recapitulation of all the effects how influential to the unsteady dusty non-Newtonian fluids mentioned in the references [94]-[98].

Non-linear thermal radiations effect is in-cooperated with heat equations for fluid and dust particles. Non-linear thermal radiations are also introduced to cope up with the temperature related problems during flows. Kumar et al. [99] discussed the MHD flow of dusty tangent hyperbolic fluid including the effect of thermal radiations. Voguish inspection of dusty flows while taking MHD and non linear thermal radiations into account mentioned in the following references[100]-[104].

Flow can be disturbed or facilitate by changing the values of different physical parameters, joule heating and viscous dissipation with convective boundary conditions. Historically the front runner of the study of viscous dissipation in natural convection was Gebhart [105]. Joule heating (also referred to as resistive or ohmic heating) describes the process where the energy of an electric current is converted into heat as it flows through a resistance. The effect of viscous dissipation in natural convection is appreciable when the induced kinetic energy becomes appreciable compared to the amount of heat transferred. Above effects are discussed in a combine way in following different references [106]-[110]. There are different solid-liquid fluid models, here are the main distribution depends upon the size of solid particles, that is micro and nano sized. The liquids contain micro or above sized particles are called dusty fluids, and nano-fluids are specified for nano sized solid particles. There are further classification of models for nano-fluids i.e, Buongiorno Model [111] and Tiwari and Das [112] two-phase Nano-fluid model. And for the dusty flows, two phase model using a continuum approach is given by Drew [12], Srivastava and Srivastava [113] and Mekheimer et al [13].

## **1.1 Solid-Liquid flow Models**

Theoretically solid-liquid flow problems can be solved by considering the different approaches of modeling. Two of the most important models are,

- Two-phase solid-liquid fluid model
- Buongiorno Nano-fluid

### **1.1.1 Two-Phase Dusty flow Model**

In two-phase model the dust size or micro-sized particles flow with the base fluid, either newtonian or non-newtonian. Due to flow of these particles drag force originates. This

model can be defined as follows:

$$\frac{\partial u}{\partial x} + \frac{\partial v}{\partial y} + \frac{\partial w}{\partial z} = 0, \quad (1.1)$$

$$\frac{\partial u_P}{\partial x} + \frac{\partial v_P}{\partial y} + \frac{\partial w_P}{\partial z} = 0, \quad (1.2)$$

$$\begin{aligned} \rho(1-C)\left[\frac{\partial u}{\partial t} + u\frac{\partial u}{\partial x} + v\frac{\partial u}{\partial y} + w\frac{\partial u}{\partial z}\right] &= -(1-C)\frac{\partial p}{\partial x} + \mu_d(C)(1-C)\left[\frac{\partial^2 u}{\partial x^2} + \frac{\partial^2 u}{\partial y^2} + \frac{\partial^2 u}{\partial z^2}\right] \\ &+ CS(u_p - u), \end{aligned} \quad (1.3)$$

$$C\rho_P\left[\frac{\partial u_P}{\partial t} + u_P\frac{\partial u_P}{\partial t} + v_P\frac{\partial u_P}{\partial y} + w_P\frac{\partial u_P}{\partial z}\right] = CS(u - u_P), \quad (1.4)$$

$$\begin{aligned} \rho(1-C)\left[\frac{\partial v}{\partial t} + u\frac{\partial v}{\partial x} + v\frac{\partial v}{\partial y} + w\frac{\partial v}{\partial z}\right] &= -(1-C)\frac{\partial p}{\partial y} + \mu_d(C)(1-C)\left[\frac{\partial^2 v}{\partial x^2} + \frac{\partial^2 v}{\partial y^2} + \frac{\partial^2 v}{\partial z^2}\right] \\ &+ CS(v_p - v), \end{aligned} \quad (1.5)$$

$$C\rho_P\left[\frac{\partial v_P}{\partial t} + u_P\frac{\partial v_P}{\partial t} + v_P\frac{\partial v_P}{\partial y} + w_P\frac{\partial v_P}{\partial z}\right] = CS(v - v_P), \quad (1.6)$$

$$\begin{aligned} \rho(1-C)\left[\frac{\partial w}{\partial t} + u\frac{\partial w}{\partial x} + v\frac{\partial w}{\partial y} + w\frac{\partial w}{\partial z}\right] &= -(1-C)\frac{\partial p}{\partial z} + \mu_d(C)(1-C)\left[\frac{\partial^2 w}{\partial x^2} + \frac{\partial^2 w}{\partial y^2} + \frac{\partial^2 w}{\partial z^2}\right] \\ &+ CS(w_p - w), \end{aligned} \quad (1.7)$$

$$C\rho_P\left[\frac{\partial w_P}{\partial t} + u_P\frac{\partial w_P}{\partial t} + v_P\frac{\partial w_P}{\partial y} + w_P\frac{\partial w_P}{\partial z}\right] = C(w - w_P), \quad (1.8)$$

$$\begin{aligned} \rho c_p(1-C)\left[\frac{\partial T}{\partial t} + u\frac{\partial T}{\partial x} + v\frac{\partial T}{\partial y} + w\frac{\partial T}{\partial z}\right] &= k(1-C)\left[\frac{\partial^2 T}{\partial x^2} + \frac{\partial^2 T}{\partial y^2} + \frac{\partial^2 T}{\partial z^2}\right] \\ &+ \frac{\rho_p c_p C}{\tau_t}(T_P - T) + CS[(u - u_P)^2 + (v - v_P)^2 + (w - w_P)^2] \\ C\left[\frac{\partial T_P}{\partial t} + u_P\frac{\partial T_P}{\partial x} + v_P\frac{\partial T_P}{\partial y} + w_P\frac{\partial T_P}{\partial z}\right] &= C\frac{c_P}{c_m \tau_T}(T - T_P), \end{aligned} \quad (1.9)$$

$S$  is Stoke's resistance (drag coefficient), there are different correlations of it according to assumptions are defined by Chhabra in his book[114]. Here the considered value for  $S$  is given below,

$$S = \frac{9}{2} \frac{\mu_o}{r^2} \lambda(C), \quad (1.10)$$

where,

$$\lambda(C) = \frac{4 + 3[8C - 3C^2]^{1/2} + 3C}{[2 - 3C]^2}. \quad (1.11)$$

Value of the above function is determined by Tam [117]. The correlation for viscosity of fluid-particle mixture is proposed by Charm and Kurland [116].

$$\mu_d = \mu_o \frac{1}{1 - qC} \quad (1.12)$$

and,

$$q = 0.07 \exp[2.49C + \frac{1107}{T} \exp(-1.69C)] \quad (1.13)$$

## 1.1.2 Buongiorno Nano-fluid Model

The Buongiorno model is used to investigate the effects of Brownian motion and thermophoresis on the flow, heat, and mass transfer. In this model, the nano-sized particles flow with the base fluid, either newtonian or non-newtonian. This model can be defined as follows:

$$\frac{\partial u}{\partial x} + \frac{\partial v}{\partial y} + \frac{\partial w}{\partial z} = 0, \quad (1.14)$$

$$\begin{aligned} \frac{\partial u}{\partial t} + u \frac{\partial u}{\partial x} + v \frac{\partial u}{\partial y} + w \frac{\partial u}{\partial z} &= -\frac{\partial p}{\partial x} + \mu \left( \frac{\partial^2 u}{\partial x^2} + \frac{\partial^2 u}{\partial y^2} + \frac{\partial^2 u}{\partial z^2} \right) \\ \frac{\partial T}{\partial t} + u \frac{\partial T}{\partial x} + v \frac{\partial T}{\partial y} + w \frac{\partial T}{\partial z} &= \alpha_m \left( \frac{\partial^2 T}{\partial x^2} + \frac{\partial^2 T}{\partial y^2} + \frac{\partial^2 T}{\partial z^2} \right) + \tau \left[ D_B \left( \frac{\partial C_n}{\partial x} \frac{\partial T}{\partial x} + \frac{\partial C_n}{\partial y} \frac{\partial T}{\partial y} + \frac{\partial C_n}{\partial z} \frac{\partial T}{\partial z} \right) \right. \\ &\left. + \frac{D_T}{D_\infty} \left( \left( \frac{\partial T}{\partial x} \right)^2 + \left( \frac{\partial T}{\partial y} \right)^2 + \left( \frac{\partial T}{\partial z} \right)^2 \right) \right], \end{aligned} \quad (1.15)$$

$$\frac{\partial C_n}{\partial t} + u \frac{\partial C_n}{\partial x} + v \frac{\partial C_n}{\partial y} + w \frac{\partial C_n}{\partial z} = D_B \left( \frac{\partial^2 C_n}{\partial x^2} + \frac{\partial^2 C_n}{\partial y^2} + \frac{\partial^2 C_n}{\partial z^2} \right) + \frac{D_T}{D_\infty} \left( \frac{\partial^2 T}{\partial x^2} + \frac{\partial^2 T}{\partial y^2} + \frac{\partial^2 T}{\partial z^2} \right), \quad (1.16)$$

$C_n$  is nanoparticle concentration.

## 1.2 Methods of finding solutions

Real problems mostly contain nonlinearity and in this dissertation, the modeled equations are non-linear differential equations. There are many analytical and numerical methods to solve the non-linear differential equation system. To solve the problem in this dissertation, the shooting method with Runge Kutta Fehlberg method and bvp4c are used methods.

## 1.3 Body forces

### 1.3.1 MHD

Study of dynamics of fluid and particles under the effect of magnetic field lies in MHD having striking importance in industry, medical diagnostics and nuclear power generation. This term can be defined by Lorentz force as:  $\mathbf{j} \times \mathbf{B}$ , where  $\mathbf{j}$  is electric current density and  $\mathbf{B}$  is magnetic field. By Ohm's law:

$$\mathbf{j} = \sigma[\mathbf{E} + \mathbf{V} \times \mathbf{B}], \quad (1.17)$$

$$(1.18)$$

where  $\sigma$  is electrical conductivity of fluid.



### 1.3.2 Thermal Radiation

Non-linear thermal radiations are also introduced to cope up with the temperature related problems during flows.  $q_r$  is the radiative heat flux can be find out by Rosseland approximation.

$$q_r = -\frac{4\sigma^*}{3k_1} \frac{\partial T^4}{\partial z}, \quad (1.19)$$

where  $\sigma^*$  is a constant called Stefan-Boltzmann and  $k_1$  is average absorption coefficient. While considering that model, optically thick radiations are considered.  $T^4$  given as below;

$$T^4 = T_\infty^4 + 4T_\infty^3(T - T_\infty) + 6T_\infty^2(T - T_\infty)^2 + \dots, \quad (1.20)$$

### 1.3.3 Heat generation/absorption

Heat generation and absorption technologies perform a distinct role in global energy and environmental issues. The current considered expression is given by,

$$Q_o = \left(\frac{kU_w(x, t)}{x\nu}\right)[A^*(T_w - T_\infty)f' + B^*(T - T_\infty)]. \quad (1.21)$$

## 1.4 Constitutive equations

### 1.4.1 Williamson Fluid

The tensor for Williamson fluid is defined by form

$$\tau = \left[\mu_\infty + \frac{(\mu_o - \mu_\infty)}{1 - \Gamma\dot{\gamma}}\right]\mathbf{A}_1. \quad (1.22)$$

Where  $\Gamma$  is a positive time constant i.e,  $\Gamma > 0$ .  $\mu_o$  is low shear rate viscosity,  $\mu_\infty$  is the high shear rate viscosity and shear rate  $\dot{\gamma}$  is defined below,

$$\dot{\gamma} = \sqrt{\frac{1}{2}\pi}, \quad (1.23)$$

and

$$\pi = \frac{1}{2}tr(\mathbf{A}_1^2). \quad (1.24)$$

Here we consider only the case for  $\mu_\infty = 0$  and  $\Gamma\dot{\gamma} < 1$ . Now extra stress tensor reduced to:

$$\tau = \left[\frac{\mu_o}{1 - \Gamma\dot{\gamma}}\right]\mathbf{A}_1. \quad (1.25)$$

By applying binomial expansion to Eq (1.18) and one can obtain following expression

$$\tau = \mu_o[1 + \Gamma\dot{\gamma}]A_1, \quad (1.26)$$

$$\dot{\gamma} = [(\frac{\partial u}{\partial x})^2 + \frac{1}{2}(\frac{\partial u}{\partial y} + \frac{\partial v}{\partial x})^2 + (\frac{\partial v}{\partial y})^2]^{\frac{1}{2}}. \quad (1.27)$$

Components of tensor depend upon the assumptions, as below are assumed for two dimensional flow.

$$\tau_{xx} = 2\mu_o[1 + \Gamma\dot{\gamma}](\frac{\partial u}{\partial x}), \quad (1.28)$$

$$\tau_{xy} = \mu_o[1 + \Gamma\dot{\gamma}](\frac{\partial u}{\partial y} + \frac{\partial v}{\partial x}), \quad (1.29)$$

$$\tau_{yy} = 2\mu_o[1 + \Gamma\dot{\gamma}](\frac{v}{y}), \quad (1.30)$$

$$\tau_{xz} = \tau_{yz} = \tau_{zx} = \tau_{zy} = \tau_{zz} = 0. \quad (1.31)$$

## 1.4.2 tangent hyperbolic Fluid

The constitutive equation for tangent hyperbolic fluid is given below,

$$\tau = [\mu_\infty + (\mu_o + \mu_\infty) \tanh(\Gamma\dot{\gamma})^n]\dot{\gamma} \quad (1.32)$$

here  $\mu_\infty$  is the infinite share rate viscosity will be consider as zero to avoid the complexity and  $\mu_o$  is zero rate viscosity of fluid,  $n$  is the power law index also known as flow behavior index which decides that if  $n = 0$  then fluid is newtonian or if  $n \neq 1$  then fluid is non-Newtonain,  $\Gamma$  is the time constant and  $\dot{\gamma}$  is defined below,

$$\dot{\gamma} = \sqrt{\frac{1}{2}tr(A_1^2)} \quad (1.33)$$

and  $A_1$  is the first Rivilin-Ereckson tensor. As tangent hyperbolic fluid belongs to shear thinning class so the condition  $\Gamma\dot{\gamma} \ll 1$  taken in account. Avoiding digress after considerations of conditions and by opening the tangent hyperbolic series Eq.(1.28) reduces to following equation,

$$\tau = \mu_o[1 + n(\Gamma\dot{\gamma} - 1)]\dot{\gamma} \quad (1.34)$$

## Chapter 2

# Numerical analysis of unsteady Magneto-biphase Williamson fluid flow with time dependent magnetic field

Numerical investigation of time dependent flow of the dusty Williamson fluid has been focused in this chapter. The flow of biphase liquid-particle suspension saturating the medium is caused by stretching of porous surface. The influence of magnetic field and heat generation/absorption are also observed. It is assumed that particle has a spherical shape and distributed uniformly in fluid matrix. Also, the concentration is small leads to negligence of collision of particles. The unsteady two dimensional problems is modeled for both fluid and particle phase using conservation of mass, momentum and heat transfer. For particles it is considered that they are non-conducting and rigid. The finalized model generates the non-dimensioned parameters, namely Weissenberg number, unsteadiness parameter, magnetic parameter, heat generation/absorption parameter, Prandtl number, fluid particle interaction parameter and mass concentration parameters. The numerical solution is obtained. Locality of skin friction and Nusselt number are focused with the help of tables and graphs.

## 2.1 Mathematical formulation

Intrinsic equations for Williamson model are defined in [27], also in (Eq.(1.18)). While formulating the constraint equations for incompressible unsteady dusty flow of Williamson fluid, magnetic field which works with time is employed long side heat source/sink. The flow is induced due to a porous sheet which is continuously stretched parallel to x-axis. Fluid deformation is defined on positive y-axis. The volume fraction of the dust granules, i.e. number density is variable. It is assumed that heat source is placed in the flow which can generate or suck energy. Considering the assumptions, controlling equations for current liquid/particle problem can be set like Manjunatha et al [115].

$$\frac{\partial u}{\partial x} + \frac{\partial v}{\partial y} = 0, \quad (2.1)$$

$$\frac{\partial u_P}{\partial x} + \frac{\partial v_P}{\partial y} = 0, \quad (2.2)$$

$$\frac{\partial u}{\partial t} + u \frac{\partial u}{\partial x} + v \frac{\partial u}{\partial y} = \nu \left[ \frac{\partial^2 u}{\partial y^2} + \sqrt{2}\Gamma \frac{\partial u}{\partial y} \frac{\partial^2 u}{\partial y^2} \right] - \frac{\sigma B^2(t)u}{\rho(1-C)} + \frac{CS}{\rho(I-C)}(u_P - u), \quad (2.3)$$

$$\frac{\partial u_P}{\partial t} + u_P \frac{\partial u_P}{\partial x} + v_P \frac{\partial u_P}{\partial y} = \frac{S}{\rho_P}(u - u_P), \quad (2.4)$$

$$\frac{\partial T}{\partial t} + u \frac{\partial T}{\partial x} + v \frac{\partial T}{\partial y} = \frac{k}{\rho c_p} \frac{\partial^2 T}{\partial y^2} + \frac{\rho_P c_p C (T_P - T)}{\rho \tau_t (1-C)} - \frac{Q_o}{\rho c_P (1-C)}, \quad (2.5)$$

$$\frac{\partial T_P}{\partial t} + u_P \frac{\partial T_P}{\partial x} + v_P \frac{\partial T_P}{\partial y} = \frac{c_P}{c_m \tau_T}(T - T_P), \quad (2.6)$$

their respective conditions at boundary are

$$u = U_w(x, t), \quad v = V_s(t), \quad T = T_w(x, t), \quad \text{at } y = 0,$$

$$u_P \rightarrow 0, \quad u \rightarrow 0, \quad v_P \rightarrow v, \quad T_P \rightarrow T_\infty, \quad T \rightarrow T_\infty, \quad \text{as } y \rightarrow \infty. \quad (2.7)$$

Here  $u(t, x, y)$  and  $u_P(t, x, y)$  are the flow components of fluid and solid particles and  $v(t, x, y)$  and  $v_P(t, x, y)$  are the components of velocity of the fluid and particles which are perpendicular to flow direction respectively.  $S$  is the Stoke's resistance (drag coefficient) [13].  $T$  and  $T_P$  are the fluid temperature and particles temperature respectively.  $Q_o$  is the non-uniform source or sink which is dependent upon space and time. The conjecture builds of the velocity of stretching wall, temperature of the wall, and mass fluid velocity are defined below:

$$U_w(x, t) = \frac{ax}{(1-ct)}, \quad V_s(t) = \frac{-V_o}{(1-ct)^{\frac{1}{2}}}, \quad T_w(x, t) = T_\infty + \frac{T_o U_w x}{\nu(1-ct)^{\frac{1}{2}}},$$

$$B(t) = \frac{B_o}{(1-ct)^{\frac{1}{2}}}, Q_o = \left(\frac{kU_w(x,t)}{x\nu}\right)[A^*(T_w - T_\infty)f' + B^*(T - T_\infty)]. \quad (2.8)$$

Here  $a$  and  $c$  are the constants with positive values,  $V_o$  is uniform suction/injection velocity and  $B_o$  is the magnetic field intensity.  $T_w$  is the temperature at the wall and  $T_\infty$  is temperature at a large distance from wall.  $A^*$  and  $B^*$  are the parameters of internal heat source/sink.

Stream functions  $\psi$  and  $\psi_P$  can be defined for both fluid and particles, such as

$$u = \frac{\partial\psi}{\partial y}, v = -\frac{\partial\psi}{\partial x}, u_P = \frac{\partial\psi_P}{\partial y}, v_P = -\frac{\partial\psi_P}{\partial x}. \quad (2.9)$$

The set of transformations for the conversion of PDE's to ODE's can be specified as

$$\begin{aligned} \eta &= y\sqrt{\frac{U_w}{\nu x}}, \psi = \sqrt{U_w\nu x}f(\eta), \psi_P = \sqrt{U_w\nu x}F(\eta) \\ \theta &= \frac{T - T_\infty}{T_w - T_\infty}, \theta_P = \frac{T_P - T_\infty}{T_w - T_\infty}. \end{aligned} \quad (2.10)$$

By manipulating *Eqs.*(2.1) – (2.7) using *Eqs.*(2.8) – (2.1) obtain following expressions,

$$f'''[1 + We f''] + f f'' - f'^2 - A[f' + \frac{\eta}{2}f''] - M^2 f' + \frac{CR}{(1-C)}(F' - f') = 0, \quad (2.11)$$

$$F''(\eta\frac{A}{2} - F) + AF' + F'^2 + R(F' - f') = 0 \quad (2.12)$$

$$\theta'' + Pr(f\theta' - 2f'\theta) - Pr\frac{A}{2}(\eta\theta' + 3\theta) + \frac{Pr\alpha\beta_T C}{(1-C)}(\theta_P - \theta) - \frac{A^*f' - B^*\theta}{(1-C)} = 0, \quad (2.13)$$

$$\theta'_P(\eta\frac{A}{2} - F) - \gamma\beta_T(\theta - \theta_P) + \theta_P(\frac{3}{2}A + 2f') = 0, \quad (2.14)$$

along with the conditions at boundary,

$$\begin{aligned} f(0) = s, \theta(0) = 1, f'(0) = 1, \\ f' \rightarrow 0, F = f, F' \rightarrow 0, \theta \rightarrow 0, \theta_P \rightarrow 0 \text{ as } \eta \rightarrow \infty. \end{aligned} \quad (2.15)$$

Here derivative is taken w.r.t  $\eta$ . The dimensionless number  $A$ ,  $M$ ,  $We$ ,  $Pr$ ,  $\alpha$ ,  $\gamma$  and  $s$  are the unsteadiness parameter, magnetic parameter, Weissenberg number, Prandtl number, mass concentration parameter, fraction of specific heat of the fluid to the particles respectively, and mass transferring parameter, for injection and suction,  $s < 0$  and  $s > 0$  are taken respectively. All of parameters are defined below

$$We = \sqrt{\frac{a^3\Gamma x^2}{\nu(1-ct)^3}}, A = \frac{c}{a}, M = \sqrt{\frac{\sigma}{\rho a}}B_o, R = \frac{S(1-ct)}{\rho a},$$

$$Pr = \frac{\mu c_p}{k}, \alpha = \frac{\rho_P}{\rho}, \beta_T = \frac{1 - ct}{a\tau_T}, \gamma = \frac{c_p}{c_m}, s = \frac{V_o}{\sqrt{\nu a}}. \quad (2.16)$$

Where,  $\tau_T$  is the thermal equilibrium time, required by particles to regulate their temperature corresponding to fluid. The skin friction and Nusselt number are the physical quantities in which engineers are interested. Relations for skin friction and Nusselt number are given in Eq (2.17),

$$C_f = \frac{\tau_w}{\frac{1}{2}\rho U_w^2}, Nu_x = \frac{xq_w}{k(T_w - T_\infty)}, \quad (2.17)$$

where,  $q_w$  denotes the heat flux of the wall. For the Williamson fluid surface shear stress and estimate of heat transfer through porous stretching wall are defined as

$$\tau_w = \mu_o \left[ \frac{\partial u}{\partial y} + \frac{\Gamma}{\sqrt{2}} \left( \frac{\partial u}{\partial y} \right)^2 \right], q_w = -k \left( \frac{\partial T}{\partial y} \right), \quad (2.18)$$

by using value of Eq (2.18) into Eq (2.17), get following relations,

$$\frac{C_f Re_x^{\frac{1}{2}}}{2} = f''(0) + \frac{We}{2} f''^2(0), Nu_x Re_x^{-\frac{1}{2}} = -\theta'(0). \quad (2.19)$$

Here,  $Re_x = \frac{Ux}{\nu}$  denotes the Reynolds number.

## 2.2 Numerical procedure of solution

Current problem is a highly non-linear system of differential equations given by Eqs (2.11)–(2.14) and to get the exact solution in quite a tedious task, therefore solution is obtained numerically and get the approximated solution. Eqs (2.11) – (2.14) can also be written as,

$$f''' = \frac{1}{1 + We f''} [f'^2 - f f'' + A(f' + \frac{\eta}{2}) + \frac{M^2 f'}{1 - C} - \frac{CR}{1 - C} (F' - f')], \quad (2.20)$$

$$F'' = \frac{-AF' - F'^2 - \beta_T(F' - f')}{\frac{A\eta}{2} - F}, \quad (2.21)$$

$$\theta'' = Pr \frac{A}{2} (\eta \theta' + 3\theta) - Pr(f\theta' - 2f'\theta) - \frac{Pr\alpha\beta_T}{(1 - C)} (\theta_P - \theta) + \frac{A^* f' + B^* \theta}{(1 - C)}, \quad (2.22)$$

$$\theta'_P = \frac{\gamma\beta_T(\theta - \theta_P) - \theta_P(\frac{3A}{2} + 2F')}{\frac{A\eta}{2} - F}. \quad (2.23)$$

Some dummy variables are introduced, shown as in Eq(2.24)

$$\begin{aligned} f &= y_1, f' = y_2, f'' = y_3, f''' = y'_3, \\ F &= y_4, F' = y_5, F'' = y'_5, \\ \theta &= y_6, \theta' = y_7, \theta'' = y'_7, \\ \theta_P &= y_8, \theta'_P = y'_8. \end{aligned} \quad (2.24)$$

The system of  $Eqs(2.20) - (2.24)$  can be converted in first order initial value problem can be shown as:

$$\frac{dy_1}{dx} = y_2, \quad (2.25)$$

$$\frac{dy_2}{dx} = y_3, \quad (2.26)$$

$$\frac{dy_3}{dx} = \frac{1}{1 + We y_3} [y_2^2 - y_1 y_3 + A(y_2 + \frac{\eta}{2} y_3) + \frac{M^2}{1 - C} y_2 - \frac{CR}{(1 - C)} (y_5 - y_2)], \quad (2.27)$$

$$\frac{dy_4}{dx} = y_5, \quad (2.28)$$

$$\frac{dy_5}{dx} = \frac{-A y_5 - y_5^2 - \beta_T (y_5 - y_2)}{\frac{A\eta}{2} - y_4}, \quad (2.29)$$

$$\frac{dy_6}{dx} = y_7, \quad (2.30)$$

$$\frac{dy_7}{dx} = -pr(y_1 y_7 - 2y_2 y_6) + Pr \frac{A}{2} (\eta y_7 + 3y_6) - \frac{Pr \alpha \beta_T}{(1 - C)} (y_8 - y_6) \quad (2.31)$$

$$+ \frac{A^* y_2 + B^* y_6}{(1 - C)},$$

$$\frac{dy_8}{dx} = \frac{\gamma \beta_T (y_6 - y_8) - y_8 (\frac{3A}{2} + 2y_5)}{\frac{A\eta}{2} - y_4}, \quad (2.32)$$

the reduced endpoint conditions are

$$\begin{aligned} y_1(a) = s, \quad y_2(a) = 1, \quad y_2(b) = s_1, \quad y_4(b) = y_1(b), \\ y_5(b) = s_2, \quad y_6(a) = 1, \quad y_6(b) = s_3, \quad y_8(b) = s_4. \end{aligned} \quad (2.33)$$

where  $s_1, s_2, s_3$  and  $s_4$  are initially guessed values in a way like integration of the system of first order ODE fulfil the endpoint conditions and obtained the desired solution for the system of ordinary differential equations (2.25)-(2.33). The choice of maximum value is  $\eta = 7$  with step size = 0.01 with simulation error as  $10^5$  and  $s = 0.3$  is fixed for all of the results in the current discussion.

## 2.3 Outcomes and discussions

Final results are gained by means of numerical method `bvp4c` in graphical and tabular form. *Fig. 2.1* is sketched for the study of the velocity profile of fluid and dust particles. As it is obvious that Weissenberg number  $We$  is the fraction of relaxation time to the retardation time. Increase in  $We$  will reduce the retardation time, which leads to

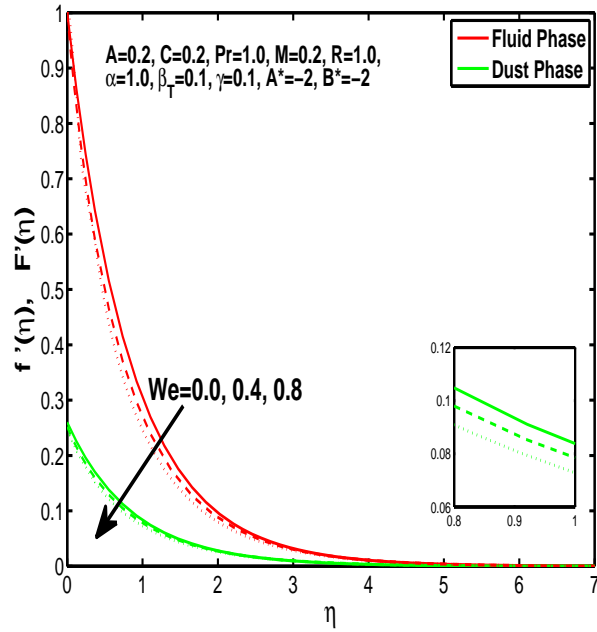


Figure 2.1: Outcome of  $We$  on velocity profile of fluid and dust particles.

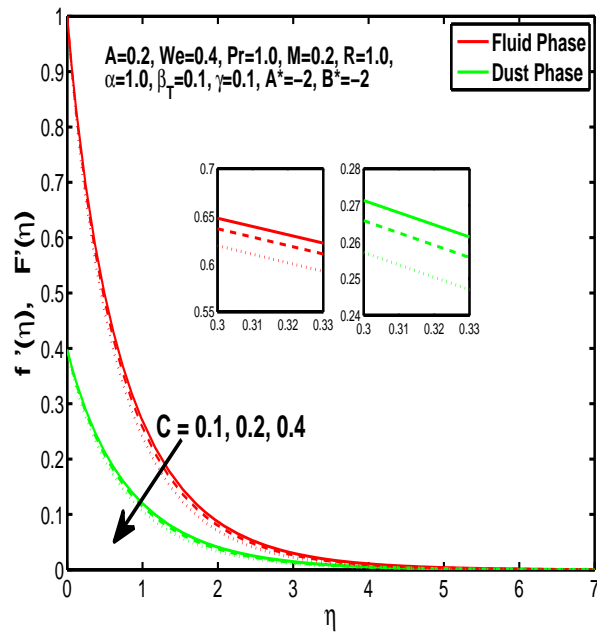


Figure 2.2: Outcome of  $C$  on velocity of fluid and dust particles.



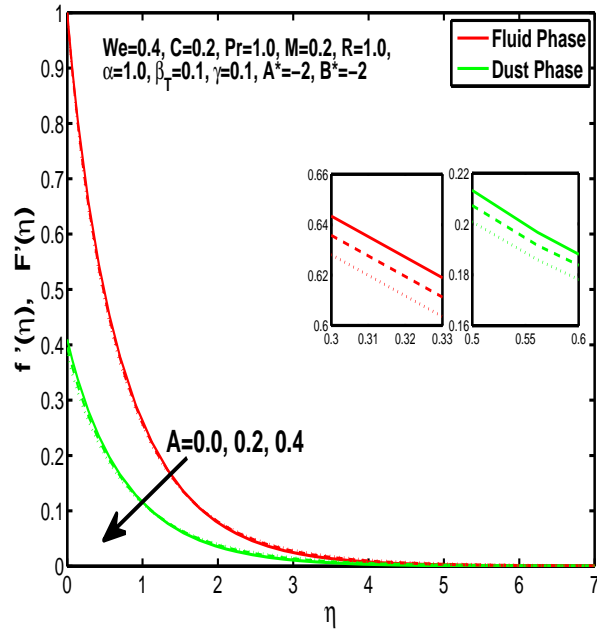


Figure 2.3: Outcome of  $A$  on velocity profile of fluid and dust particles.

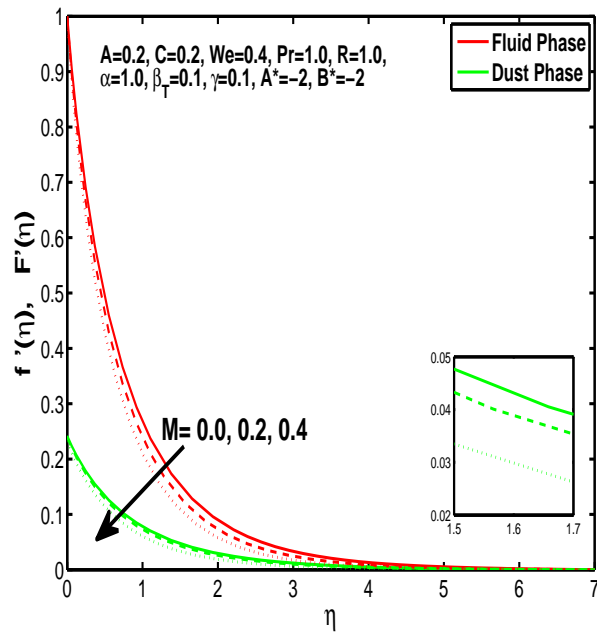


Figure 2.4: Outcome of  $M$  on velocity of fluid and dust particles.

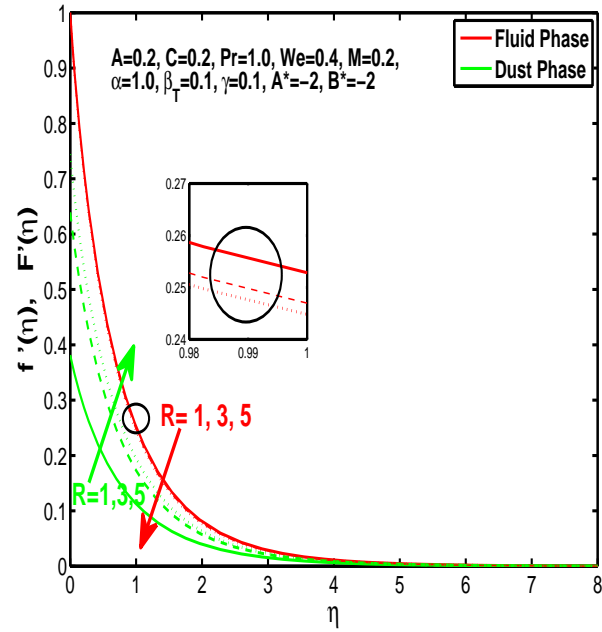


Figure 2.5: Outcome of  $R$  on velocity profile of fluid and dust.

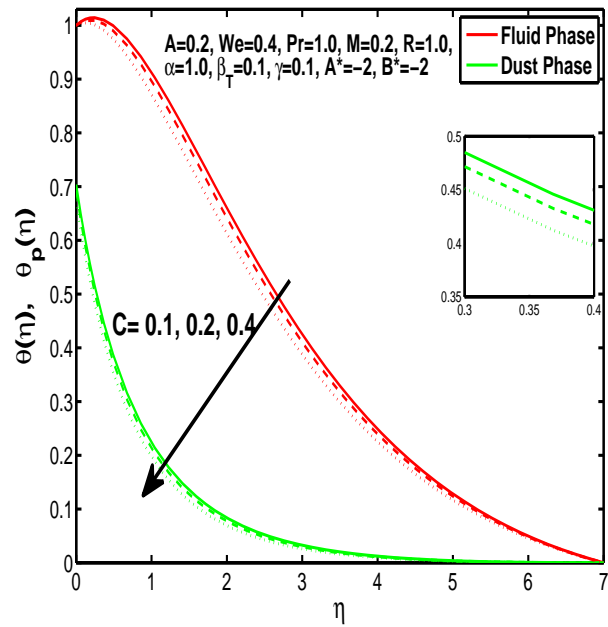


Figure 2.6: Outcome of  $C$  on temperature profile of fluid and dust particles.

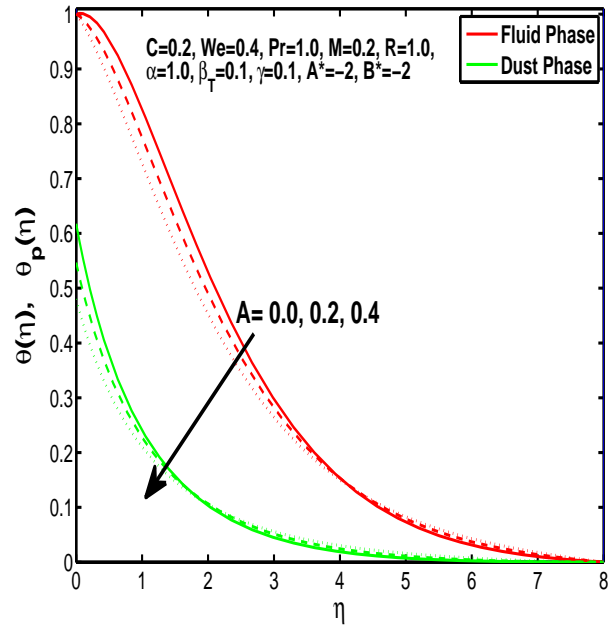


Figure 2.7: Outcome of  $A$  on temperature profile of fluid and dust particles.

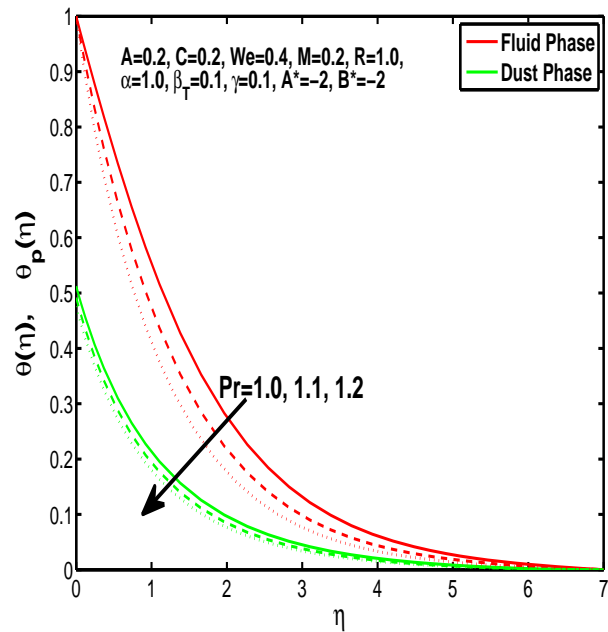


Figure 2.8: Outcome of  $Pr$  on temperature profile of fluid and dust particles.

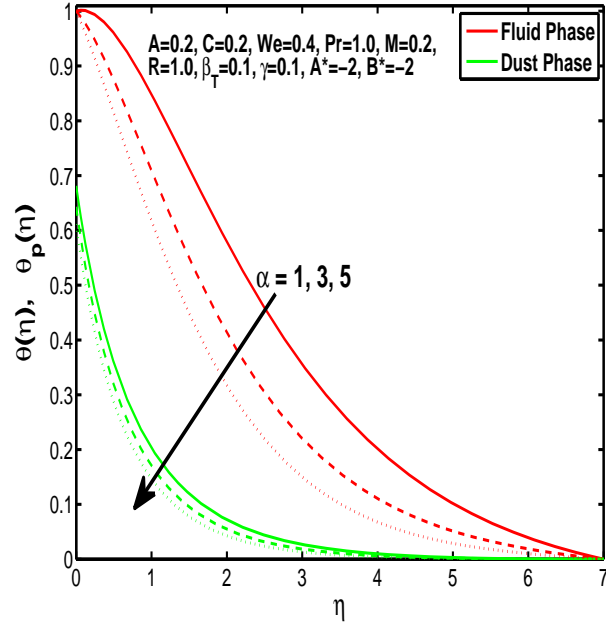


Figure 2.9: Outcome of  $\alpha$  on temperature profile of fluid and dust particles.

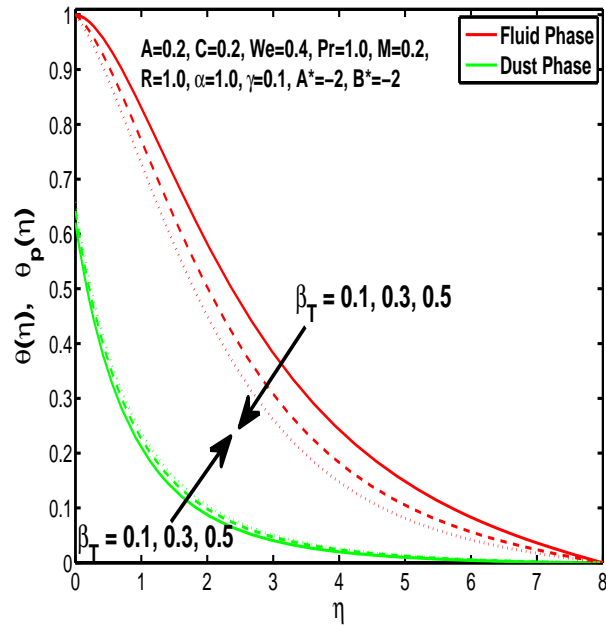


Figure 2.10: Outcome of  $\beta_T$  on temperature of fluid and dust particles.

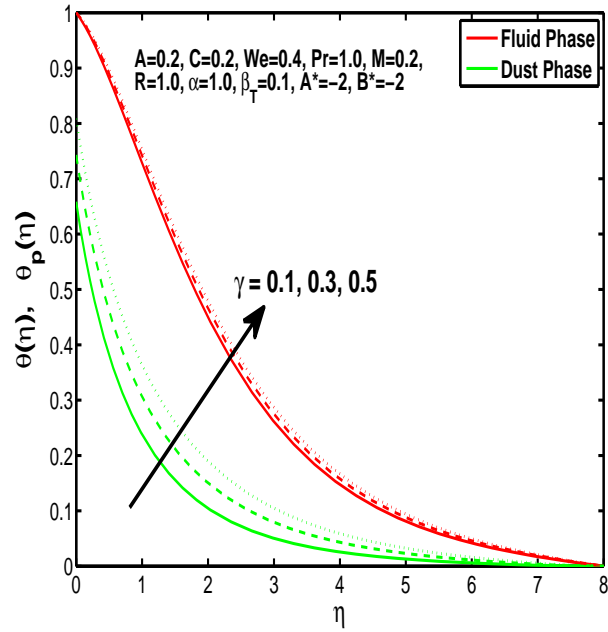


Figure 2.11: Outcome of  $\gamma$  on temperature profile of fluid and dust particles.

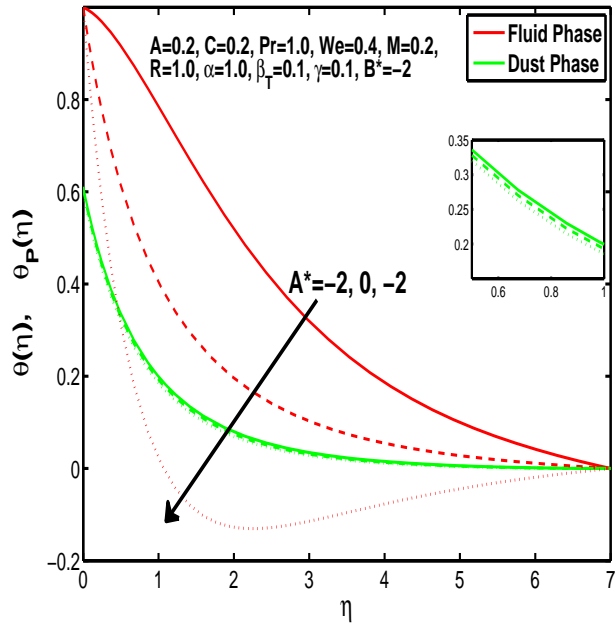


Figure 2.12: Outcome of  $A^*$  on temperature profile of fluid and dust particles.

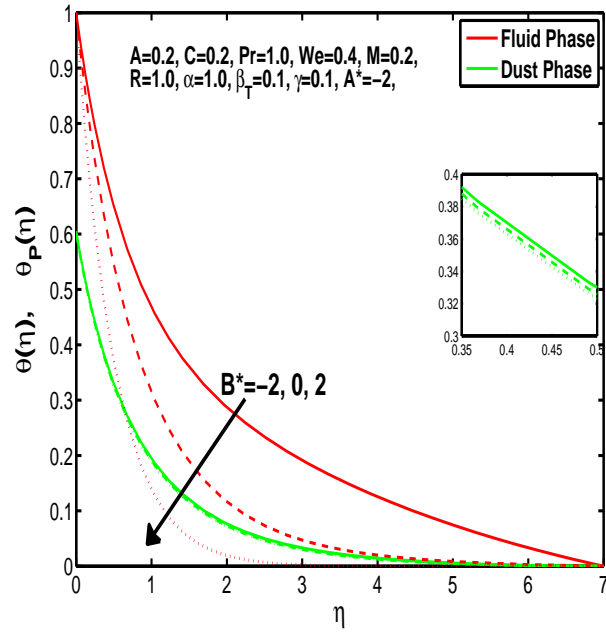


Figure 2.13: Outcome of  $B^*$  on temperature profile of fluid and dust particles.

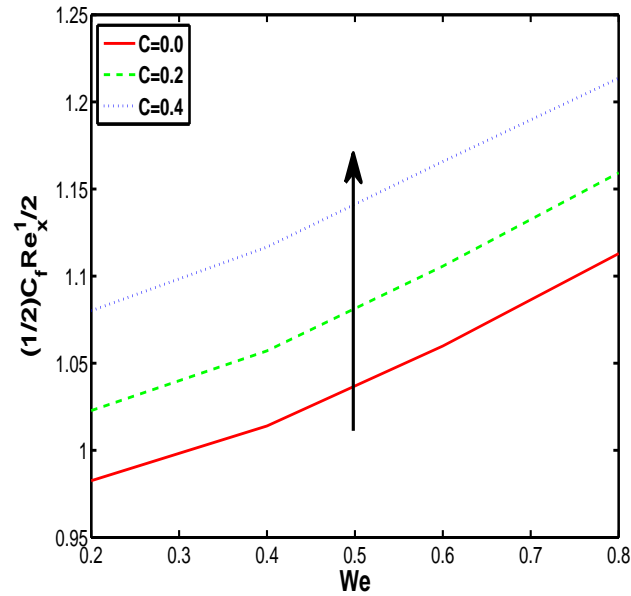


Figure 2.14: Variation of skin friction according to change in volume fraction parameter  $C$  and Weissenberg parameter  $We$ .

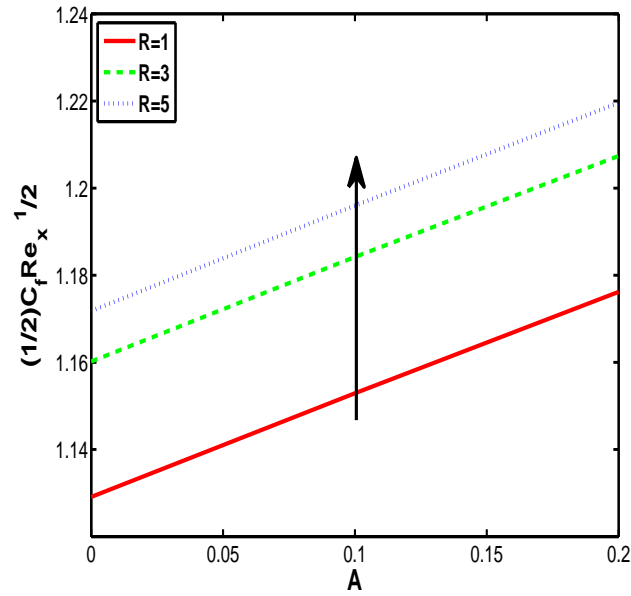


Figure 2.15: Variation of skin friction according to change in fluid-particle interaction  $R$  and unsteadiness parameter  $A$ .

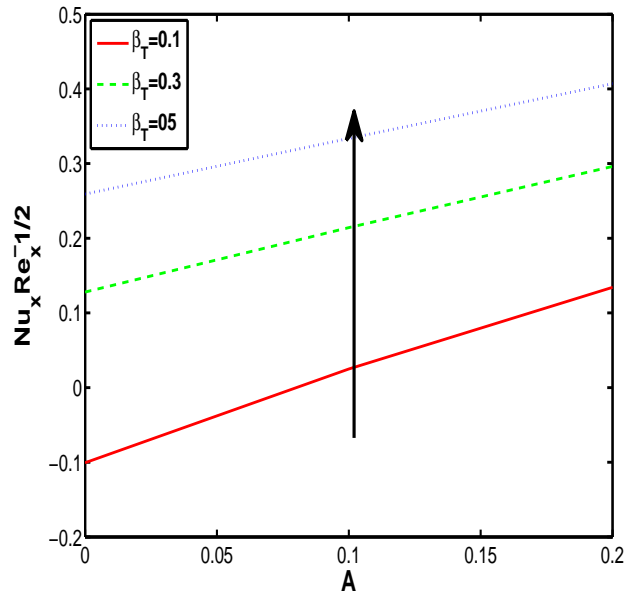


Figure 2.16: Variation of Nusselt number according to change in fluid-particle interaction  $\beta_T$  and unsteadiness parameter  $A$ .

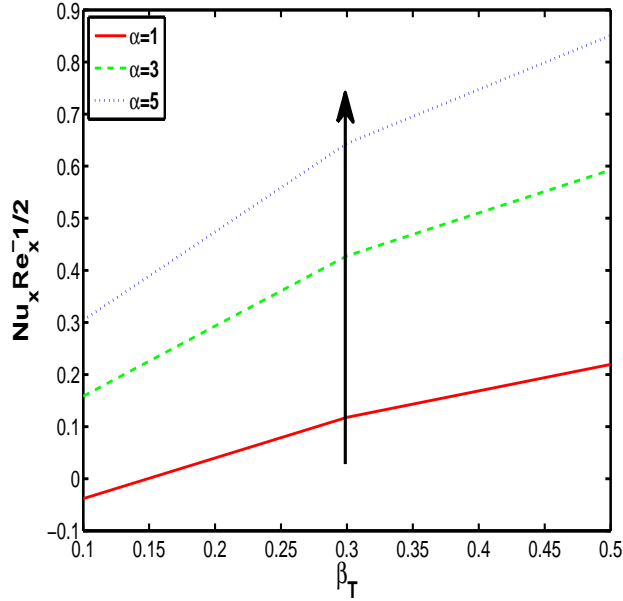


Figure 2.17: Variation of Nusselt number according to change in mass concentration  $\alpha$  and fluid-particle parameter  $\beta_T$ .

resistance to flow in very short time. In simple words, one can say that increment of the Weissenberg number depreciates the fluid velocity as well as the dust phase velocity. The consequence of volume fraction  $C$  on the momentum boundary layer is delineated in *Fig. 2.2*. Substantially the volume taken by the dust particles is high in the fluid then increment of  $C$  will inflate the concentration of fluid overall, due to which velocity of fluid as well as dust particles will depreciate. *Fig. 2.3*. depicts that velocity profile of the fluid decreases with the improvement of unsteadiness parameter  $A$ . Due to rapid increment in time there is a reduction in stretching rate, which is cause of flow. So lesser stretching rate causes thinner momentum boundary layer of fluid and dust particles. *Fig. 2.4*. portrays the consequence of magnetic field on momentum boundary layer. According to the fact that addendum of magnetic parameter evolves the resistive force against the flow, which is predominantly known as Lorentz force. Due to this resistive force velocity profile reduces both for the fluid and dust particle. *Fig. 2.5*. indicate the turn-out of fluid particle interaction parameter on momentum boundary layer. Graph's out-come depicts that with the improvement of fluid interaction reduces the velocity of fluid and enhances the velocity of dust particles. *Fig. 2.6*. is sketched for the effect of volume fraction of temperature boundary layer. When the number of particles increases the fluid temperature decreases



Table 2.1: Analogy of Skin friction coefficient with already published results by keeping  $A = 0$  and  $We = 0$ .

M	Akbar et al. <sup>34</sup>	Fathizadeh et al. <sup>35</sup>	Kumar et al. <sup>21</sup>	Present results
1	-1.41421	-1.41421	-1.41421	-1.41421
5	-2.44948	-2.44948	-2.44949	-2.44948
10	-3.31662	-3.31662	-3.31662	-3.31662
50	-7.14142	-7.14142	-7.14143	-7.14142
500	-22.3830	-22.3830	-22.3830	-22.38302
1000	-31.6386	-31.6386	-31.63858	-31.63858

as the internal energy is utilized to keep the temperature of the mixture at equilibrium. *Fig. 2.7.* depicts that behavior of the unsteadiness parameter on temperature profile. As explained above that due to concentration depreciates the temperature boundary layer after attaining peak value to normalized the temperature of the fluid and dust granules. *Fig. 2.8.* portray the discernible results for dimensionless Prandtl number. As the rise in Prandtl number dwindle the thermal conductivity of fluid which leads to decline of thermal boundary layer of fluid and particles as well. *Fig. 2.9.* shows that increase of mass concentration  $\alpha$  decreases the temperature boundary layer of fluid after gaining maximum value to stabilized the temperature of the fluid and dust particles as well. *Fig. 2.10.* indicates that the enhancement of fluid-particle interaction reduces the temperature of fluid phase and raises the temperature profile of dust phase. It may happen because the interaction of dust particles is for the enhancement of thermal conductivity. *Fig. 2.11.* depicts that increase in the specific heat capacity ratio enlarge the temperature boundary layer of fluid and dust phase as well and this is the obvious result. *Fig. 2.12.* and *Fig. 2.13.* exhibits the influence of heat source/sink parameters upon the temperature profile. Graphical results inform that there is decrease in internal heat of fluid and solid particles due to increase in heat generation parameter. And opposite behavior is observed in heat absorption case. *Fig. 2.14.* shows that increase of volume fraction of dust granules enhances the skin friction that's because the increment of volume of dust particles causes the resistive force with the wall. Same the case with fluid-particle interaction parameter shown in *Fig. 2.15.* Nusselt number is the change in temperature from wall to fluid and it increases with the increase in fluid-particle interaction and mass concentration because of addition of internal energy due to resistive force after collisions of particles shown in *Fig. 2.16* and *Fig. 2.17.* For the authentication of current results with previous results one

Table 2.2: Numeric findings for Skin friction.

$A$	$R$	$C$	$\alpha$	$M$	$We$	$\frac{1}{2}C_f Re_x^{-\frac{1}{2}}$
0.0	-	-	-	-	-	1.1640
0.1	-	-	-	-	-	1.1927
0.2	1	-	-	-	-	1.2212
-	2	-	-	-	-	1.2327
-	3	0.1	-	-	-	1.2392
-	-	0.2	-	-	-	1.2955
-	-	0.3	1	-	-	1.3645
-	-	-	2	-	-	1.5120
-	-	-	3	0.2	-	1.6464
-	-	-	-	0.4	-	1.6945
-	-	-	-	0.6	0.2	1.7702
-	-	-	-	-	0.3	1.6659

can consult the *Table. 2.1.* which shows the comparable closed results. Variation of local skin friction against different parameter  $A, R, C, \alpha, M$  and  $We$  is given in *Table. 2.2.* And results show that skin friction increases with the increase of unsteadiness, fluid particle interaction and volume fraction of dust particles but decreases due to Weissenberg effect. The variation of local Nusselt number against different parameters  $A, \beta_T, \alpha, \gamma, Pr, A^*$  and  $B^*$  is given in *Table. 2.3.* And Nusselt number increases with the increase in unsteadiness, fluid-particle interaction, mass concentration, specific heat ratio, Prandtl number and heat source but reduces due to heat sink.

## 2.4 Concluding remarks

The two dimensional unsteady dusty flow of Williamson fluid is studied in this chapter. The effects of magnetic field and heat generation/absorption are discussed for fluid and dust particles as well. Following are the outcomes of the current effort:

- Enhancement of Weissenberg number, unsteady parameter, volume fraction parameter, magnetic parameter, and mass concentration parameter depreciates the velocity of fluid  $f'(\eta)$  and velocity of dust granules  $F'(\eta)$  as well.
- Enhancement of fluid-particle interaction reduces the velocity of fluid  $f'(\eta)$  but give rise to the velocity of dust granules  $F'(\eta)$ .

Table 2.3: Numeric findings for Nusselt number.

$A$	$\beta_T$	$\alpha$	$\gamma$	$Pr$	$A'$	$B'$	$Nu_x Re_x^{-1/2}$
0.0	-	-	-	-	-	-	2.6347
0.1	-	-	-	-	-	-	2.6452
0.2	-	-	-	-	-	-	2.6559
0.3	0.1						2.6668
-	0.2	-	-	-	-	-	2.6676
-	0.3	1	-	-	-	-	2.6687
-	-	2	-	-	-	-	2.6653
-	-	3	0.1	-	-	-	2.6652
-	-	-	0.2	-	-	-	2.6669
-	-	-	0.3	0.7	-	-	2.6685
-	-	-	-	0.9	-	-	2.8204
-	-	-	-	1.1	2	-	2.9475
-	-	-	-	-	0	-	2.3560
-	-	-	-	-	-2	2	1.7645
-	-	-	-	-	-	0	1.0838
-	-	-	-	-	-	-2	-0.1625

- Enhancement of Prandtl number, volume fraction parameter, unsteadiness parameter and mass concentration parameter depreciates the temperature of the fluid  $\theta$  and temperature of dust granules  $\theta_P$  as well.
- Enhancement of fluid-particle interaction reduces the temperature of fluid  $\theta$  but give rise to the temperature of dust granules  $\theta_P$ .
- Enhancement of the ratio of specific heat capacities increases the heat of fluid  $\theta$  and heat of dust granules  $\theta_P$  as well.
- Enhancement in heat generation reduces the heat of fluid and solid particles and opposite vogue is followed in absorption case.
- Enhancement of volume fraction of dust granules and fluid-particle interaction increases the local Skin friction.
- Enhancement of mass concentration and fluid-particle interaction increases the local Nusselt number.

## Chapter 3

# Numerical investigation of unsteady solid-liquid flow of tangent hyperbolic fluid with variable thermal conductivity and convective boundary

This chapter contains the computational estimations of magnetized particulate flow of tangent hyperbolic fluid due to linearized stretching of porous sheet. Heat flow with added heat generation/absorption and variable thermal conductivity, alongside convective boundary conditions is accounted. According to modeling of particulate flow separate PDE's for fluid and particles (two-phase model) are modeled. With due assistance of boundary layer approximation and appropriate transformations these PDE's are converted into nonlinear ODE's. Approximate results are generated with the help of numerical technique `bvp4c`. Upshots of emerging parameters such as unsteadiness parameter, magnetic parameter, Biot number etc, of ongoing study are elaborated with the support of graphs and numeric values.

### 3.1 Mathematical formulation

Examining the two dimensional incompressible unsteady MHD two phase tangent hyperbolic fluid flowing over infinite stretching sheet, which stretches linearly parallel to x-axis.

The effects of variable thermal conductivity and heat source sink under the convective boundary conditions are accounted in heat transfer equation. Fluid is restricted to positive y-axis. Magnetic force of magnitude  $B_o$  is imposed at right angle to the flow of fluid. The stress tensor for tangent hyperbolic fluid is given in Eq.(1.3). Governing equations for current problem can be writtellows:

$$\frac{\partial u}{\partial x} + \frac{\partial v}{\partial y} = 0, \quad (3.1)$$

$$\frac{\partial u_P}{\partial x} + \frac{\partial u_P}{\partial y} = 0, \quad (3.2)$$

$$\begin{aligned} \frac{\partial u}{\partial t} + u \frac{\partial u}{\partial x} + v \frac{\partial u}{\partial y} &= \nu[(1-n) \frac{\partial^2 u}{\partial y^2} + \sqrt{2n}\Gamma \frac{\partial u}{\partial y} \frac{\partial^2 u}{\partial y^2}] - \frac{\sigma B^2(t)u}{\rho(1-C)} \\ &+ \frac{CS}{\rho(I-C)}(u_p - u), \end{aligned} \quad (3.3)$$

$$C\rho_P \left( \frac{\partial u_P}{\partial t} + u_P \frac{\partial u_P}{\partial t} + v_P \frac{\partial u_P}{\partial y} \right) = CS(u - u_P), \quad (3.4)$$

$$\begin{aligned} \frac{\partial T}{\partial t} + u \frac{\partial T}{\partial x} + v \frac{\partial T}{\partial y} &= \frac{k}{\rho c_P} \frac{\partial}{\partial y} \left[ \alpha'(t) \frac{\partial T}{\partial y} \right] + \frac{\rho_P C}{\rho \tau_t} \frac{(T_P - T)}{(1-C)} + \frac{CS(u - u_P)^2}{(1-C)} \\ &- \frac{Q_o}{\rho c_P(1-C)}, \end{aligned} \quad (3.5)$$

$$C \frac{\partial T_P}{\partial t} + u_P \frac{\partial T_P}{\partial x} + v_P \frac{\partial T_P}{\partial y} = C \frac{c_P}{c_m \tau_T} (T - T_P), \quad (3.6)$$

their respective conditions at boundary are

$$u = U_w(x, t), \quad v = V_s(t), \quad -k \frac{\partial T}{\partial y} = h_f(T_w - T), \quad \text{at } y = 0,$$

$$u_P \rightarrow 0, \quad u \rightarrow 0, \quad v_P \rightarrow v, \quad T_P \rightarrow T_\infty \quad T \rightarrow T_\infty, \quad \text{as } y \rightarrow \infty. \quad (3.7)$$

The conjecture builds of the velocity of stretching wall, temperature of the wall, and mass fluid velocity are defined in Eq.(2.8) and:

$$\alpha'(t) = \alpha_\infty(1 + \varepsilon\theta),$$

$\alpha_\infty$  denotes thermal conductivity far away from sheet and  $\varepsilon$  is the small parameter depends upon the nature of material or fluid. Stream functions  $\psi$  and  $\psi_P$  can be defined as in Eq.(2.9) and the set of transformations for the conversion of PDE's to ODE's are same as

Eq.(2.10) Hence Eqs.(3.1) – (3.10) after using Eqs.(2.9) – (2.10) becomes,

$$f'''[(1-n) + nWef''] + ff'' - A[f' + \frac{\eta}{2}f''] - f'^2 - M^2 f' + \frac{CR}{(1-C)}(F'(\eta) - f'(\eta)) = 0, \quad (3.8)$$

$$F''(\eta\frac{A}{2} - F) + AF' + F'^2 + \beta_T(F' - f') = 0 \quad (3.9)$$

$$\theta''(1 + \varepsilon\theta) + \varepsilon\theta'^2 + Pr(f\theta' - 2f'\theta) - Pr\frac{A}{2}(\eta\theta' + 3\theta) + \frac{Pr\alpha\beta_TC}{(1-C)}(\theta_P - \theta) - \frac{CEc^*}{(1-C)}(f' - F')^2 - \frac{A^*f' - B^*\theta}{(1-C)} = 0, \quad (3.10)$$

$$\theta'_P(\eta\frac{A}{2} - F) - \gamma\beta_T(\theta - \theta_P) + \theta_P(\frac{3}{2}A + 2f') = 0, \quad (3.11)$$

along with the conditions at boundary,

$$f(0) = s, f'(0) = 1, \theta'(0) = -\zeta[1 - \theta(0)], \\ f' \rightarrow 0, F' \rightarrow 0, F = f, \theta \rightarrow 0, \theta_P \rightarrow 0 \text{ as } \eta \rightarrow \infty. \quad (3.12)$$

$\zeta$  and  $Ec^*$  are Biot number and viscous dissipation parameter are defined below

$$\zeta = \frac{h_f}{k} \sqrt{\frac{\nu(1-ct)}{a}}, \quad Ec^* = \frac{S\nu^2(1-ct)^2}{T_0k}. \quad (3.13)$$

Intrinsic relations for skin friction and Nusselt number are given in Eq (3.17),

$$C_f = \frac{\tau_w}{\frac{1}{2}\rho U_w^2}, \quad Nu_x = \frac{xq_w}{k(T_w - T_\infty)}, \quad (3.14)$$

here

$$\tau_w = \mu_o[(1-n)\frac{\partial u}{\partial y} + n\frac{\Gamma}{\sqrt{2}}(\frac{\partial u}{\partial y})^2], \quad q_w = -k(\frac{\partial T}{\partial y}), \quad (3.15)$$

settle the Eq (3.21) into Eq (3.20),to get following relations,

$$\frac{C_f Re_x^{\frac{1}{2}}}{2} = (1-n)f''(0) + \frac{n}{2}Wef''^2(0), \quad Nu_x Re_x^{-\frac{1}{2}} = -\theta'(0). \quad (3.16)$$

## 3.2 Numerical procedure of solution

The modeled problem shows the nonlinear nature of differential equations and it seems to be difficult to find the closed form or exact solution for the presumed problem. So the better option to find the approximated solution by using numerical method. Ongoing

problem is solved by `bvp4c` by using MATLAB software. Rearrangement of  $Eqs$  (3.14) – (3.17) according to required form can be written as

$$f''' = \frac{1}{(1-n) + nWe_f f''} [f'^2 + A(f' + \frac{\eta}{2}) - ff'' + \frac{M^2 f'}{1-C} - \frac{CR}{1-C}(F' - f')], \quad (3.17)$$

$$F'' = \frac{-AF' - F'^2 - \beta_T(F' - f')}{\frac{A\eta}{2} - F}, \quad (3.18)$$

$$\theta'' = \frac{1}{1 + \varepsilon\theta} [Pr \frac{A}{2}(\eta\theta' + 3\theta) - Pr(f\theta' - 2f'\theta) - \frac{Pr\alpha\beta_T C}{1-C}(\theta_P - \theta) - \varepsilon\theta'^2 + \frac{CEc^*}{(1-C)}(f' - F')^2 + \frac{A^*f' + B^*}{(1-C)}\theta], \quad (3.19)$$

$$\theta'_P = \frac{\gamma\beta_T(\theta - \theta_P) - \theta_P(\frac{3A}{2} + 2F')}{\frac{A\eta}{2} - F}. \quad (3.20)$$

There is demand of dummy variables,

$$f = y_1, f' = y_2, f'' = y_3, f''' = y'_3, \\ F = y_4, F' = y_5, F'' = y'_5, \quad (3.21)$$

$$\theta = y_6, \theta' = y_7, \theta'' = y'_7, \\ \theta_P = y_8, \theta'_P = y'_8. \quad (3.22)$$

The system of  $Eqs$ (3.23) – (3.26) can be converted in the initial value problem as:

$$\frac{dy_1}{dx} = y_2, \quad (3.23)$$

$$\frac{dy_2}{dx} = y_3, \quad (3.24)$$

$$\frac{dy_3}{dx} = \frac{1}{1 + We y_3} [y_2^2 - y_1 y_3 + A(y_2 + \frac{\eta}{2} y_3) + \frac{M^2}{1-C} y_2 - \frac{CR}{(1-C)}(y_5 - y_2)], \quad (3.25)$$

$$\frac{dy_4}{dx} = y_5, \quad (3.26)$$

$$\frac{dy_5}{dx} = \frac{-Ay_5 - y_5^2 - \beta_T(y_5 - y_2)}{\frac{A\eta}{2} - y_4}, \quad (3.27)$$

$$\frac{dy_6}{dx} = y_7, \quad (3.28)$$

$$\frac{dy_7}{dx} = \frac{1}{1 + \varepsilon y_6} [-pr(y_1 y_7 - 2y_2 y_6) + Pr \frac{A}{2}(\eta y_7 + 3y_6) - \frac{Pr\alpha\beta_T C}{1-C}(y_8 - y_6) - \varepsilon y_7^2 + \frac{CEc^*}{(1-C)}(y_2 - y_5)^2 + \frac{A^* y_2 + B^* y_6}{(1-C)}], \quad (3.29)$$

$$\frac{dy_8}{dx} = \frac{\gamma\beta_T(y_6 - y_8) - y_8(\frac{3A}{2} + 2y_5)}{\frac{A\eta}{2} - y_4}, \quad (3.30)$$

the reduced endpoint conditions are

$$\begin{aligned} y_1(a) = s, \quad y_2(a) = 1, \quad y_2(b) = s_1, \quad y_4(b) = y_1(b), \quad y_5(b) = s_2, \\ y_6(b) = s_3, \quad y_7(a) = -\zeta(1 - y_6(a)), \quad y_8(b) = s_4. \end{aligned} \quad (3.31)$$

where  $s_1, s_2, s_3$  and  $s_4$  are initially guessed values in a way like integration of the system of first order ODEs fulfil the endpoint conditions and obtained the desired solution for the system of ordinary differential equations (3.29)-(3.36). The choice of maximum value is  $\eta = 7$  with step size = 0.01 with simulation error as  $10^5$  and  $s = 0.3$  is fixed for the whole of the results in the current discussion.

### 3.3 Outcomes and discussions

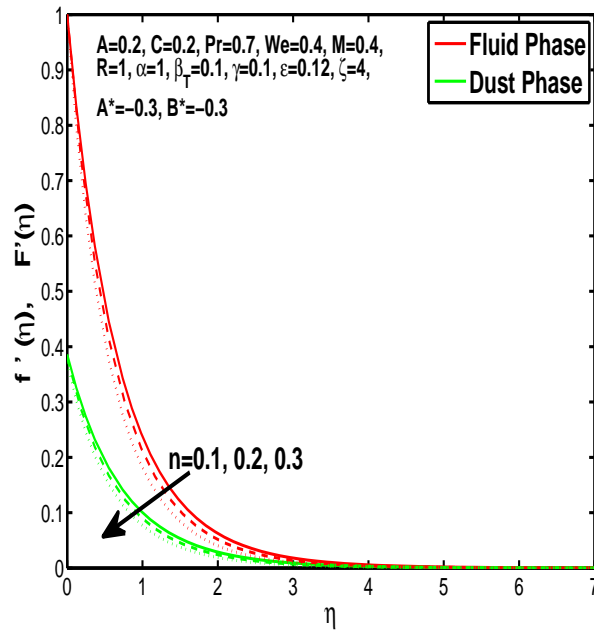


Figure 3.1: Outcome of  $n$  on velocity profile of fluid and dust particles.

Boundary layers of velocity and temperature obtained for fluid and granules through numerical technique that is bvp4c while using MATLAB software. *Fig. 3.1.* is plotted to observe the behavior of power law index  $n$  which is also known as flow consistency index. It is clearly shown that increase in flow index causes decrease in momentum boundary layer of both fluid and granules. *Fig. 3.2.* is sketched to notice the change in boundary layers



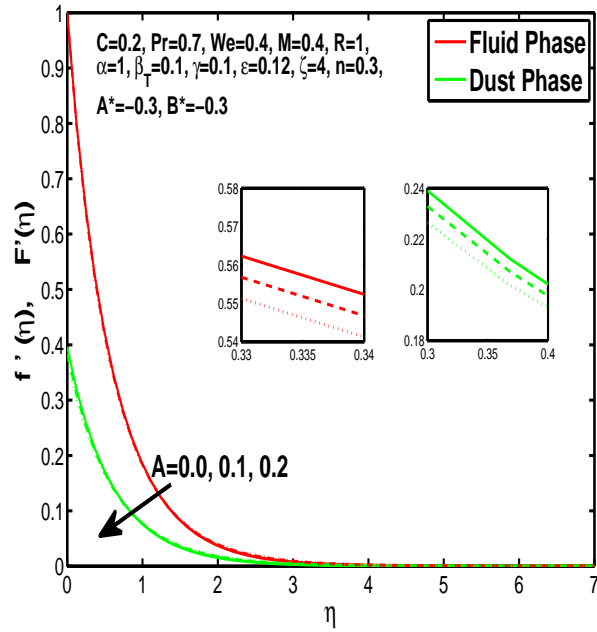


Figure 3.2: Outcome of  $A$  on velocity profile of fluid and dust particles.

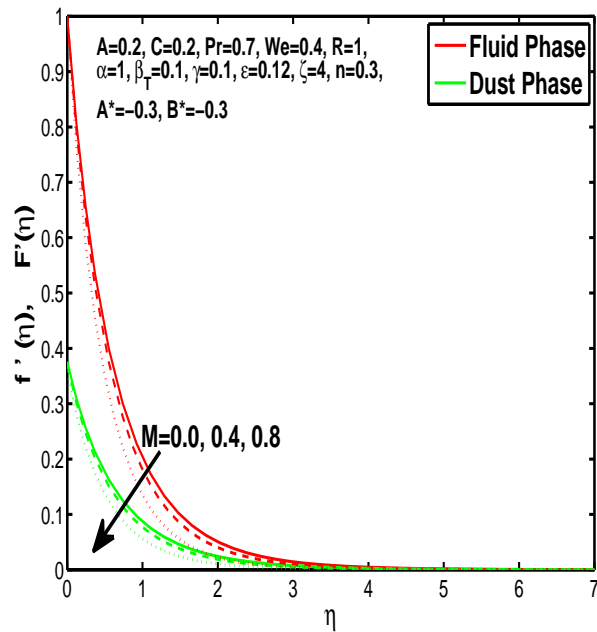


Figure 3.3: Outcome of  $M$  on velocity profile of fluid and dust particles.

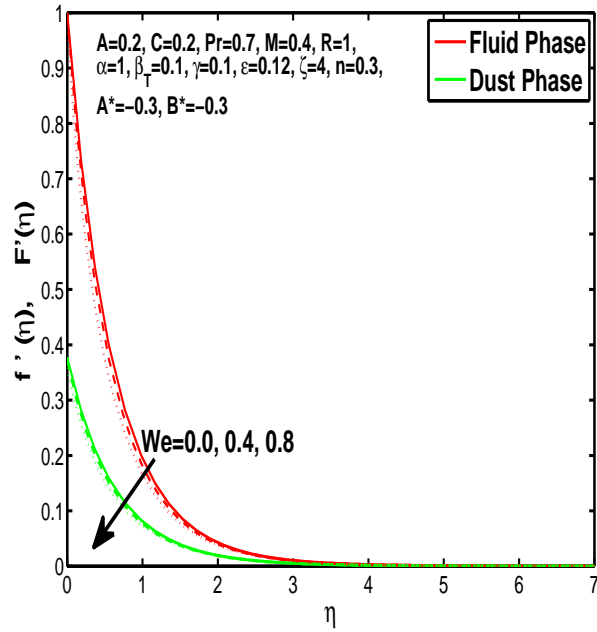


Figure 3.4: Outcome of  $We$  on velocity profile of fluid and dust particles.

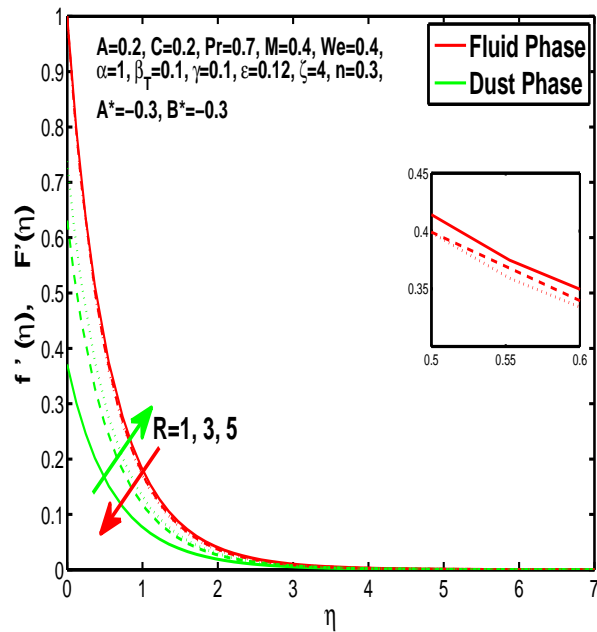


Figure 3.5: Outcome of  $R$  on velocity of fluid and dust.

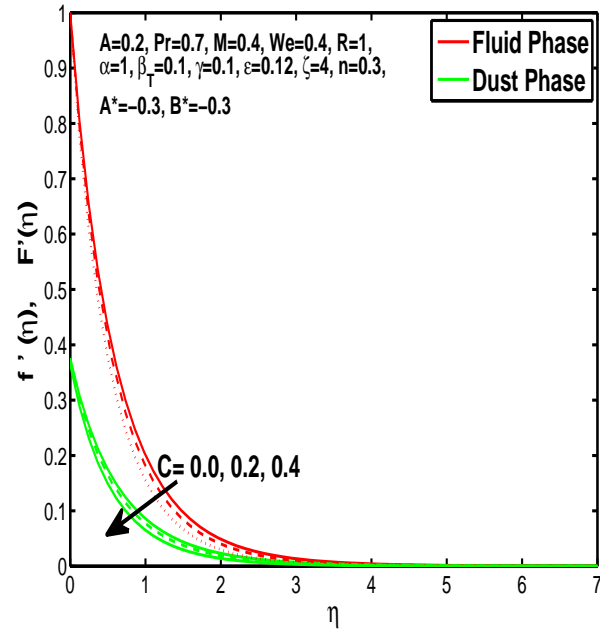


Figure 3.6: Outcome of  $C$  on velocity profile of fluid and dust particles.

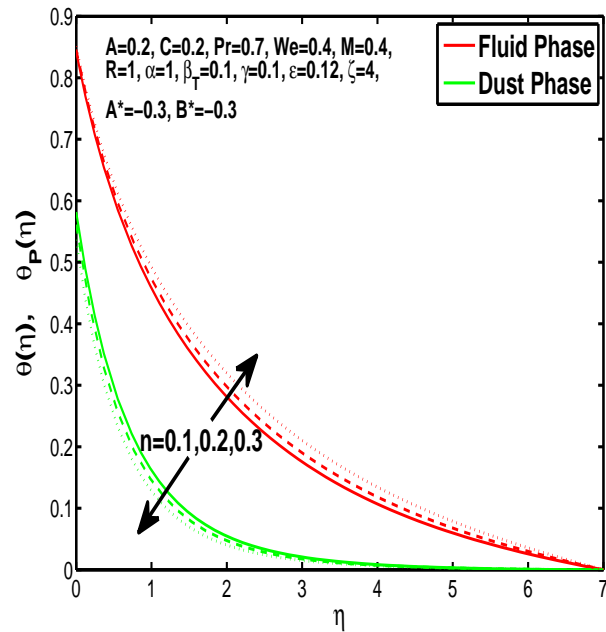


Figure 3.7: Outcome of  $n$  on temperature profile of fluid and dust particles.

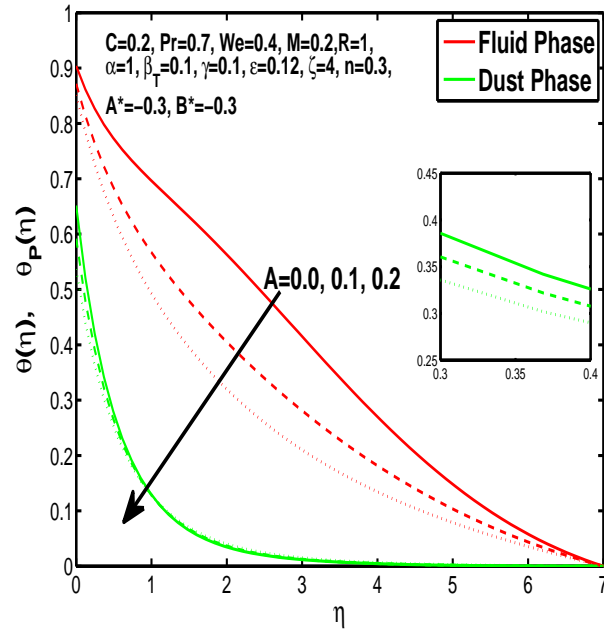


Figure 3.8: Outcome of  $A$  on temperature profile of fluid and dust particles.

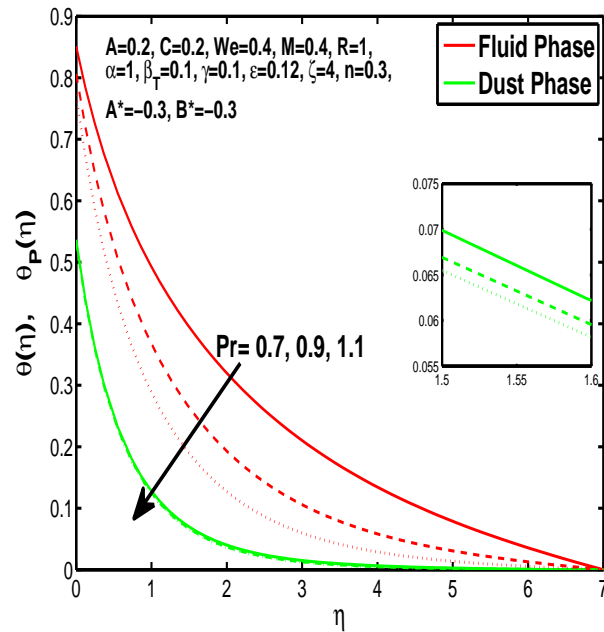


Figure 3.9: Outcome of  $Pr$  on temperature profile of fluid and dust particles.

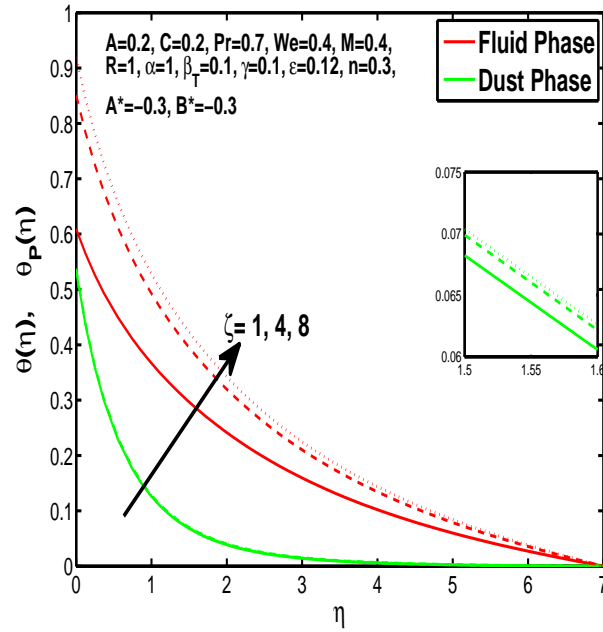


Figure 3.10: Outcome of  $\zeta$  on temperature profile of fluid and dust particles.

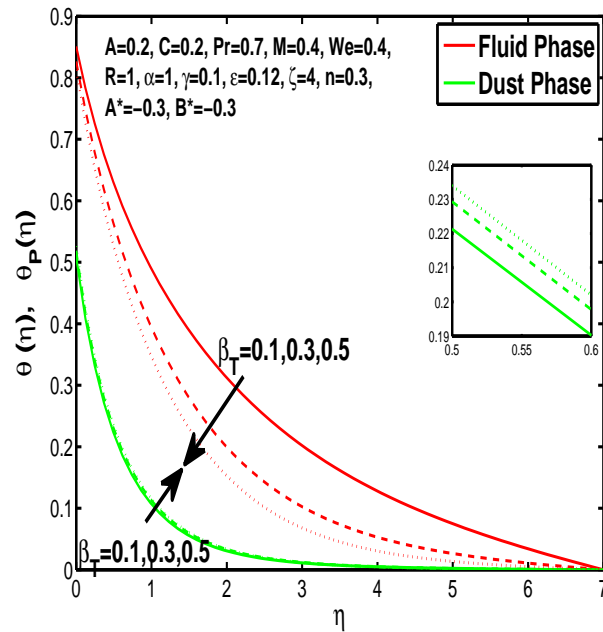


Figure 3.11: Outcome of  $\beta_T$  on temperature of fluid and dust particles.

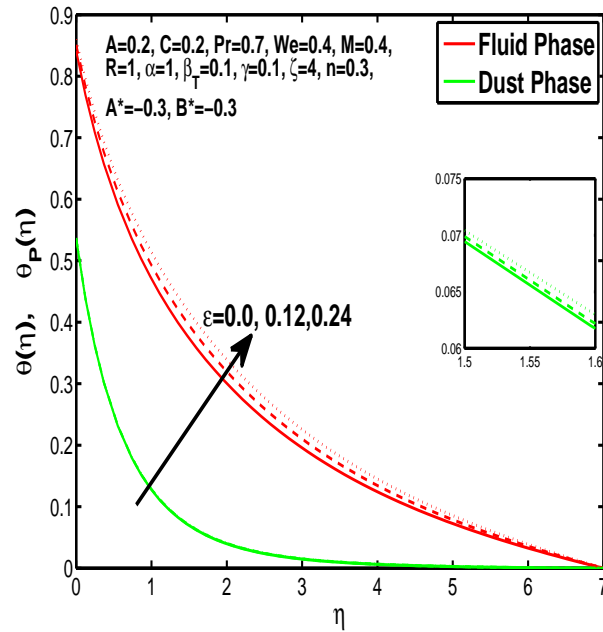


Figure 3.12: Outcome of  $\varepsilon$  on temperature profile of fluid and dust particles.

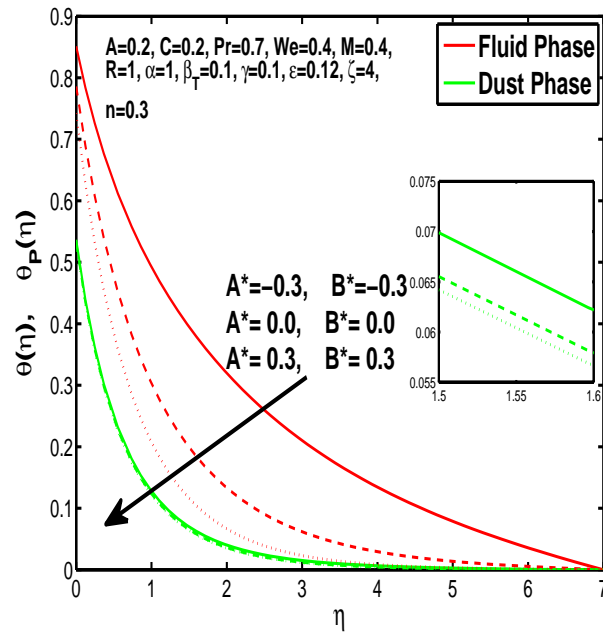


Figure 3.13: Outcome of  $A^*$  and  $B^*$  on temperature profile of fluid and dust particles.

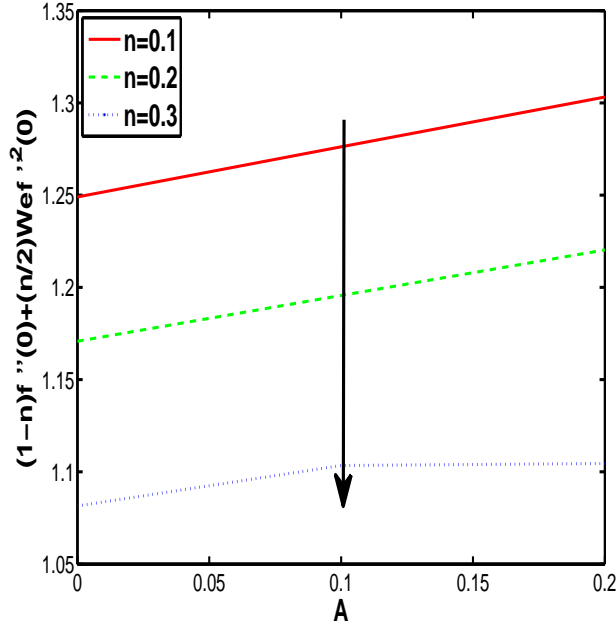


Figure 3.14: Variations of skin friction according to change in unsteadiness parameter  $A$  and power law index  $n$ .

due to change in unsteadiness parameter  $A$ . Graph shows the increment of unsteadiness parameter reduces the velocity of fluid and particles. *Fig. 3.3.* delineate the effects of well known parameter that is magnetic field parameter  $M$ . It is obvious that due to magnetic field parameter there is origination of resistive Lorentz force which diminishes the thickness of momentum boundary layer of fluid and granules as well. *Fig. 3.4.* is for describing the Weissenberg effect which is tangible for non-Newtonian fluids. Weissenberg number  $We$  is dependent upon time constant, boost of weissenberg causes falloff of retardation time will depress the velocity of fluid and particles. *Fig. 3.5.* assimilate the out-turn of fluid-particle interaction  $R$ . As in current problem two-phase that is fluid and dust phase has been considered, so in combined flow there is interaction between fluid particles and dust particles. This interaction sequel the velocity of fluid and dust particles in such a way that more the interaction more the flow of particles but at the same time enhances the resistance due to which velocity of fluid reduces. *Fig. 3.6.* depict the upshot of volume fraction parameter and results are obvious that accretion of concentration will shrink the momentum boundary layer due to resistance to flow. *Fig. 3.7.* illustrate the power law index behavior on temperature boundary layer. An interesting denouement rise that flow

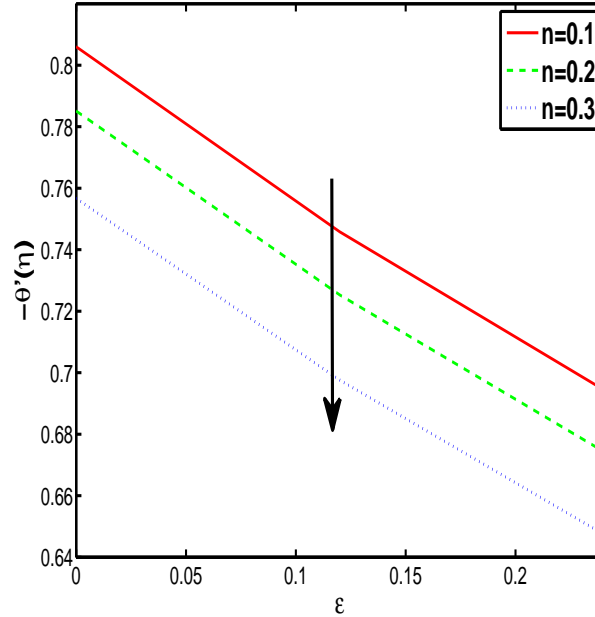


Figure 3.15: Variation of Nusselt number according to change in  $n$  and  $\varepsilon$ .

index enhances the heat flow of fluid but lessens the temperature of dust phase. *Fig. 3.8.* displays the same graphical decline of heat due to increase in unsteadiness parameter as for velocity. *Fig. 3.9.* portrays the discernible results for dimensionless Prandtl number. As the rise in Prandtl number dwindles the thermal conductivity of fluid which leads to a decline of the thermal boundary layer of fluid and particles as well. *Fig. 3.10.* exhibits the graphical change due to change in mass Biot number. Biot number has a direct relation with convection and an inverse relation with conduction. So it is clear from this association that conduction will be reduced with the enhancement of Biot number which leads to a decline in the temperature boundary layer of fluid and solid particles as well. *Fig. 3.11.* specifically describes the fluid-particle interaction for the temperature boundary layer. Results are the same as for the momentum boundary layer; that is, the increment of fluid-particle interaction depreciates the fluid temperature and side-by-side resistance due to interaction increases the temperature of solid particles. *Fig. 3.12.* evidently sketches that enhancement of thermal conduction gives rise to the temperature of fluid and particles. *Fig. 3.13.* graphically depicts that heat generation by the system of fluid and solid particle reduces the temperature of the system, contrarily, heat absorption by the system from surroundings increases the temperature of both of the fluid and particles. *Fig. 3.14.* exhibits the combined effect



Table 3.1: Analogy of coefficient of Skin friction with already published results by keeping  $s = 2$ ,  $M = 3$ ,  $n = 0$ ,  $A = 0$  and  $R = 0$ .

$\eta$	$f_n$	$f_m$	$f'_n$	$f'_m$	$f''_n$	$f''_m$
0.000000	2.000000	2.000000	1.000000	1.000000	-3.236068	-3.236068
0.408163	2.226537	2.226535	0.266910	0.266916	-0.863739	-0.863758
0.816327	2.287002	2.287002	0.071241	0.071242	-0.230540	-0.230546
1.224490	2.303141	2.303141	0.019015	0.019015	-0.061534	-0.061535
1.632653	2.307449	2.307449	0.005075	0.005075	-0.016424	-0.016424
2.040816	2.308598	2.308598	0.001355	0.001355	-0.004384	-0.004384
2.448980	2.308905	2.308905	0.000362	0.000362	-0.001170	-0.001170
2.857143	2.308987	2.308987	0.000096	0.000096	-0.000312	-0.000312
3.265306	2.309009	2.309009	0.000026	0.000026	-0.000083	-0.000083
3.673469	2.309015	2.309015	0.000007	0.000007	-0.000022	-0.000022
4.081633	2.309016	2.309016	0.000002	0.000002	-0.000006	-0.000006
4.489796	2.309017	2.309017	0.000000	0.000000	-0.000002	-0.000002
4.897959	2.309017	2.309017	0.000000	0.000000	-0.000001	-0.000001
5.000000	2.309017	2.309017	0.000000	0.000000	0.000000	0.000000

of unsteadiness parameter and flow index on local skin friction. Increment of flow index reduces the skin friction. Certification of the ongoing study and results could be check out in *Table. 3.1.* by the comparison of results with the published article by the Vajravelu and Nayfeh [75] in which they have solved the problem by numerical technique that is Finite Difference and also gives the comparison with exact solution of already published data, where  $f_n$ ,  $f'_n$  and  $f''_n$  are the values obtained previously by finite difference method but  $f_m$ ,  $f'_m$  and  $f''_m$  are the values calculated presently by bvp4c method. *Table. 3.2.* and *Table. 3.3.* depicts the fluctuation of local skin friction and Nusselt number for different values of various parameter. Results show that skin friction increases with the increase of unsteadiness, fluid particle interaction, volume fraction of dust particles, mass concentration and magnetic field but decreases due to Weissenberg effect and power law index. And Nusselt number increases with the increase in unsteadiness, fluid-particle interaction, mass concentration, specific heat ratio, Prandtl number Biot number and heat source but reduces due to heat sink and variable thermal conductivity parameter.

Table 3.2: Numeric findings for Skin friction.

A	R	C	$\alpha$	M	We	n	$(1-n)f''(0) + \frac{n}{2}We f''^2(0)$
0.0	-	-	-	-	-	-	1.1552
0.1	-	-	-	-	-	-	1.1844
0.2	1	-	-	-	-	-	1.2134
-	2	-	-	-	-	-	1.2254
-	3	0.1	-	-	-	-	1.2321
-	-	0.2	-	-	-	-	1.2909
-	-	0.3	1	-	-	-	1.3636
-	-	-	2	-	-	-	1.5206
-	-	-	3	0.2	-	-	1.6659
-	-	-	-	0.4	-	-	1.6921
-	-	-	-	0.8	0.2	-	1.9097
-	-	-	-	-	0.4	-	1.8955
-	-	-	-	-	0.8	0.1	1.8652
-	-	-	-	-	-	0.2	1.6741

### 3.4 Concluding remarks

The two dimensional unsteady dusty flow of tangent hyperbolic fluid is studied in this chapter. The effects of magnetic field and variable thermal conductivity with convection are discussed for fluid and dust particles as well. Evolved conclusions of the current problem are given below. Most of the parameter cause retardation to flows, let have a overlook,

- Boost of magnetic field, Power-law index, concentration of particles, Weissenberg effect, unsteadiness parameter diminishes the momentum boundary layer of fluid and dust particles.
- Boost of interaction between fluid and particles drops the flow rate of fluid but at the same time enhance the velocity and temperature of dust particles.
- Boost of Power-law index expand the heat flow of fluid but at the same time drops the temperature of dust particles.
- Boost of variable thermal conductivity and Biot number expand the temperature boundary layer but boost of unsteadiness parameter and the Prandtl number lessen the heat of fluid and dust particles as well.

Table 3.3: Numeric findings for Nusselt number.

A	$\beta_T$	$\alpha$	$\gamma$	Pr	$A^*$	$B^*$	$\epsilon$	$\zeta$	$-\theta'(\eta)$
0.0	-	-	-	-	-	-	-	-	0.3289
0.1	-	-	-	-	-	-	-	-	0.3733
0.2	0.1	-	-	-	-	-	-	-	0.4046
-	0.2	-	-	-	-	-	-	-	0.4172
-	0.3	1	-	-	-	-	-	-	0.4254
-	-	2	-	-	-	-	-	-	0.4427
-	-	3	0.1	-	-	-	-	-	0.4552
-	-	-	0.2	-	-	-	-	-	0.4538
-	-	-	0.3	0.7	-	-	-	-	0.4523
-	-	-	-	0.9	-	-	-	-	0.4980
-	-	-	-	1.1	-0.3	-	-	-	0.5308
-	-	-	-	-	0	-	-	-	0.5674
-	-	-	-	-	0.3	-0.3	-	-	0.6041
-	-	-	-	-	-	0	-	-	0.6188
-	-	-	-	-	-	0.3	0.12	-	0.6315
-	-	-	-	-	-	-	0.24	-	0.6153
-	-	-	-	-	-	-	0.36	1	0.6191
-	-	-	-	-	-	-	-	4	1.1630
-	-	-	-	-	-	-	-	8	1.3480
-	-	-	-	-	-	-	-	12	1.4213

- Heat generation by the system reduces the temperature and heat absorption by the system from surroundings increase the temperature of fluid and dust particles as well.
- Boost of unsteadiness parameter and Power-law index collectively lessen the local skin-friction.
- Boost of thermal conductivity and Power-law index collectively reduces the Nusselt number.

## Chapter 4

# Numerical analysis of unsteady flow of three dimensional Williamson fluid-particle suspension with MHD and non-linear thermal radiations

In this chapter time dependent 3D flow of a non-Newtonian Williamson fluid has been considered. Flow is generated by the stretching of a sheet with constant velocity and effected by MHD, dust particles and non-linear thermal radiations. Problem controlling PDEs are converted into ODEs by using appropriate transformations. Finalized equations are solved by 'bvp4c method'. The numerical results are compared with already published data. Non-dimensionalised parameters such as first and second ordered radiation parameter, the fluid particle interaction, the unsteadiness parameter, the stretching parameter, and others are discussed that for these affect the velocity and temperature distribution. Physical quantities Nusselt number and Skin friction are also analyzed numerically as well as graphically.

### 4.1 Mathematical formulation

In this study the time dependent incompressible 3D solid-liquid Williamson non-Newtonian fluid for momentum and heat flow are evaluated. The effects of MHD and nonlinear thermal radiations are also considered. Flow distribution is due to stretching sheet which

is assumed to be placed in xy-plane and fluid is placed along the z-axis. Solid particles emersed in the fluid are small enough but have density, velocity and other physical properties. The tensor for Williamson fluid is mentioned in section 1.5.1. Modeling for assumed problem using laws of conservation of mass, momentum and energy are,

$$\frac{\partial u}{\partial x} + \frac{\partial v}{\partial y} + \frac{\partial w}{\partial z} = 0, \quad (4.1)$$

$$\frac{\partial u_P}{\partial x} + \frac{\partial v_P}{\partial y} + \frac{\partial w_p}{\partial z} = 0, \quad (4.2)$$

$$\begin{aligned} \rho(1-C)\left[\frac{\partial u}{\partial t} + u\frac{\partial u}{\partial x} + v\frac{\partial u}{\partial y} + w\frac{\partial u}{\partial z}\right] &= \mu(1-C)\frac{\partial}{\partial z}\left[(1 + \sqrt{2}\Gamma\sqrt{\left(\frac{\partial u}{\partial z}\right)^2 + \left(\frac{\partial v}{\partial z}\right)^2}\right)\frac{\partial u}{\partial z} \\ &- \sigma B^2(t)u + CS(u_p - u), \end{aligned} \quad (4.3)$$

$$C\rho_P\left(\frac{\partial u_P}{\partial t} + u_P\frac{\partial u_P}{\partial x} + v_P\frac{\partial u_P}{\partial y} + w_p\frac{\partial u_p}{\partial z}\right) = CS(u - u_P), \quad (4.4)$$

$$\begin{aligned} \rho(1-C)\left[\frac{\partial v}{\partial t} + u\frac{\partial v}{\partial x} + v\frac{\partial v}{\partial y} + w\frac{\partial v}{\partial z}\right] &= \mu(1-C)\frac{\partial}{\partial z}\left[(1 + \sqrt{2}\Gamma\sqrt{\left(\frac{\partial u}{\partial z}\right)^2 + \left(\frac{\partial v}{\partial z}\right)^2}\right)\frac{\partial v}{\partial z} \\ &- \sigma B^2(t)v + CS(v_p - v), \end{aligned} \quad (4.5)$$

$$C\rho_P\left(\frac{\partial v_P}{\partial t} + u_P\frac{\partial v_P}{\partial x} + v_P\frac{\partial v_P}{\partial y} + w_p\frac{\partial v_p}{\partial z}\right) = CS(v - v_P), \quad (4.6)$$

$$\begin{aligned} \rho c_p(1-C)\left[\frac{\partial T}{\partial t} + u\frac{\partial T}{\partial x} + v\frac{\partial T}{\partial y} + w\frac{\partial T}{\partial z}\right] &= k(1-C)\frac{\partial^2 T}{\partial z^2} + \frac{\rho_p c_p C}{\tau_t}(T_P - T) \\ &+ CS[(u - u_P)^2 + (v - v_P)^2] - \frac{\partial q_r}{\partial z} \end{aligned} \quad (4.7)$$

$$C\left(\frac{\partial T_P}{\partial t} + u_P\frac{\partial T_P}{\partial x} + v_P\frac{\partial T_P}{\partial y} + w_p\frac{\partial T_p}{\partial z}\right) = C\frac{c_P}{c_m \tau_T}(T - T_P), \quad (4.8)$$

conditions at boundary are:

$$u = U_w(x, t), \quad v = V_w(y, t), \quad w = 0, \quad T = T_w(x, t), \quad \text{at } z = 0,$$

$$u_P = u = 0, \quad v_P = v = 0, \quad w_p = w, \quad T \rightarrow T_\infty, \quad T_P \rightarrow T_\infty \quad \text{as } z \rightarrow \infty. \quad (4.9)$$

In above equation array the  $u(t, x, y, z)$ ,  $v(t, x, y, z)$  and  $w(t, x, y, z)$  are the components of fluid velocity in abscissa, ordinate and applicate axis direction. Similarly  $u_P(x, y, t)$ ,  $v_P(t, x, y, z)$  and  $w_p(t, x, y, z)$  are components of particles velocity in above mentioned three dimensions.  $q_r$  is radiative heat flux, defined below by Rosseland approximation.

$$q_r = -\frac{4\sigma^*}{3k_1}\frac{\partial T^4}{\partial z}, \quad (4.10)$$

where  $\sigma^*$  is a constant called Stefan-Boltzmann and  $k_1$  is average absorption coefficient. While considering that model, optically thick radiations are considered. Relation for  $T^4$

given in Eq.(1.20) As we know its difficult to solve the PDE's, so there is requirement of similarity transformations for the turning of PDE into ODE as follows,

$$\begin{aligned}
u &= \frac{ax}{1-ct}f'(\eta), \quad v = \frac{ay}{1-ct}g'(\eta), \quad w = -\sqrt{\frac{\nu a}{1-ct}}(f(\eta) + g(\eta)), \\
u_P &= \frac{ax}{1-ct}F'(\eta), \quad v_P = \frac{ay}{1-ct}G'(\eta), \quad w_P = -\sqrt{\frac{\nu a}{1-ct}}(F(\eta) + G(\eta)), \\
\theta &= \frac{T - T_\infty}{T_w - T_\infty}, \quad \theta_P = \frac{T_P - T_\infty}{T_w - T_\infty},
\end{aligned} \tag{4.11}$$

and to be noted that,

$$\begin{aligned}
U_w(x, t) &= \frac{ax}{1-ct}, \quad V_w(y, t) = \frac{by}{1-ct}, \quad \eta = z\sqrt{\frac{U_w}{\nu x}}, \\
T_w(x, t) &= T_\infty + \frac{T_o U_w x}{\nu(1-ct)^{\frac{1}{2}}}, \quad B(t) = \frac{B_o}{(1-ct)^{\frac{1}{2}}}.
\end{aligned} \tag{4.12}$$

Utilize Eqs.(4.10) – (4.12) into Eqs.(4.1) – (4.9) and get the following equalizations,

$$\begin{aligned}
f'''[1 + We_x(\sqrt{f'^2 + g'^2} + \frac{f''^2}{\sqrt{f'^2 + g'^2}})] + We_x \frac{f''g''g'''}{\sqrt{f'^2 + g'^2}} + (f + g)f'' \\
-f'^2 - A[f' + \frac{\eta}{2}f''] - \frac{M^2}{(1-C)}f' + \frac{CR}{(1-C)}(F'(\eta) - f'(\eta)) = 0,
\end{aligned} \tag{4.13}$$

$$\frac{A}{2}\eta F'' + AF' + F'^2 - (F + G)F'' + R(F' - f') = 0 \tag{4.14}$$

$$\begin{aligned}
g'''[1 + We_y(\sqrt{f'^2 + g'^2} + \frac{g''^2}{\sqrt{f'^2 + g'^2}})] + We_y \frac{g''f''f'''}{\sqrt{f'^2 + g'^2}} + (f + g)g'' \\
-g'^2 - A[g' + \frac{\eta}{2}g''] - \frac{M^2}{(1-C)}g' + \frac{CR}{(1-C)}(G'(\eta) - g'(\eta)) = 0,
\end{aligned} \tag{4.15}$$

$$\frac{A}{2}\eta G'' + G'^2 + R(G' - g') + AG' - (F + G)G'' = 0 \tag{4.16}$$

$$\begin{aligned}
\theta''(1 - 5R_d + R_1^*\theta) + R_1^*\theta'^2 + Pr(f\theta' - 2f'\theta) - Pr\frac{A}{2}(\eta\theta' + 3\theta) \\
+ Pr\theta'(f + g) + \frac{Pr\alpha\beta_T C}{(1-C)}(\theta_P - \theta) + \frac{CEc^*}{(1-C)}(f' - F')^2 + \frac{CEc^*}{(1-C)}(g' - G')^2 = 0,
\end{aligned} \tag{4.17}$$

$$\theta'_P(\eta\frac{A}{2} - 2F - G) - \gamma\beta_T(\theta - \theta_P) + \theta_P(\frac{3}{2}A + 2f') = 0, \tag{4.18}$$

along with the boundary conditions

$$\begin{aligned}
f(0) = 0, \quad f'(0) = 1, \quad g(0) = 0, \quad g'(0) = \lambda, \quad \theta(0) = 1, \\
f' \rightarrow 0, \quad F' \rightarrow 0, \quad F = f, \quad g' \rightarrow 0, \quad G' \rightarrow 0, \quad G = g, \\
\theta \rightarrow 0, \quad \theta_P \rightarrow 0 \quad as \quad \eta \rightarrow \infty.
\end{aligned} \tag{4.19}$$

As the multiple dependence shifted to unique  $\eta$  derivative is extracted with respect to it.  $We_x$  is Weissenberg along x-direction,  $We_y$  is Weissenberg number along y-direction,  $\lambda$  is stretching ratio parameter and  $R_d, R_1^*$  are the nonlinear thermal radiation parameters are defined below

$$We_x = \sqrt{\frac{2a^3\Gamma x^2}{\nu(1-ct)^3}}, \quad We_y = \sqrt{\frac{2a^3\Gamma y^2}{\nu(1-ct)^3}}, \quad \lambda = \frac{b}{a},$$

$$R_d = \frac{16\sigma^*T_\infty^3}{3k_1k}, \quad R_1^* = \frac{3R_d}{(1-ct)} \left[ \frac{T_w}{T_\infty} - 1 \right]. \quad (4.20)$$

Mathematical Expressions of skin friction for three dimensional flow are given in Eq (4.25),

$$C_{fx} = \frac{\tau_{xz}}{\frac{1}{2}\rho U_w^2}, \quad C_{fy} = \frac{\tau_{yz}}{\frac{1}{2}\rho V_w^2}, \quad (4.21)$$

By using boundary layer approximation shear stress rates at wall in x, y directions and coefficients will be reduced to

$$\tau_{xz} = \mu_o \left[ \frac{\partial u}{\partial z} + \left( \frac{\Gamma}{\sqrt{2}} \sqrt{\frac{\partial u^2}{\partial z} + \frac{\partial v^2}{\partial z}} \right) \frac{\partial u}{\partial z} \right]_{z=0},$$

$$\tau_{yz} = \mu_o \left[ \frac{\partial v}{\partial z} + \left( \frac{\Gamma}{\sqrt{2}} \sqrt{\frac{\partial u^2}{\partial z} + \frac{\partial v^2}{\partial z}} \right) \frac{\partial v}{\partial z} \right]_{z=0}, \quad (4.22)$$

by inserting Eq (4.26), into Eq (4.25), one can get,

$$C_{fx} Re_x^{\frac{1}{2}} = f''(0) + \frac{We_x}{2} \sqrt{f''(0)^2 + g''(0)^2} f''(0),$$

$$C_{fy} Re_y^{\frac{1}{2}} = g''(0) + \frac{We_y}{2} \sqrt{f''(0)^2 + g''(0)^2} g''(0). \quad (4.23)$$

Now expression for another physical quantity that is Nusselt number give in Eq (4.28),

$$Nu_x = \frac{xq_w}{k(T_w - T_\infty)}, \quad q_w = -k \left( \frac{\partial T}{\partial z} + q_r \right) \quad (4.24)$$

where  $q_w$  denotes the heat flux of the wall. Settle the value of  $q_w$  into  $Nu$  while considering the thermal radiations effective, one can get following relation for Nusselt number,

$$Nu_x Re_x^{-\frac{1}{2}} = -[1 - R_d k - R_1^* k \theta] \theta'(0). \quad (4.25)$$

Here  $Re_x = \frac{U_w x}{\nu}$  and  $Re_y = \frac{V_w y}{\nu}$  are the Reynolds numbers in x and y-directions respectively. The considered flow is laminar and for that flow Reynolds number will be of low range.

## 4.2 Numerical procedure of solution

Conjecture built of three dimensional flow became more complicated as compare to two dimensional flow and evidently the non-linearity rate of equations is high. So its preferable to get the solution numerically. Here the solution of problem is find out by bvp4c method by using the software MATLAB. For this method, the equations are reduced to first order equations for the purpose firstly we write:

$$f''' = \frac{1}{[1 + We_x(\sqrt{f'^2 + g'^2} + \frac{f''^2}{\sqrt{f'^2 + g'^2}})]} [-We_x \frac{f'' g'' g'''}{\sqrt{f'^2 + g'^2}} + f'^2 + A(f' + \frac{\eta}{2} f'') + \frac{M^2 f'}{1 - C} - \frac{CR}{1 - C} (F' - f') - f''(f + g)], \quad (4.26)$$

$$F'' = \frac{-AF' - F'^2 - R(F' - f')}{\frac{A\eta}{2} - 2F - G}, \quad (4.27)$$

$$g''' = \frac{1}{[1 + We_y(\sqrt{f'^2 + g'^2} + \frac{g''^2}{\sqrt{f'^2 + g'^2}})]} [-We_y \frac{g'' f'' f'''}{\sqrt{f'^2 + g'^2}} + g'^2 + A(g' + \frac{\eta}{2} g'') + \frac{M^2 g'}{1 - C} - \frac{CR}{1 - C} (G' - g') - g''(f + g)], \quad (4.28)$$

$$G'' = \frac{-AG' - sG'^2 - R(G' - g')}{\frac{A\eta}{2} - F - G}, \quad (4.29)$$

$$\theta'' = \frac{1}{1 - 5R_d + R_1^* \theta} [Pr \frac{A}{2} (\eta \theta' + 3\theta) - Pr(f\theta' - 2f'\theta) - \frac{Pr\alpha\beta_T C}{1 - C} (\theta_P - \theta) - Pr\theta'(f + g) - R_1^* \theta'^2 - \frac{CEc^*}{(1 - C)} (f' - F')^2 - \frac{CEc^*}{1 - C} (g' - G')^2], \quad (4.30)$$

$$\theta'_P = \frac{\gamma\beta_T(\theta - \theta_P) - \theta_P(\frac{3A}{2} + 2F')}{\frac{A\eta}{2} - 2F - G}. \quad (4.31)$$

There is requirement of method to assume the dummy variables as shown in Eq(4.32).

$$\begin{aligned} f &= y_1, \quad f' = y_2, \quad f'' = y_3, \quad f''' = y'_3, \quad F = y_4, \quad F' = y_5, \quad F'' = y'_5, \\ g &= y_6, \quad g' = y_7, \quad g'' = y_8, \quad g''' = y'_8, \quad G = y_9, \quad G' = y_{10}, \quad G'' = y'_{10}, \\ \theta &= y_{11}, \quad \theta' = y_{12}, \quad \theta'' = y'_{12}, \quad \theta_P = y_{13}, \quad \theta'_P = y'_{13}. \end{aligned} \quad (4.32)$$

Set of Eqs(4.30) – (4.35) can be molded in the initial value problem as:



$$\frac{dy_1}{dx} = y_2, \quad (4.33)$$

$$\frac{dy_2}{dx} = y_3, \quad (4.34)$$

$$\begin{aligned} \frac{dy_3}{dx} = & \frac{1}{[1 + We_x(\sqrt{y_2^2 + y_7^2} + \frac{y_3^2}{\sqrt{f_2^2 + y_7^2}})]} [-We_x \frac{y_3 y_8 y_8'}{\sqrt{y_2^2 + y_7^2}} + y_2^2 - y_3(y_1 + y_6) \\ & + A(y_2 + \frac{\eta}{2}y_3) + \frac{M^2}{1-C}y_2 - \frac{CR}{(1-C)}(y_5 - y_2)], \end{aligned} \quad (4.35)$$

$$\frac{dy_4}{dx} = y_5, \quad (4.36)$$

$$\frac{dy_5}{dx} = \frac{-Ay_5 - y_5^2 - R(y_5 - y_2)}{\frac{A\eta}{2} - 2y_4} - y_9, \quad (4.37)$$

$$\frac{dy_6}{dx} = y_7, \quad (4.38)$$

$$\frac{dy_7}{dx} = y_8, \quad (4.39)$$

$$\begin{aligned} \frac{dy_8}{dx} = & \frac{1}{[1 + We_y(\sqrt{y_2^2 + y_7^2} + \frac{y_8^2}{\sqrt{y_2^2 + y_7^2}})]} [-We_y \frac{y_8 y_3 y_3'}{\sqrt{y_2^2 + y_7^2}} + y_7^2 - y_8(y_1 + y_6) \\ & + A(y_7 + \frac{\eta}{2}y_8) + \frac{M^2}{1-C}y_7 - \frac{CR}{(1-C)}(y_{10} - y_7)], \end{aligned} \quad (4.40)$$

$$\frac{dy_9}{dx} = y_{10}, \quad (4.41)$$

$$\frac{dy_{10}}{dx} = \frac{-Ay_{10} - sy_{10}^2 - R(y_{10} - y_7)}{\frac{A\eta}{2} - y_4} - y_9, \quad (4.42)$$

$$\frac{dy_{11}}{dx} = y_{12}, \quad (4.43)$$

$$\begin{aligned} \frac{dy_{12}}{dx} = & \frac{1}{1 - 5R_d + R_1^*y_{11}} [-Pr(y_1y_{12} - 2y_2y_{11}) + Pr\frac{A}{2}(\eta y_{12} + 3y_{11}) - R_1^*y_{12}^2 \\ & - \frac{Pr\alpha\beta_T C}{1-C}(y_{13} - y_{11}) - Pr y_{12}(y_1 + y_6) - \frac{CEc^*}{(1-C)}(y_2 - y_5)^2 - \frac{CEc^*}{(1-C)}(y_7 - y_{10})^2], \end{aligned} \quad (4.44)$$

$$\frac{dy_{13}}{dx} = \frac{\gamma\beta_T(y_{11} - y_{13}) - y_{13}(\frac{3A}{2} + 2y_5)}{\frac{A\eta}{2} - 2y_4 - y_9}, \quad (4.45)$$

the reduced endpoint conditions are

$$\begin{aligned} y_1(a) &= 0, \quad y_2(a) = 1, \quad y_2(b) = s_1, \quad y_4(b) = y_1(b), \\ y_5(b) &= s_2, \quad y_6(a) = 0, \quad y_7(a) = \lambda, \quad y_7(b) = s_3, \\ y_9(b) &= y_6(b), \quad y_{10}(b) = s_4, \quad y_{11}(a) = 1, \quad y_{11}(b) = s_5, \\ y_{13}(b) &= s_6. \end{aligned} \quad (4.46)$$

Here we need to find some initial guesses that are  $s_1, s_2, s_3, s_4, s_5$  and  $s_6$  by hit and trial in a way like integration of the system of first order ODEs fulfil the endpoint conditions and obtained the solution for the system of equations (4.37)-(4.49). The choice of highest value is  $\eta = 7$  with step size= 0.01 with simulation error is chosen  $10^{-5}$ .

### 4.3 Outcomes and discussions

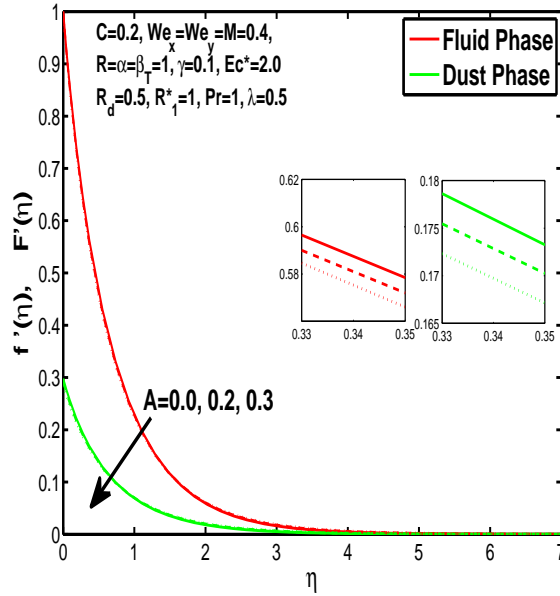


Figure 4.1: Effect of unsteadiness parameter "A" on momentum boundary layer of fluid and particles in x-direction.

Outcomes of the boundary layer flow effected by the different parameters find out by the numerical method, displayed graphically and numerically. *Fig. 4.1* and *Fig. 4.2*. are plotted to check the change in momentum boundary layers due to change in unsteadiness parameter  $A$ . Graphs exhibits that rise in unsteadiness parameter decreases the speed of fluid and granules in both x and y-directions. We can observe in the graph that just about the surface velocity decreases and increases apart from surface. *Fig. 4.3*. and *Fig. 4.4*. delineate the effects of magnetic field parameter  $M$ . As we know that magnetic field parameter causes a resistive Lorentz force and create hindrance in the fluid flow, decreases the momentum boundary layer of fluid and dust particles as well and in both x and y-directions. *Fig. 4.5*. and *Fig. 4.6*. are for describing the Weissenberg effect which

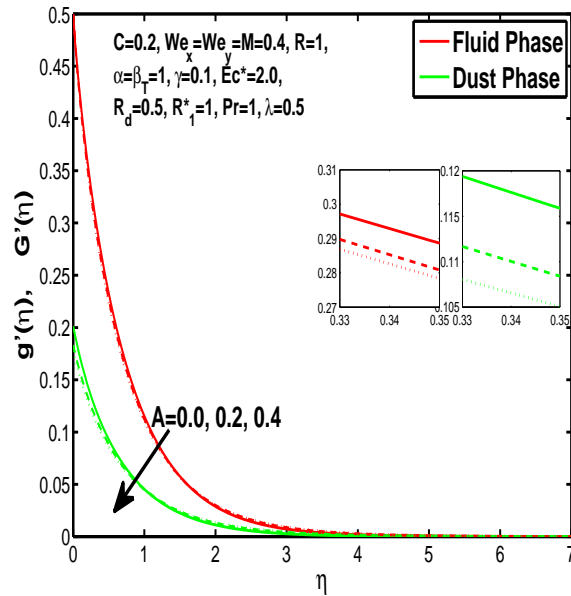


Figure 4.2: Effect of unsteadiness parameter "A" on momentum boundary layer of fluid and particles in y-direction.

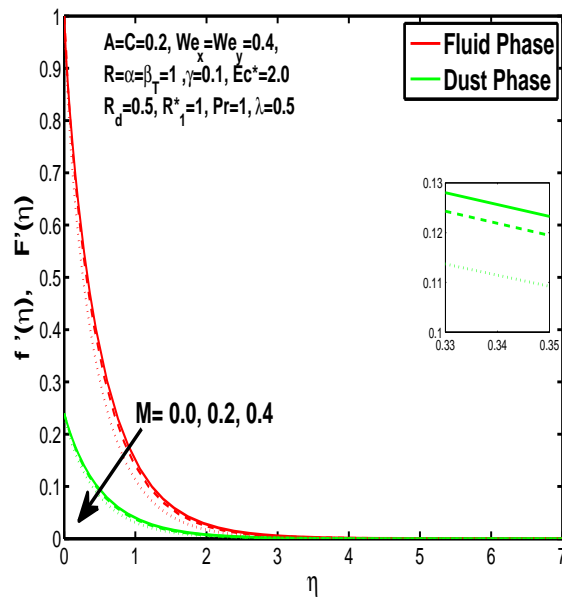


Figure 4.3: Effect of magnetic parameter "M" on the velocity of fluid and particles in x-direction.

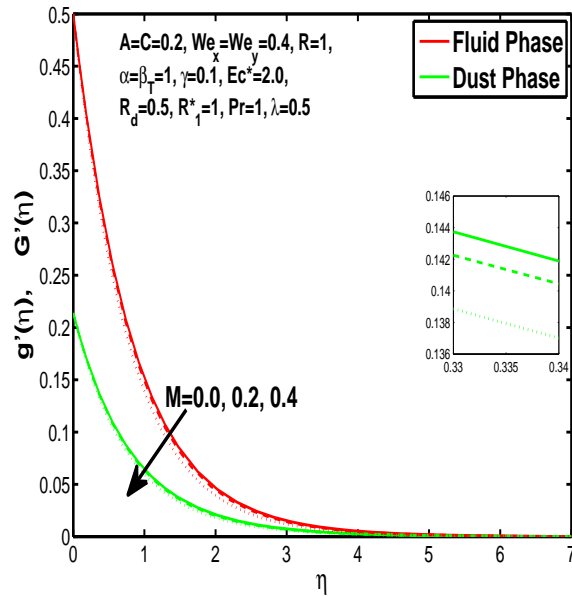


Figure 4.4: Effect of magnetic parameter "M" on momentum boundary layer of fluid and particles in y-direction.

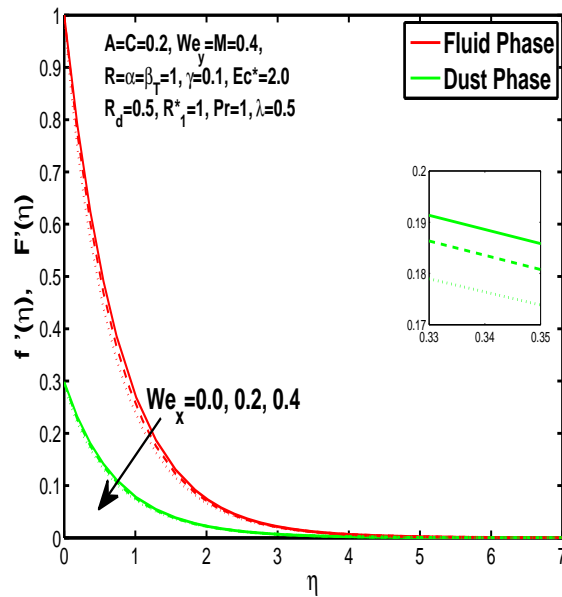


Figure 4.5: Effect of Weissenberg number "We\_x" on momentum boundary layer of fluid and particles in x-direction.

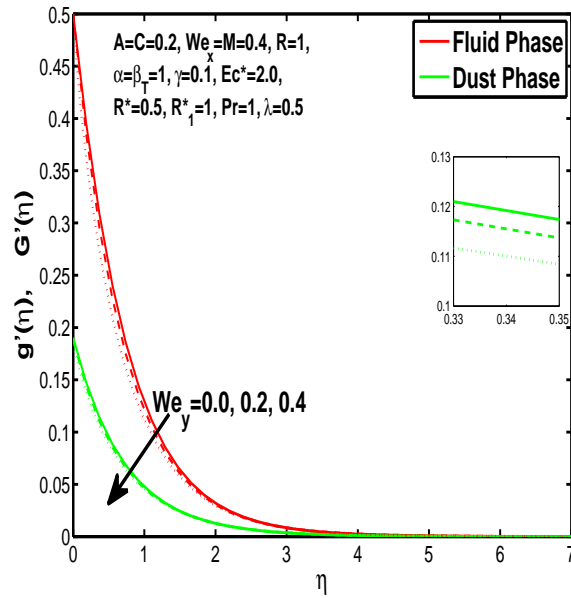


Figure 4.6: Effect of Weissenberg number " $We_y$ " on momentum boundary layer of fluid and particles in  $y$ -direction.

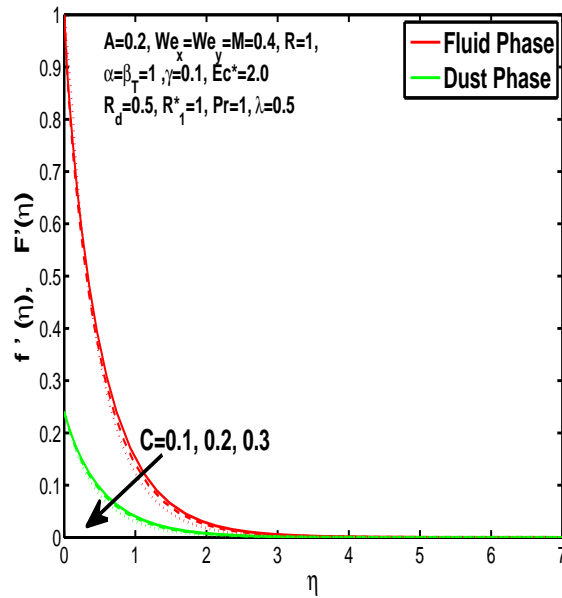


Figure 4.7: Effect of " $C$ " on velocity of fluid and particles in  $x$ -direction.

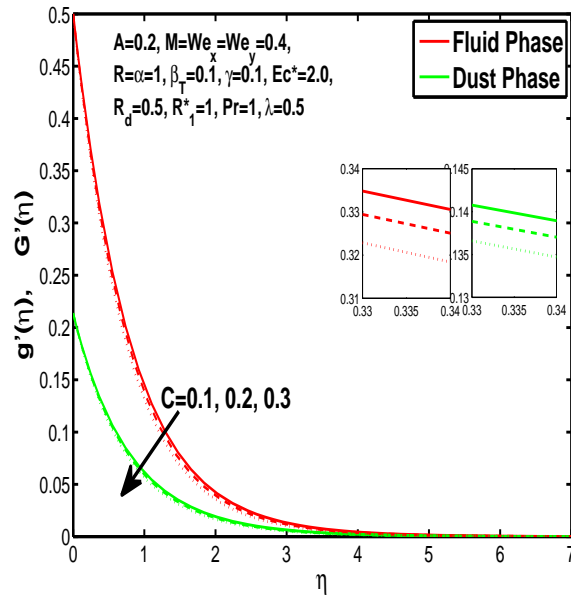


Figure 4.8: Effect of "C'" on velocity of fluid and particles in y-direction.

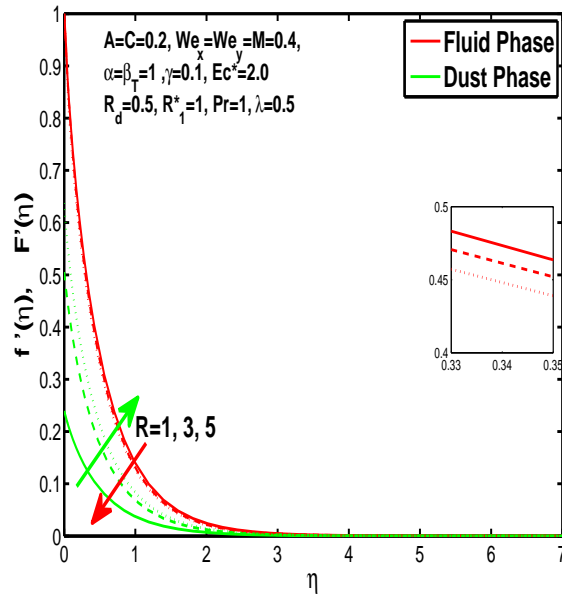


Figure 4.9: Effect of fluid-particle interaction parameter "R" on momentum boundary layer of fluid and particles in x-direction.

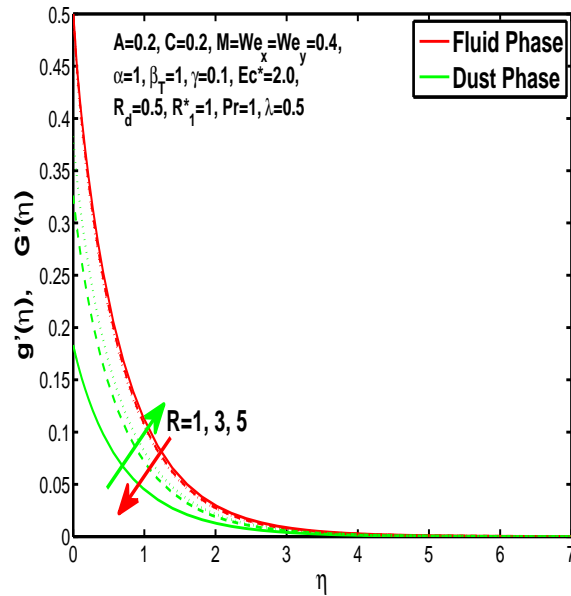


Figure 4.10: Effect of fluid-particle interaction parameter "R" on momentum boundary layer of fluid and particles in y-direction.

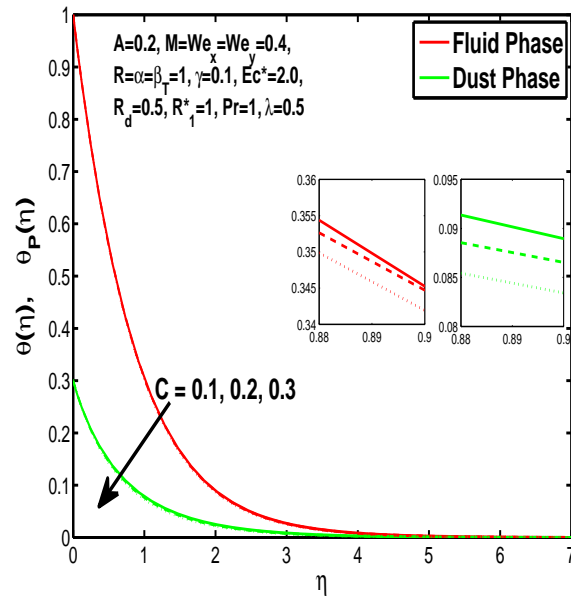


Figure 4.11: Outcome of "C" on temperature boundary layer of fluid and particles.

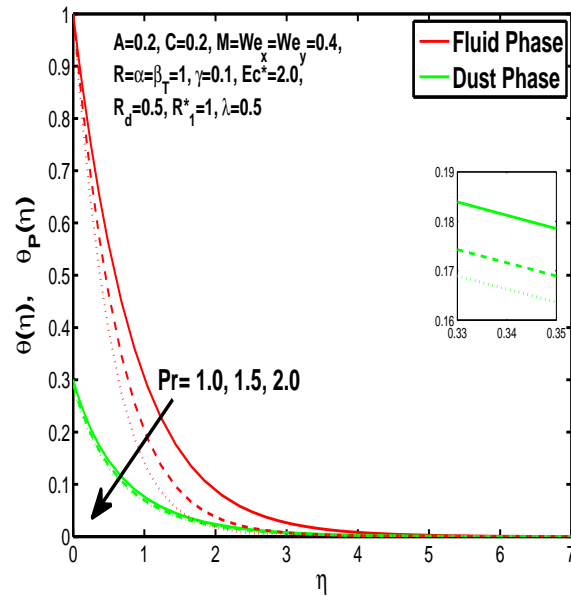


Figure 4.12: Effect of Prandtl number "Pr" on temperature boundary layer of fluid and particles.

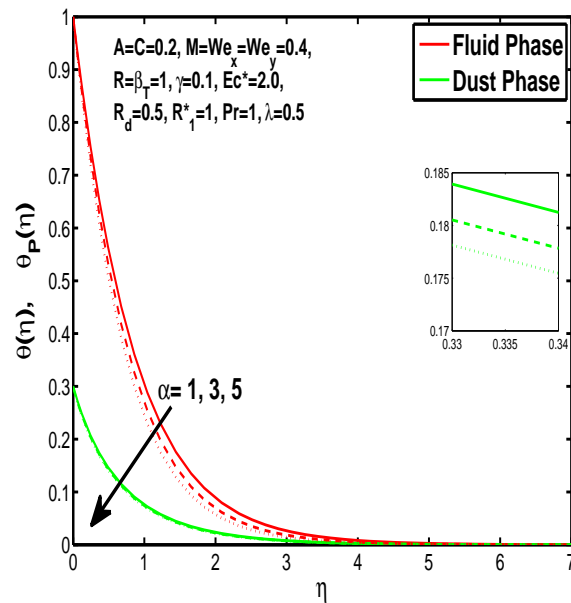


Figure 4.13: Effect of concentration parameter "α" on temperature boundary layer of fluid and particles.



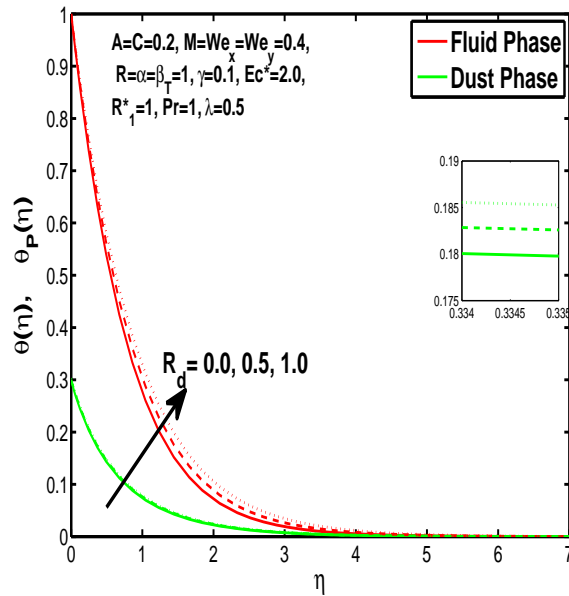


Figure 4.14: Effect of radiation parameter " $R_d$ " on temperature boundary layer of fluid and particles.

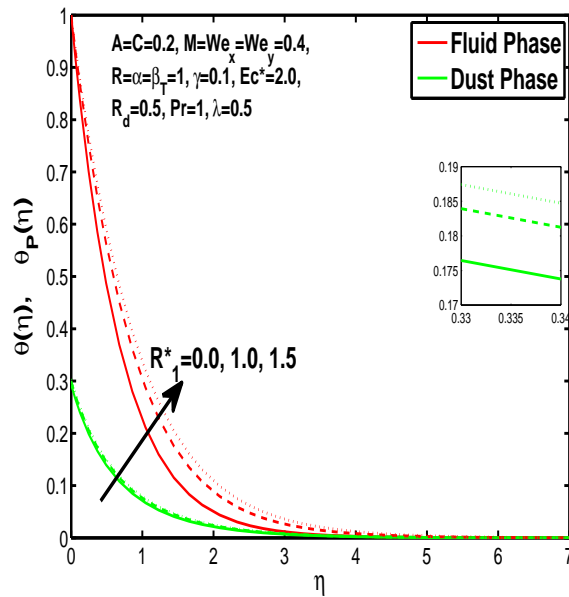


Figure 4.15: Effect of non-linear radiation parameter " $R_1^*$ " on temperature boundary layer of fluid and particles.

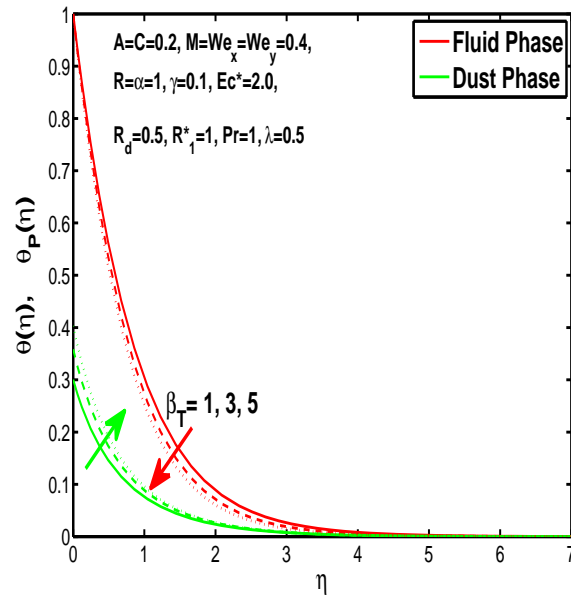


Figure 4.16: Effect of fluid-particle interaction parameter " $\beta_T$ " on temperature boundary layer of fluid and particles.

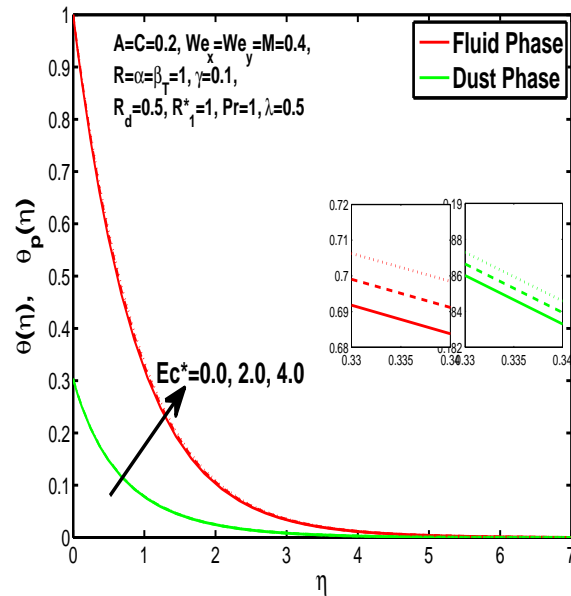


Figure 4.17: Effect of " $Ec^*$ " on temperature profile of fluid and particles.

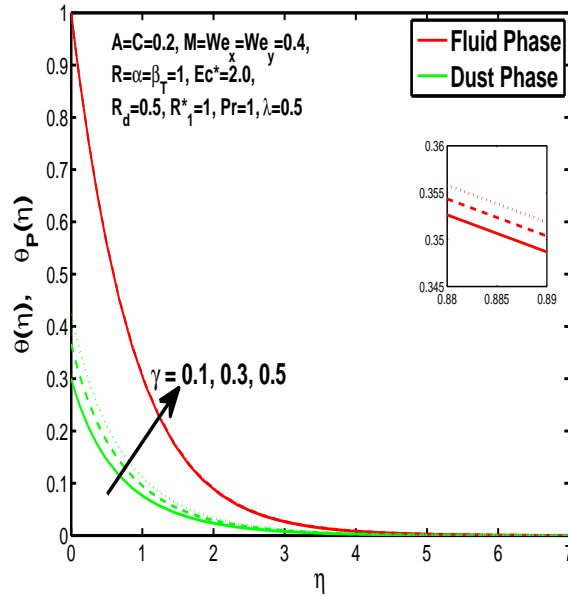


Figure 4.18: Effect of " $\gamma$ " on temperature boundary layer of fluid and particles.

is essential for fluids having non-Newtonian property. Weissenberg numbers  $We_x$  and  $We_y$  are dependent upon time constant, in the x and y-direction. Boost of weissenberg causes falloff of retardation time will depress the velocity of fluid and granules. *Fig. 4.7.* and *Fig. 4.8.* depict the upshot of volume fraction parameter and results are obvious that accretion of concentration enhances the resistance to flow in x and y-direction due to which boundary layer becomes shorten in both directions. *Fig. 4.9.* and *Fig. 4.10.* assimilate the result of fluid-particle interaction  $R$ . As in current problem two-phase that is fluid and granules has been considered, so there is an interaction between fluid particles and granules. This interaction enhances the velocity of liquid and solid phase in such a way that more the interaction more the particles will flow but at the same time due to interaction the resistance increases due to which velocity of fluid reduces. Same results are shown in x and y-directions. *Fig. 4.11.* describes the effect of volume fraction of granules  $C$  on temperature boundary layer. Due to increase in number of particles the temperature boundary layer decreases because increase in fraction of granules causes resistance results in the generation of internal energy turns to utilized to keep the temperature of the mixture at state of equilibrium. *Fig. 4.12.* shows the results for dimensionless Prandtl number. There is an inverse relation of thermal conduction of fluid with Prandtl number, the enhancement of  $Pr$  decreases of temperature boundary layer of fluid and particles as

well. *Fig. 4.13.* shows that increase of mass concentration  $\alpha$  decreases the temperature boundary layer of fluid after gaining maximum value to stabilized the temperature of the fluid and dust particles as well. *Fig. 4.14.* and *Fig. 4.15.* exhibits the obvious results that increase in the radiations enhances the temperature of fluid and particles.  $R_d$  and  $R_1^*$  are the non linear thermal radiations parameters and it is well known that the fastest way of heat transfer is radiation. *Fig. 4.16.* shows that the increment of fluid-particle interaction  $\beta_T$  reduces the heat of fluid and increases the temperature of solid particles. It may happen due to thermal conductivity of the particles. *Fig. 4.17.* shows that increment of viscous dissipation  $Ec^*$  raises the temperature of the system because heat generate during the dissipation due to viscous or resistive forces. And this heat absorbed by the fluid and thicken the thermal boundary layer of fluid and dust granules. *Fig. 4.18.* depicts that rise in the specific heat capacity ratio enlarge the temperature boundary layer of liquid and dust particles as well and this is the obvious result. *Fig. 4.19.* depicts that enhancement of stretching ratio decreases the speed of fluid in x-direction and increases in y-direction. And the reason is clear that  $\lambda = \frac{b}{a}$ ,  $\lambda$  has direct relation with  $b$  and inverse relation with  $a$ . So increase in  $\lambda$  increases  $b$  which is coefficient of  $V_w$  and decreases the  $a$  which is coefficient of  $U_w$ . In *Table. 4.1.* we have compared the of results with the online published articles by the Ariel [61] and Hayat et al.[65] in which they have solved the problem by exact method and numerical technique. The values find out presently by bvp4c numerical method also gives the comparison with already published data. *Table. 4.2.* illustrate the evaluations of skin-friction and *Table. 4.3.* illustrate Nusselt number. Results show that skin friction increases with the increase of unsteadiness, fluid particle interaction, volume fraction of dust particle, stretching ratio and magnetic field, but decreases due to Weissenberg effect. And Nusselt number increases with the increase in unsteadiness, fluid-particle interaction, mass concentration, specific heat ratio and Prandtl number but reduces due to viscous dissipation and non-linear thermal radiations.

## 4.4 Concluding remarks

The three dimensional unsteady dusty flow of Williamson fluid is studied in this chapter. The effects of magnetic field and non-linear thermal radiations are discussed for fluid and dust particles as well. Evolved conclusions of the current problem are mentioned below. Most of the parameter cause hindrance to flows, let have a glance to the results,

- Rise in magnetic field, Weissenberg effect, concentration of dust particles, unsteady-

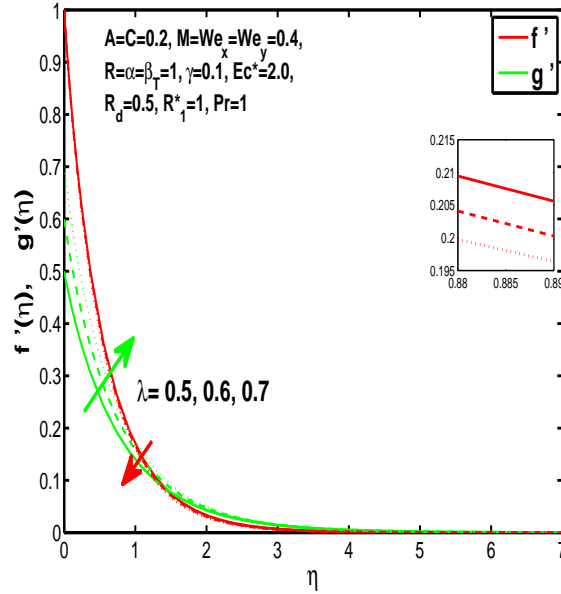


Figure 4.19: Effect of stretching ratio parameter  $\lambda$  on momentum boundary layer of fluid in x and y-direction.

ness parameter reduces the momentum boundary layer of fluid and dust granules in both x and y-directions.

- Increase in interaction between fluid and particles drops the flow of fluid, simultaneously increases the flow rate (in both x and y-directions) and temperature of dust granules.
- Increase in Prandtl number reduces the temperature boundary layer of fluid and dust granules as well.
- Increase in viscous dissipation and non-linear thermal radiations rise the heat of the system, increase the temperature of fluid and dust particles as well.

Table 4.1: Similarity of values of Skin friction coefficient with published data [61] and [65] by keeping  $M = 0$ ,  $A = 0$ ,  $R = 0$ ,  $We_x = 0$  and  $We_y = 0$ .

s	-f''(0)			-g''(0)		
	Exact results	Approximate results	Present findings	Exact results	Approximate results	Present findings
0	1	1	1.000172075	0	0	0.000000013
0.1	1.02025978	1.01952736	1.020660804	0.06684715	0.06684715	0.062427429
0.2	1.03949519	1.03827716	1.040423786	0.14873691	0.15018484	0.134408200
0.3	1.05795478	1.05642139	1.059440011	0.24335980	0.24476799	0.217419213
0.4	1.07578811	1.07406868	1.077719687	0.34920865	0.35039176	0.312560997
0.5	1.09309502	1.09129272	1.095289353	0.46520485	0.46606428	0.420667298
0.6	1.10994694	1.10814635	1.112183080	0.59052892	0.59101139	0.542377495
0.7	1.12639752	1.10814635	1.128437063	0.72453174	0.72460900	0.678186868
0.8	1.14248862	1.14089185	1.144088858	0.86668292	0.86634122	0.828485294
0.9	1.15825383	1.15683905	1.159176650	1.01653870	1.01577291	0.993585147
1.0	1.17372074	1.17253093	1.172544500	1.1737274	1.17253093	1.172020638

Table 4.2: Numeric values of Skin-friction.

A	We <sub>x</sub>	We <sub>y</sub>	M	C	R	λ	-f''(0)	-g''(0)	$f''(0) + \frac{We_x}{2} \sqrt{f''(0)^2 + g''(0)f''(0)^2}$	$g''(0) + \frac{We_y}{2} \sqrt{f''(0)^2 + g''(0)g''(0)^2}$
0.0	-	-	-	-	-	-	1.1797	0.4427	1.1101	0.4378
0.1	-	-	-	-	-	-	1.2115	0.4605	1.1381	0.4552
0.2	-	-	-	-	-	-	1.2432	0.4783	1.1659	0.4726
0.3	0.1	0.1	-	-	-	-	1.2749	0.4960	1.1936	0.4898
-	0.2	0.2	-	-	-	-	1.3439	0.4988	1.1633	0.4864
-	0.3	0.3	-	-	-	-	1.4392	0.5013	1.1285	0.4825
-	0.4	0.4	0.1	-	-	-	1.5976	0.5036	1.0871	0.4782
-	-	-	0.2	-	-	-	1.6259	0.5126	1.0972	0.4863
-	-	-	0.3	-	-	-	1.6743	0.5274	1.1136	0.4996
-	-	-	0.4	0.1	-	-	1.7446	0.5474	1.1359	0.5174
-	-	-	-	0.2	-	-	1.8618	0.5722	1.1685	0.5395
-	-	-	-	0.3	1	-	2.6378	0.6028	1.2462	0.5665
-	-	-	-	0.1	2	-	1.7827	0.5526	1.1471	0.5221
-	-	-	-	-	3	-	1.8045	0.5545	1.1533	0.5238
-	-	-	-	-	4	0.5	1.8178	0.5553	1.1569	0.5245
-	-	-	-	-	-	0.7	1.8911	0.9041	1.1758	0.7897
-	-	-	-	-	-	0.9	1.9599	1.4391	1.1917	1.0663

Table 4.3: Numerical values of Nusselt number for different values of  $A, \beta_T, \alpha, \gamma, Pr, C, R_d, R_1^*$  and  $Ec^*$ .

$A$	$Pr$	$Ec^*$	$\alpha$	$R^*$	$R_1^*$	$\beta_T$	$C$	$\gamma$	$-\theta'(0)$	$-\theta'(0)[1 - R_d k - R_1^* k \theta]$
0.0	-	-	-	-	-	-	-	-	1.0850	0.6510
0.1	-	-	-	-	-	-	-	-	1.1037	0.6622
0.2	-	-	-	-	-	-	-	-	1.1222	0.6733
0.3	0.7	-	-	-	-	-	-	-	1.1404	0.6842
-	0.9	-	-	-	-	-	-	-	1.3273	0.7964
-	1.1	-	-	-	-	-	-	-	1.4951	0.8971
-	1.3	0.5	-	-	-	-	-	-	1.6486	0.9892
-	-	1	-	-	-	-	-	-	1.6431	0.9859
-	-	1.5	-	-	-	-	-	-	1.6376	0.9826
-	-	2	1	-	-	-	-	-	1.6288	0.9773
-	-	-	2	-	-	-	-	-	1.6560	0.9936
-	-	-	3	-	-	-	-	-	1.6827	1.0096
-	-	-	4	1	-	-	-	-	1.7087	1.0252
-	-	-	-	1.5	-	-	-	-	1.7012	0.9640
-	-	-	-	2	1	-	-	-	1.6949	0.9039
-	-	-	-	-	1.5	-	-	-	1.5976	0.5858
-	-	-	-	-	2	1	-	-	1.5149	0.3030
-	-	-	-	-	-	2	-	-	1.5277	0.3055
-	-	-	-	-	-	3	-	-	1.6054	0.3211
-	-	-	-	-	-	4	0.1	-	1.6756	0.3351
-	-	-	-	-	-	-	0.2	-	1.9802	0.3960
-	-	-	-	-	-	-	0.3	-	2.3074	0.4615
-	-	-	-	-	-	-	0.1	0.1	1.6756	0.3351
-	-	-	-	-	-	-	-	0.2	1.6496	0.3299
-	-	-	-	-	-	-	-	0.3	1.6265	0.3253
-	-	-	-	-	-	-	-	0.4	1.6060	0.3212

## Chapter 5

# Numerically analysis of unsteady flow of three dimensional tangent hyperbolic fluid-particle suspension with MHD, viscous dissipation and joule heating with convective boundary conditions

This chapter explores the impact of MHD and viscous dissipation on stretching flow of particulate tangent hyperbolic fluid in 3D. A time-dependent magnetic field is applied along the z-axis and the sheet stretches along the xy-plane with some velocity. The effects of joule's heating and convective boundary conditions on the heat transfer analysis of particle-fluid flow. The fluid and dust particles motions are coupled through momentum and heat drag between them. The effect of dissipation due to viscosity and particle interaction in natural convection is appreciable since, induced kinetic energy becomes appreciable compared to the amount of heat transferred. A well known bvp4c method has been used to find the fruitful results. Graphs and tables show the facts and figures for physical properties according to different parameters.



## 5.1 Mathematical formulation

The incompressible 3D unsteady dusty tangent hyperbolic non-Newtonian fluid momentum and heat flow under the effect of MHD, Joule heating and viscous dissipation with convective boundary conditions. Flow distribution is due to stretching sheet which is assumed to be placed in xy-plane and fluid is placed along the z-axis. Solid particles emersed in the fluid are small enough but have density, velocity and other physical properties. The stress tensor for tangent hyperbolic fluid is mentioned in section 1.5.2. Modeling for assumed situation is given as:

$$\frac{\partial u}{\partial x} + \frac{\partial v}{\partial y} + \frac{\partial w}{\partial z} = 0, \quad (5.1)$$

$$\frac{\partial u_P}{\partial x} + \frac{\partial v_P}{\partial y} + \frac{\partial w_P}{\partial z} = 0, \quad (5.2)$$

$$\begin{aligned} \rho(1-C) \left[ \frac{\partial u}{\partial t} + u \frac{\partial u}{\partial x} + v \frac{\partial u}{\partial y} + w \frac{\partial u}{\partial z} \right] &= \mu(1-C) \frac{\partial}{\partial z} [((1-n) \\ &+ \sqrt{2n}\Gamma \sqrt{(\frac{\partial u}{\partial z})^2 + (\frac{\partial v}{\partial z})^2}) \frac{\partial u}{\partial z}] - \sigma B^2(t)u + CS(u_p - u), \end{aligned} \quad (5.3)$$

$$C\rho_P \left( \frac{\partial u_P}{\partial t} + u_P \frac{\partial u_P}{\partial x} + v_P \frac{\partial u_P}{\partial y} + w_P \frac{\partial u_P}{\partial z} \right) = CS(u - u_P), \quad (5.4)$$

$$\begin{aligned} \rho(1-C) \left[ \frac{\partial v}{\partial t} + u \frac{\partial v}{\partial x} + v \frac{\partial v}{\partial y} + w \frac{\partial v}{\partial z} \right] &= \mu(1-C) \frac{\partial}{\partial z} [((1-n) \\ &+ \sqrt{2n}\Gamma \sqrt{(\frac{\partial u}{\partial z})^2 + (\frac{\partial v}{\partial z})^2}) \frac{\partial v}{\partial z}] - \sigma B^2(t)v + CS(v_p - v), \end{aligned} \quad (5.5)$$

$$C\rho_P \left( \frac{\partial v_P}{\partial t} + u_P \frac{\partial v_P}{\partial x} + v_P \frac{\partial v_P}{\partial y} + w_P \frac{\partial v_P}{\partial z} \right) = CS(v - v_P), \quad (5.6)$$

$$\begin{aligned} \rho c_p(1-C) \left[ \frac{\partial T}{\partial t} + u \frac{\partial T}{\partial x} + v \frac{\partial T}{\partial y} + w \frac{\partial T}{\partial z} \right] &= k(1-C) \frac{\partial^2 T}{\partial z^2} + \frac{\rho_p c_p C}{\tau_t} (T_P - T) \\ &+ CS[(u - u_p)^2 + (v - v_p)^2] - \mu \left[ \left( \frac{\partial u}{\partial z} \right)^2 + \left( \frac{\partial v}{\partial z} \right)^2 \right] + \sigma B^2(u^2 + v^2) \end{aligned} \quad (5.7)$$

$$C \left( \frac{\partial T_P}{\partial t} + u_P \frac{\partial T_P}{\partial x} + v_P \frac{\partial T_P}{\partial y} + w_P \frac{T_P}{z} \right) = C \frac{c_P}{c_m \tau_T} (T - T_P), \quad (5.8)$$

conditions at the boundary are:

$$u = U_w(x, t), \quad v = V_w(y, t), \quad w = 0, \quad -k \frac{\partial T}{\partial z} = h_f(T_w - T), \quad \text{at } z = 0, \quad (5.9)$$

$$u_P = u = 0, \quad v_P = v = 0, \quad w_P = w, \quad T \rightarrow T_\infty, \quad T_P \rightarrow T_\infty \text{ as } z \rightarrow \infty. \quad (5.10)$$

$S$  is the drag force.  $B(t)$  is the time dependent magnetic field.  $U_w$  and  $V_w$  are the stretching velocities of the sheet.  $T_w$  is the wall temperature of stretching sheet.

As we know its difficult to solve the PDE's, so there is requirement of similarity transformations for the turning of PDEs into ODEs. Similarity transformations required for the conversion of PDE's to ODE's are defined as in *Eqs.*(4.11) – (4.12)

$$\begin{aligned}
u &= \frac{ax}{1-ct}f'(\eta), \quad v = \frac{ay}{1-ct}g'(\eta), \quad w = -\sqrt{\frac{\nu a}{1-ct}}(f(\eta) + g(\eta)), \\
u_P &= \frac{ax}{1-ct}F'(\eta), \quad v_P = \frac{ay}{1-ct}G'(\eta), \quad w_P = -\sqrt{\frac{\nu a}{1-ct}}(F(\eta) + G(\eta)), \\
\theta &= \frac{T - T_\infty}{T_w - T_\infty}, \quad \theta_P = \frac{T_P - T_\infty}{T_w - T_\infty},
\end{aligned} \tag{5.11}$$

and to be noted that,

$$\begin{aligned}
U_w(x, t) &= \frac{ax}{1-ct}, \quad V_w(y, t) = \frac{by}{1-ct}, \quad \eta = z\sqrt{\frac{U_w}{\nu x}}, \\
T_w(x, t) &= T_\infty + \frac{T_o U_w x}{\nu(1-ct)^{\frac{1}{2}}}, \quad B(t) = \frac{B_o}{(1-ct)^{\frac{1}{2}}}.
\end{aligned} \tag{5.12}$$

Utilize *Eqs.*(4.11) – (4.12) into *Eqs.*(5.1) – (5.10) and get the following equalizations,

$$\begin{aligned}
&f'''[(1-n) + nW e_x(\sqrt{f'^2 + g'^2} + \frac{f''^2}{\sqrt{f'^2 + g'^2}})] + nW e_x \frac{f''g''g'''}{\sqrt{f'^2 + g'^2}} \\
&+ (f+g)f'' - f'^2 - A[f' + \frac{\eta}{2}f'''] - \frac{M^2}{(1-C)}f' + \frac{CR}{(1-C)}(F'(\eta) - f'(\eta)) = 0
\end{aligned} \tag{5.13}$$

$$\frac{A}{2}\eta F'' + AF' + F'^2 - (F+G)F'' + R(F' - f') = 0, \tag{5.14}$$

$$\begin{aligned}
&g'''[(1-n) + nW e_y(\sqrt{f'^2 + g'^2} + \frac{g''^2}{\sqrt{f'^2 + g'^2}})] + nW e_y \frac{g''f''f'''}{\sqrt{f'^2 + g'^2}} \\
&+ (f+g)g'' - g'^2 - A[g' + \frac{\eta}{2}g'''] - \frac{M^2}{(1-C)}g' + \frac{CR}{(1-C)}(G'(\eta) - g'(\eta)) = 0,
\end{aligned} \tag{5.15}$$

$$\frac{A}{2}\eta G'' + AG' + R(G' - g') + G'^2 - (F+G)G'' = 0, \tag{5.16}$$

$$\begin{aligned}
&\theta'' + Pr(f\theta' - 2f'\theta) - Pr\frac{A}{2}(\eta\theta' + 3\theta) + Pr\theta'(f+g) + \frac{Pr\alpha\beta_T C}{(1-C)}(\theta_P - \theta) + \\
&\frac{CEc^*}{(1-C)}(f' - F')^2 + \frac{CEc^*}{(1-C)}(g' - G')^2 + \frac{Ec_x f''^2}{(1-C)} + \frac{Ec_y g''^2}{(1-C)} \\
&+ \frac{M^2 Ec_x f'^2}{(1-C)} + \frac{M^2 Ec_y g'^2}{(1-C)} = 0,
\end{aligned} \tag{5.17}$$

$$\theta'_P(\eta\frac{A}{2} - 2F - G) - \gamma\beta_T(\theta - \theta_P) + \theta_P(\frac{3}{2}A + 2f') = 0, \tag{5.18}$$

along with the conditions at boundary,

$$\begin{aligned} f(0) = 0, f'(0) = 1, g(0) = 0, g'(0) = \lambda, \theta'(0) = -\zeta[1 - \theta(0)], \\ f' \rightarrow 0, F' \rightarrow 0, F = f, g' \rightarrow 0, G' \rightarrow 0, G = g, \theta \rightarrow 0, \theta_P \rightarrow 0 \text{ as } \eta \rightarrow \infty. \end{aligned} \quad (5.19)$$

As the multiple dependence shifted to unique  $\eta$  derivative is extract with respect to it. The dimensionless number  $A$  is unsteadiness parameter,  $M$  is magnetic parameter,  $We_x$  is Weissenberg along x-direction,  $We_y$  is Weissenberg number along y-direction,  $Pr$  is Prandtl number,  $R$  fluid-particle interaction parameter for momentum,  $\beta_T$  is fluid-particle interaction parameter for temperature,  $C$  is volume fraction of the granules,  $\alpha$  is mass concentration parameter,  $\gamma$  is fraction of specific heat of the fluid to the particles,  $\lambda$  is stretching ratio parameter,  $Ec^*$  is viscous dissipation parameter and  $Ec_x, Ec_y$  are Eckert numbers in x and y-direction, defined below

$$\begin{aligned} We_x = \sqrt{\frac{2a^3\Gamma x^2}{\nu(1-ct)^3}}, We_y = \sqrt{\frac{2a^3\Gamma y^2}{\nu(1-ct)^3}}, A = \frac{c}{a}, M = \sqrt{\frac{\sigma}{\rho a}}B_o, \\ Pr = \frac{\mu C_p}{k}, R = S \frac{(1-ct)}{\rho a}, \alpha = \frac{\rho_P}{\rho}, \gamma = \frac{c_p}{c_m}, \beta_T = \frac{1-ct}{a\tau_T}, \lambda = \frac{b}{a}, \\ Ec^* = \frac{S\nu^2(1-ct)^2}{T_o k}, Ec_x = \frac{U_w^2}{c_p(T_f - T_\infty)}, Ec_y = \frac{V_w^2}{c_p(T_f - T_\infty)}. \end{aligned} \quad (5.20)$$

Where  $\tau_T$  is the thermal equilibrium time, required by particles to manage their temperature corresponding to fluid. Mathematical Expressions of skin friction for three dimensional flow are given in Eq (5.24),

$$C_{fx} = \frac{\tau_{xz}}{\frac{1}{2}\rho U_w^2}, C_{fy} = \frac{\tau_{yz}}{\frac{1}{2}\rho V_w^2}, \quad (5.21)$$

By using boundary layer approximation shear stress rates at wall in x, y directions and coefficients will be reduced to

$$\begin{aligned} \tau_{xz} = \mu_o[(1-n)\frac{\partial u}{\partial z} + n(\frac{\Gamma}{\sqrt{2}}\sqrt{\frac{\partial u^2}{\partial z} + \frac{\partial v^2}{\partial z}})\frac{\partial u}{\partial z}]_{z=0}, \\ \tau_{yz} = \mu_o[(1-n)\frac{\partial v}{\partial z} + n(\frac{\Gamma}{\sqrt{2}}\sqrt{\frac{\partial u^2}{\partial z} + \frac{\partial v^2}{\partial z}})\frac{\partial v}{\partial z}]_{z=0}, \end{aligned} \quad (5.22)$$

by inserting Eq (5.25), into Eq (5.24), one can get,

$$C_{fx} Re_x^{\frac{1}{2}} = (1-n)f''(0) + n\frac{We_x}{2}\sqrt{f''(0)^2 + g''(0)^2}f''(0),$$

$$C_{fy}Re_y^{\frac{1}{2}} = (1 - n)g''(0) + n\frac{We_y}{2}\sqrt{f''(0)^2 + g''(0)^2}g'''(0). \quad (5.23)$$

Now expression for another physical quantity that is Nusselt number give in Eq (5.27),

$$Nu_x = \frac{xq_w}{k(T_w - T_\infty)}, \quad q_w = -k\left(\frac{\partial T}{\partial z}\right) \quad (5.24)$$

where  $q_w$  denotes the heat flux of the wall. Settle the value of  $q_w$  into  $Nu_x$  while considering the thermal radiations effective, one can get following relation for Nusselt number,

$$Nu_xRe_x^{-\frac{1}{2}} = -\theta'(0) \quad . \quad (5.25)$$

The considered flow is laminar and for that flow Reynolds number will be of low range.

## 5.2 Numerical procedure of solution

Conjecture built of three dimensional flow became more complicated as compare to two dimensional flow and evidently the non-linearity rate of equations is high. So its preferable to get the solution numerically. Here the solution of problem is find out by bvp4c method by using the software MATLAB. For this method we have to convert equations in he

following form:

$$f''' = \frac{1}{[(1-n) + nWe_x(\sqrt{f'^2 + g'^2} + \frac{f''^2}{\sqrt{f'^2 + g'^2}})]} [-nWe_x \frac{f'' g'' g'''}{\sqrt{f'^2 + g'^2}} + f'^2 + A(f' + \frac{\eta}{2} f'') + \frac{M^2 f'}{1-C} - \frac{CR}{1-C} (F' - f') - f''(f + g)], \quad (5.26)$$

$$F'' = \frac{-AF' - F'^2 - R(F' - f')}{\frac{A\eta}{2} - 2F - G}, \quad (5.27)$$

$$g''' = \frac{1}{[(1-n) + nWe_y(\sqrt{f'^2 + g'^2} + \frac{g''^2}{\sqrt{f'^2 + g'^2}})]} [-nWe_x \frac{g'' f'' f'''}{\sqrt{f'^2 + g'^2}} + g'^2 + A(g' + \frac{\eta}{2} g'') + \frac{M^2 g'}{1-C} - \frac{CR}{1-C} (G' - g') - g''(f + g)], \quad (5.28)$$

$$G'' = \frac{-AG' - sG'^2 - R(G' - g')}{\frac{A\eta}{2} - F - G}, \quad (5.29)$$

$$\theta'' = Pr \frac{A}{2} (\eta \theta' + 3\theta) - Pr(f\theta' - 2f'\theta) - \frac{Pr\alpha\beta_T C}{1-C} (\theta_P - \theta) - Pr\theta'(f + g) + Ec_x f''^2 + Ec_y g''^2 + M^2 Ec_x f'^2 + M^2 Ec_y g'^2 - \frac{CEc^*}{(1-C)} (f' - F')^2 \quad (5.30)$$

$$- \frac{CEc^*}{1-C} (g' - G')^2, \quad \theta'_P = \frac{\gamma\beta_T(\theta - \theta_P) - \theta_P(\frac{3A}{2} + 2F')}{\frac{A\eta}{2} - 2F - G}. \quad (5.31)$$

There is requirement of method to assume the dummy variables as shown in Eq(5.35).

$$\begin{aligned} f &= y_1, f' = y_2, f'' = y_3, f''' = y'_3, F = y_4, F' = y_5, F'' = y'_5, \\ g &= y_6, g' = y_7, g'' = y_8, g''' = y'_8, G = y_9, G' = y_{10}, G'' = y'_{10}, \\ \theta &= y_{11}, \theta' = y_{12}, \theta'' = y'_{12}, \theta_P = y_{13}, \theta'_P = y'_{13}. \end{aligned} \quad (5.32)$$

Set of Eqs(5.29) – (5.34) can be molded in the initial value problem as:

$$\frac{dy_1}{dx} = y_2, \quad (5.33)$$

$$\frac{dy_2}{dx} = y_3, \quad (5.34)$$

$$\begin{aligned} \frac{dy_3}{dx} = & \frac{1}{[(1-n) + nWe_x(\sqrt{y_2^2 + y_7^2} + \frac{y_3^2}{\sqrt{y_2^2 + y_7^2}})]} [-nWe_x \frac{y_3 y_8 y_8'}{\sqrt{y_2^2 + y_7^2}} \\ & + y_2^2 - y_3(y_1 + y_6) + A(y_2 + \frac{\eta}{2}y_3) + \frac{M^2}{1-C}y_2 - \frac{CR}{(1-C)}(y_5 - y_2)], \end{aligned} \quad (5.35)$$

$$\frac{dy_4}{dx} = y_5, \quad (5.36)$$

$$\frac{dy_5}{dx} = \frac{-Ay_5 - y_5^2 - R(y_5 - y_2)}{\frac{A\eta}{2} - 2y_4} - y_9, \quad (5.37)$$

$$\frac{dy_6}{dx} = y_7, \quad (5.38)$$

$$\frac{dy_7}{dx} = y_8, \quad (5.39)$$

$$\begin{aligned} \frac{dy_8}{dx} = & \frac{1}{[(1-n) + nWe_y(\sqrt{y_2^2 + y_7^2} + \frac{y_8^2}{\sqrt{y_2^2 + y_7^2}})]} [-nWe_x \frac{y_8 y_3 y_3'}{\sqrt{y_2^2 + y_7^2}} \\ & + y_7^2 - y_8(y_1 + y_6) + A(y_7 + \frac{\eta}{2}y_8) + \frac{M^2}{1-C}y_7 - \frac{CR}{(1-C)}(y_{10} - y_7)], \end{aligned} \quad (5.40)$$

$$\frac{dy_9}{dx} = y_{10}, \quad (5.41)$$

$$\frac{dy_{10}}{dx} = \frac{-Ay_{10} - sy_{10}^2 - R(y_{10} - y_7)}{\frac{A\eta}{2} - y_4} - y_9, \quad (5.42)$$

$$\frac{dy_{11}}{dx} = y_{12}, \quad (5.43)$$

$$\begin{aligned} \frac{dy_{12}}{dx} = & -Pr(y_1 y_{12} - 2y_2 y_{11}) + Pr \frac{A}{2}(\eta y_{12} + 3y_{11}) - \frac{Pr\alpha\beta_T C}{1-C}(y_{13} - y_{11}) \\ & - Pr y_{12}(y_1 + y_6) + Ec_x y_3^2 + Ec_y y_8^2 + M^2 Ec_x y_2^2 + M^2 Ec_y y_7^2 \\ & - \frac{CEc^*}{(1-C)}(y_2 - y_5)^2 - \frac{CEc^*}{(1-C)}(y_7 - y_{10})^2, \end{aligned} \quad (5.44)$$

$$\frac{dy_{13}}{dx} = \frac{\gamma\beta_T(y_{11} - y_{13}) - y_{13}(\frac{3A}{2} + 2y_5)}{\frac{A\eta}{2} - 2y_4 - y_9}, \quad (5.45)$$

the reduced endpoint conditions are

$$\begin{aligned}
 y_1(a) &= 0, \quad y_2(a) = 1, \quad y_2(b) = s_1, \quad y_4(b) = y_1(b), \\
 y_5(b) &= s_2, \quad y_6(a) = 0, \quad y_7(a) = \lambda, \quad y_7(b) = s_3, \\
 y_9(b) &= y_6(b), \quad y_{10}(b) = s_4, \quad y_{12}(a) = -\zeta(1 - y_{11}(a)), \\
 y_{11}(b) &= s_5, \quad y_{13}(b) = s_6.
 \end{aligned} \tag{5.46}$$

Here we need to find some initial guesses that are  $s_1, s_2, s_3, s_4, s_5$  and  $s_6$  in a way like integration of the system of first order ODEs fulfil the endpoint conditions and obtained the solution for the system of equations (5.36)-(5.48). The choice of highest value is  $\eta = 7$  with step size= 0.01 with simulation error is chosen  $10^5$ .

### 5.3 Outcomes and discussions

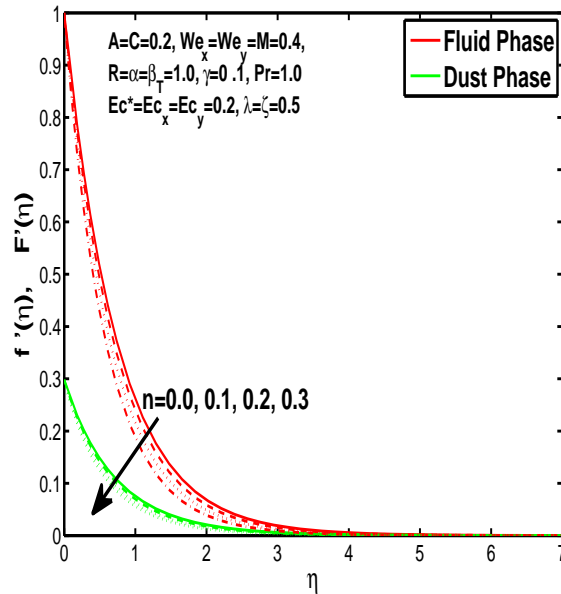


Figure 5.1: Effect of power law index "n" on momentum boundary layer of fluid and particles in x-direction.

In this section the results of the momentum and temperature boundary layers effected by the different parameters find out by the numerical method, displayed graphically and numerically. *Fig. 5.1* and *Fig. 5.2*. are plotted to show the behavior of the power-law

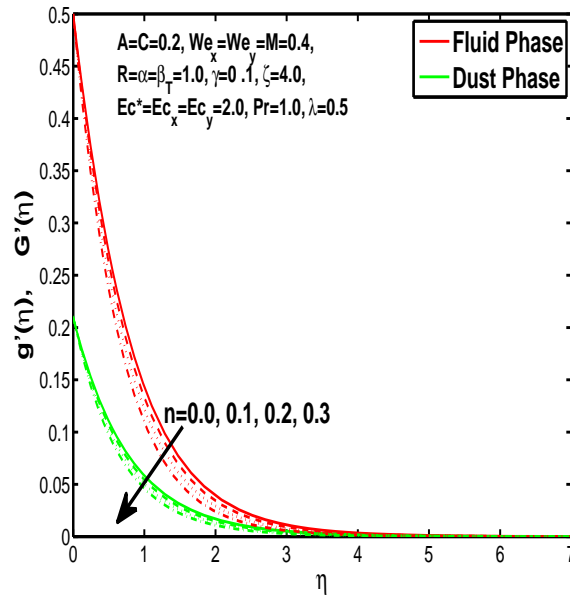


Figure 5.2: Effect of power law index "n" on momentum boundary layer of fluid and particles in y-direction.

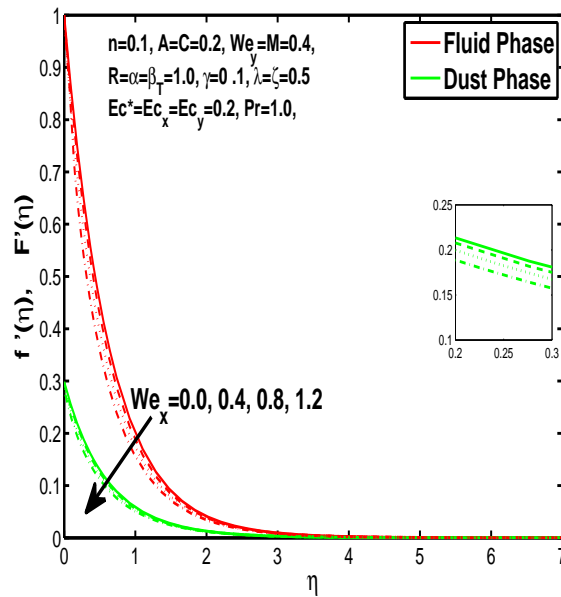


Figure 5.3: Effect of Weissenberg number "We\_x" on momentum boundary layer of fluid and particles in x-direction.



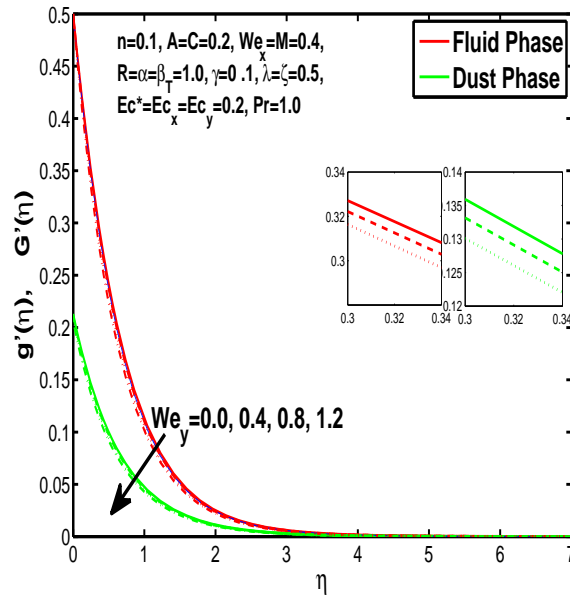


Figure 5.4: Outcome of Weissenberg number " $We_y$ " on momentum boundary layer of fluid and particles in y-direction.

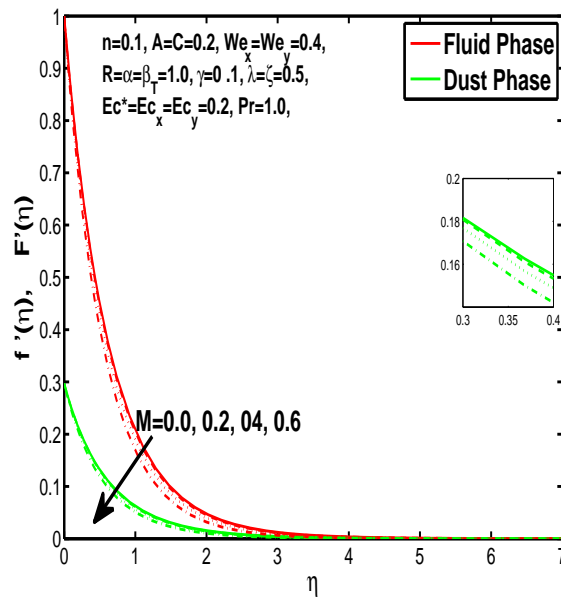


Figure 5.5: Effect of magnetic parameter " $M$ " on velocity of fluid and particles in x-direction.

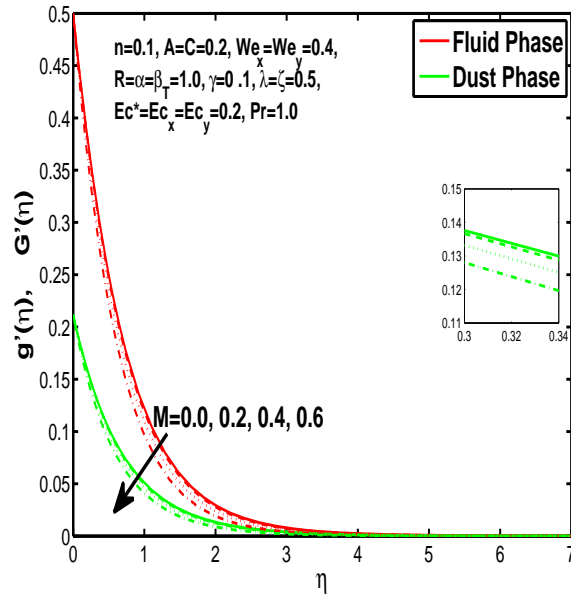


Figure 5.6: Effect of magnetic parameter "M" on velocity of fluid and particles in y-direction.

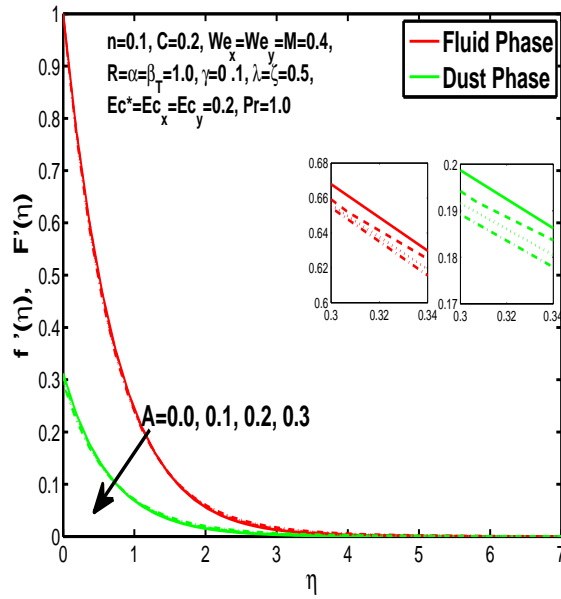


Figure 5.7: Effect of unsteadiness parameter "A" on momentum boundary layer of fluid and particles in x-direction.

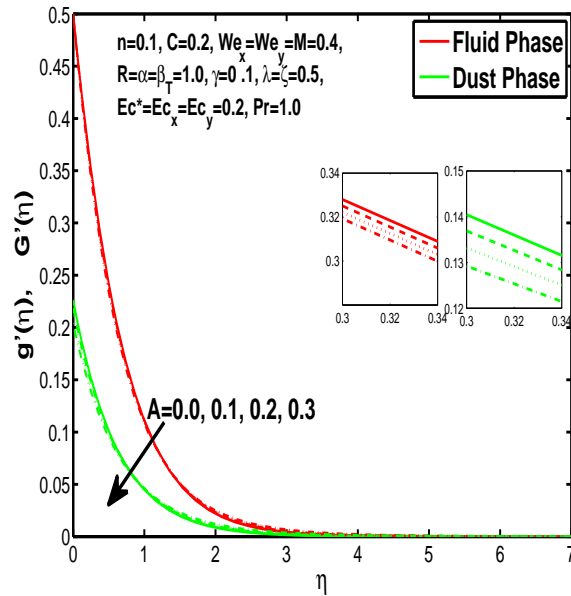


Figure 5.8: Effect of unsteadiness parameter "A" on momentum boundary layer of fluid and particles in y-direction.

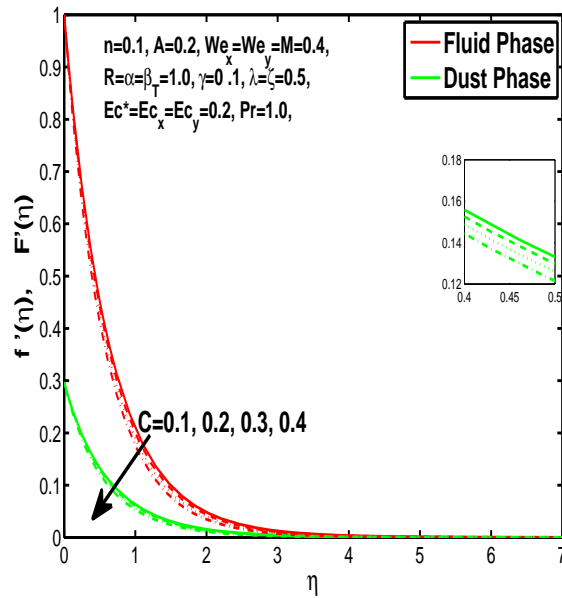


Figure 5.9: Effect of "C" on velocity of fluid and particles in x-direction.

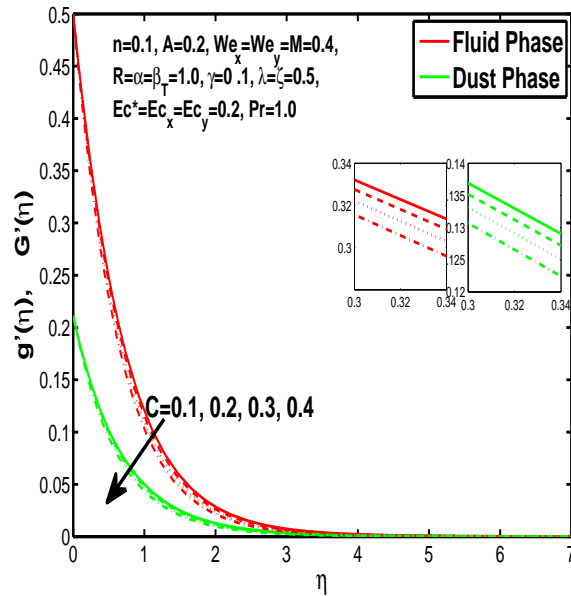


Figure 5.10: Effect of "C" on momentum boundary layer of fluid and particles in y-direction.

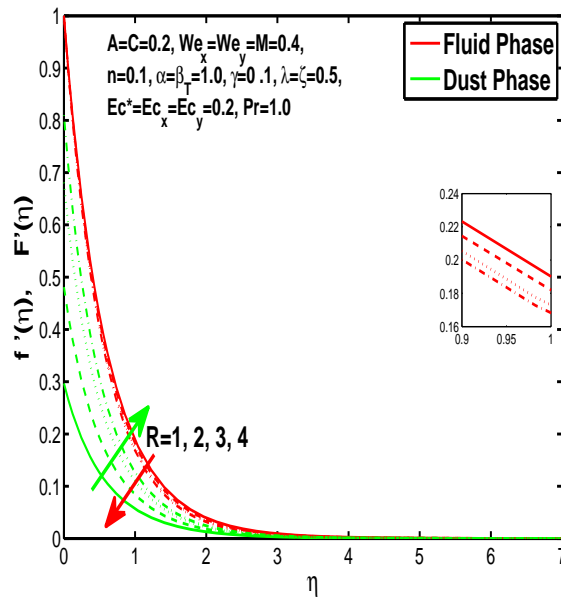


Figure 5.11: Effect of fluid-particle interaction parameter "R" on momentum boundary layer of fluid and particles in x-direction.

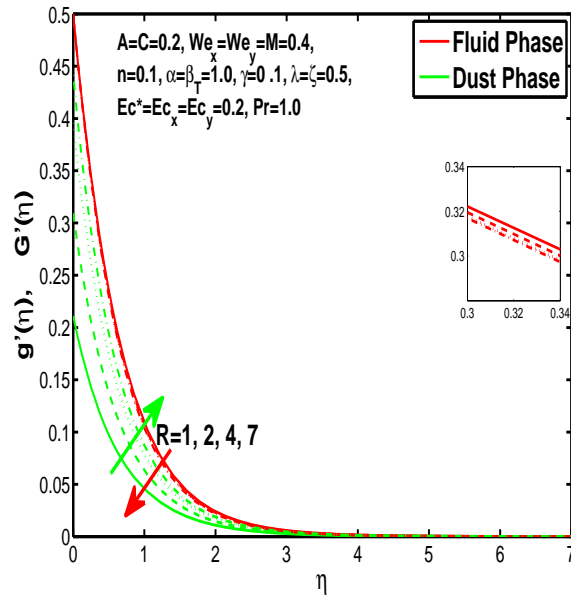


Figure 5.12: Effect of fluid-particle interaction parameter "R" on momentum boundary layer of fluid and particles in y-direction.

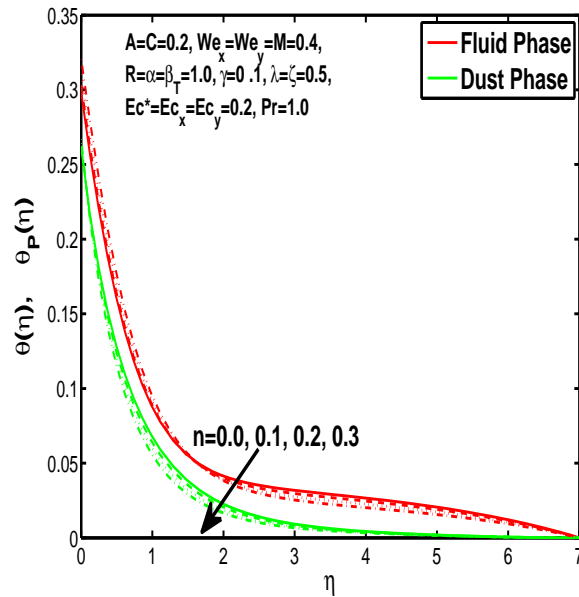


Figure 5.13: Effect of power law index "n" on temperature boundary layer of fluid and particles.

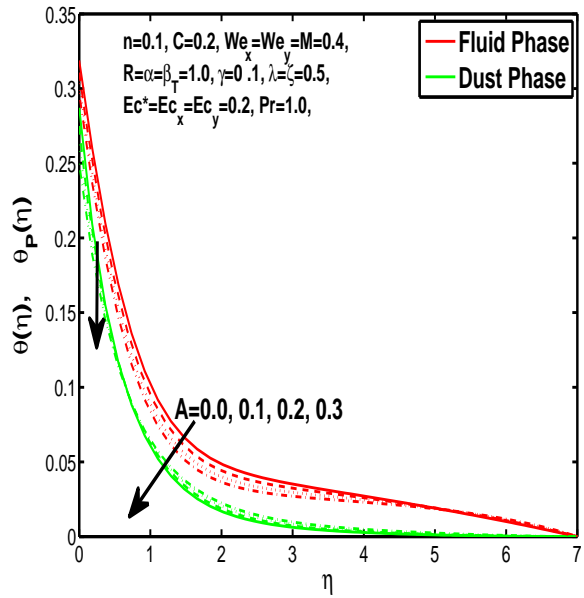


Figure 5.14: Effect of unsteadiness parameter "A on temperature boundary layer of fluid and particles.

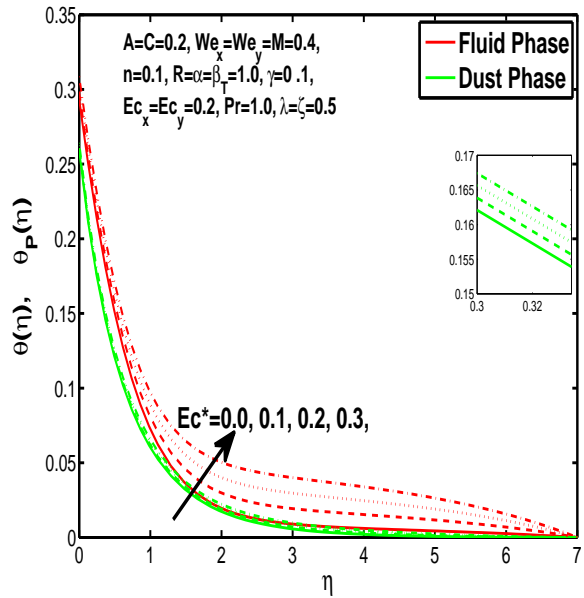


Figure 5.15: Effect of "Ec\*" on temperature boundary layer of fluid and particles.

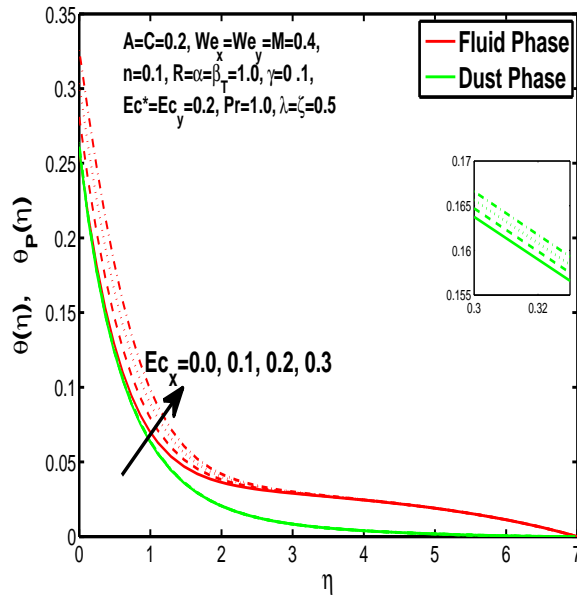


Figure 5.16: Effect of Eckert number " $Ec_x$ " on temperature boundary layer of fluid and particles in x-direction.

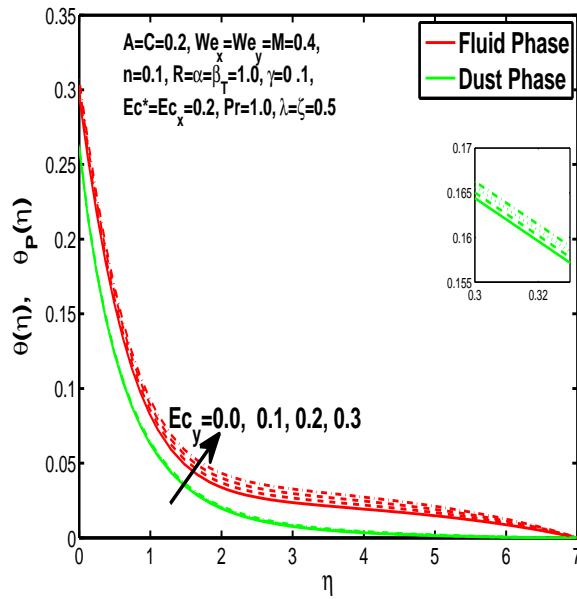


Figure 5.17: Effect of Eckert number " $Ec_y$ " on temperature boundary layer of fluid and particles in y-direction.

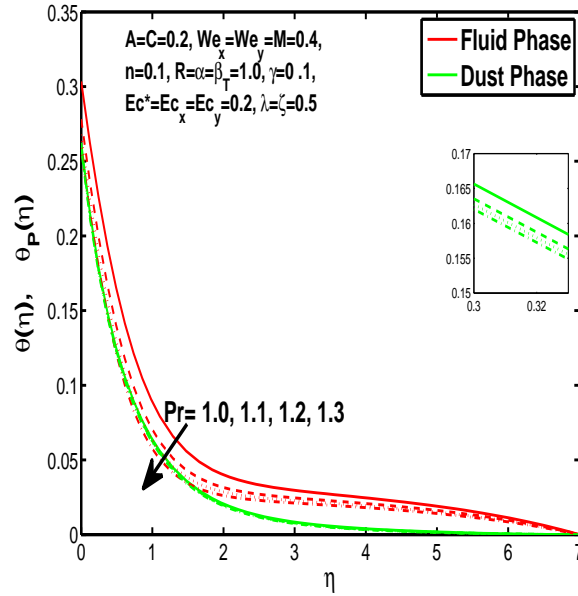


Figure 5.18: Effect of Prandtl number "Pr" on temperature boundary layer of fluid and particles.

index  $n$  which is also known as flow consistency index. It is clearly shown that the increase in flow index reduces the speed of both fluid and granules in both  $x$  and  $y$ -directions. *Fig. 5.3* and *Fig. 5.4*. are for describing the Weissenberg effect which is essential for fluids having non-Newtonian property. Weissenberg parameters  $We_x$  and  $We_y$  are dependent upon time constant, in the  $x$  and  $y$ -direction. Increase in Weissenberg parameter causes falloff of retardation time will depress the velocity of fluid and granules. *Fig. 5.5*. and *Fig. 5.6*. delineate the effects of magnetic field parameter  $M$ . As we know that magnetic field parameter causes Lorentz force which is a resistive force and create hindrance in the fluid flow, in result of which decreases the momentum boundary layer of fluid and dust particles as well and in both  $x$  and  $y$ -directions. *Fig. 5.7*. and *Fig. 5.8*. are plotted to check the change in momentum boundary layers due to change in unsteadiness parameter  $A$ . Graphs reveal that the rise in unsteadiness parameter decreases the flow rate of fluid and granules in both  $x$  and  $y$ -directions. We can observe in the graph that near the surface, velocity decreases and increases off from surface. As  $A$  is defined as inversely proportional to stretching coefficient  $a$ . The increase in unsteadiness parameter  $A$  reduces the  $a$ , in result of which velocity of fluid and granules decreases. *Fig. 5.9*. and *Fig. 5.10*. depict the upshot of volume fraction parameter and results are obvious



that accretion of concentration enhances the resistance to flow in x and y-direction due to which boundary layer becomes shorten in both directions. *Fig. 5.11.* and *Fig. 5.12.* assimilate the out-turn of fluid-particle interaction  $R$ . As in current problem two-phase that is fluid and granules has been considered, so there is an interaction between fluid particles and granules. This interaction enhances the speed of fluid and particles as well, in such a way that more the interaction more the particles will flow but at the same time due to interaction the resistance increases due to which velocity of fluid reduces. Same results are shown in x and y-directions. *Fig. 5.13.* shows that while enhancing the power law index reduces the temperature of the fluid. *Fig. 5.14.* shows the same graphical as for the velocity profile that unsteadiness decreases of the temperature of system. Increase in unsteadiness parameter reduces the velocity of fluid in turn decreases the temperature of fluid. *Fig. 5.15.*, *Fig. 5.16.* and *Fig. 5.17.* show that increment of viscous dissipation parameters  $Ec^*$ ,  $Ec_x$  and  $Ec_y$  raises the temperature of the system because heat generate during the dissipation due to viscous or resistive forces. And this heat absorbed by the fluid and thicken the temperature boundary layer of liquid and granules. *Fig. 5.18.* shows the results for dimensionless Prandtl number. Because of inverse relation of Prandtl number with the thermal conduction of fluid, the enhancement of  $Pr$  decreases of temperature boundary layer of fluid and particles as well. *Fig. 5.19.* shows that increase of mass concentration  $\alpha$  decreases the temperature boundary layer of fluid after gaining maximum value to stabilized the temperature of the fluid and dust particles as well. *Fig. 5.20.* reveal that the increment of fluid-particle interaction  $\beta_T$  reduces the temperature of liquid phase and increases the temperature of solid particles. It may happen due to thermal conductivity of the particles. *Fig. 5.21.* describes the effect of volume fraction of granules  $C$  on temperature boundary layer. Due to increase in number of particles the temperature boundary layer decreases because increase in fraction of granules causes resistance results in the generation of internal energy turns to utilized to keep the temperature of the mixture at state of equilibrium. *Fig. 5.22.* depicts that rise in Biot number increases the heat of system. This is due to the fact that the convective heat exchange at the surface leads to enhance the thermal boundary layer thickness. *Fig. 5.23.* shows that the increase in stretching ratio decreases the speed in x-direction and increases in y-direction. And the reason is clear that  $\lambda = \frac{b}{a}$ ,  $\lambda$  has direct relation with  $b$  and inverse relation with  $a$ . So increase in  $\lambda$  increases  $b$  which is coefficient of  $V_w$  and decreases the  $a$  which is coefficient of  $U_w$ . *Table. 5.1.* and *Table. 5.2.* illustrate the variation of skin friction and also Nusselt number for different values of considered parameters. Results show that skin friction

increases with the increase of unsteadiness, fluid particle interaction, volume fraction of dust particles, stretching ratio and magnetic field, but decreases due to Weissenberg effect and power law index. And Nusselt number increases with the increase in unsteadiness, fluid-particle interaction, mass concentration, specific heat ratio, Prandtl number Biot number and heat source but reduces due to power law index and viscous dissipation .

### 5.4 Concluding remarks

The three dimensional unsteady dusty flow of tangent hyperbolic fluid is studied in this chapter. The effects of magnetic field and viscous dissipation with convection are discussed for fluid and dust particles as well. Evolved out-turns of the current problem are mentioned below. Most of the parameter cause hindrance to flows, let have a glance to the results,

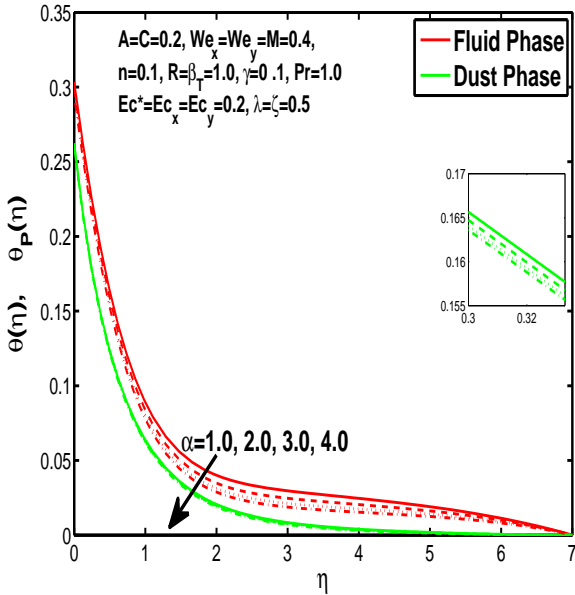


Figure 5.19: Effect of concentration parameter  $\alpha$  on temperature boundary layer of fluid and particles.

- Increase in power law index, Weissenberg effect, magnetic field, concentration of dust particles, and unsteadiness parameter reduces the momentum boundary layer of fluid and dust granules in both x and y-directions.

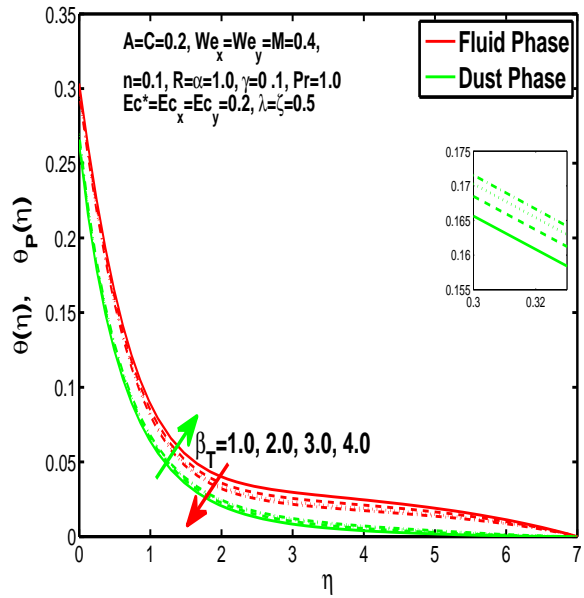


Figure 5.20: Effect of fluid-particle interaction parameter  $\beta_T$  on temperature boundary layer of fluid and particles.

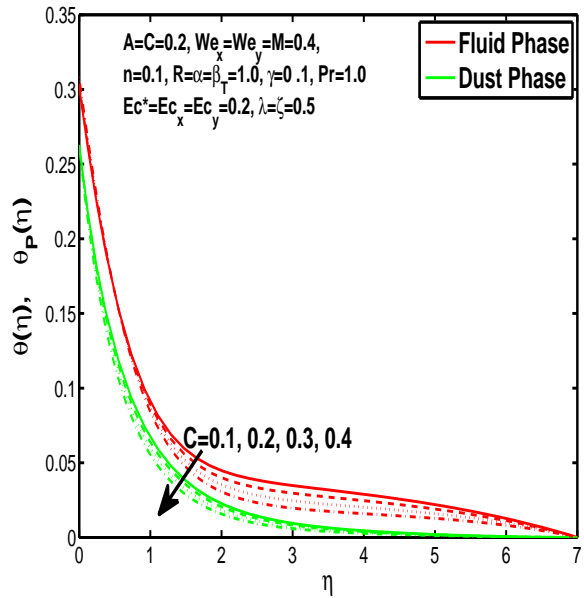


Figure 5.21: Effect of  $C$  on temperature of fluid and particles.

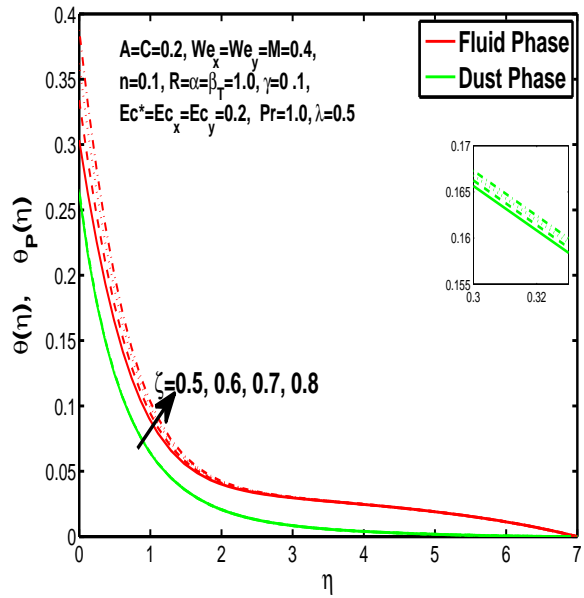


Figure 5.22: Effect of mass Biot number  $\zeta$  on temperature boundary layer of fluid and particles.

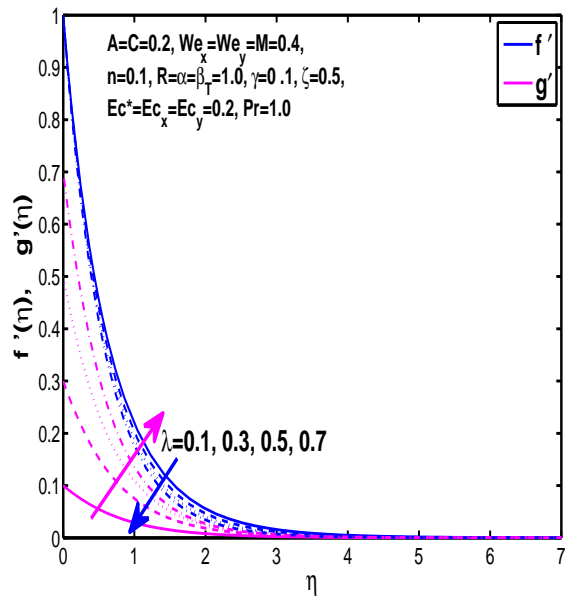


Figure 5.23: Effect of stretching ratio parameter  $\lambda$  on momentum boundary layer of fluid in x and y-direction.

Table 5.1: Numeric findings of Skin-friction.

$A$	$n$	$We_x$	$We_y$	$M$	$C$	$R$	$\lambda$	$-f''(0)$	$-g''(0)$	$\frac{(1-n)f''(0)}{2} + \frac{nWe_x}{2} \sqrt{f''(0)^2 + g''(0)f''(0)}$	$\frac{(1-n)g''(0)}{2} + \frac{nWe_y}{2} \sqrt{f''(0)^2 + g''(0)g''(0)}$
0.0	-	-	-	-	-	-	-	1.2439	0.5322	1.1118	0.4776
0.1	-	-	-	-	-	-	-	1.2742	0.5493	1.1387	0.4929
0.2	0.1	-	-	-	-	-	-	1.3044	0.5664	1.1655	0.5082
-	0.2	-	-	-	-	-	-	1.3927	0.6023	1.0948	0.4782
-	0.3	0.1	0.1	-	-	-	-	1.5036	0.6463	1.0186	0.4461
-	-	0.2	0.2	-	-	-	-	1.5387	0.6516	1.0061	0.4434
-	-	0.3	0.3	-	-	-	-	1.5787	0.6572	0.9929	0.4406
-	-	0.4	0.4	0.1	-	-	-	1.6249	0.6631	0.9790	0.4378
-	-	-	-	0.2	-	-	-	1.6474	0.6743	1.9903	0.4474
-	-	-	-	0.3	-	-	-	1.6845	0.6927	1.0089	0.4561
-	-	-	-	0.4	0.2	-	-	1.7357	0.7177	1.0342	0.4715
-	-	-	-	-	0.3	-	-	1.8242	0.7540	1.0773	0.4937
-	-	-	-	-	0.4	1	-	1.9388	0.8001	1.1316	0.5217
-	-	-	-	-	-	2	-	2.0678	0.8342	1.1909	0.5422
-	-	-	-	-	-	3	-	2.1054	0.8431	1.2078	0.5475
-	-	-	-	-	-	4	0.5	2.1790	0.8548	1.2404	0.5545
-	-	-	-	-	-	-	0.7	2.2077	1.0812	1.2530	0.6867
-	-	-	-	-	-	-	0.9	2.2629	1.5948	1.2768	1.0663

- Increase in interaction between fluid and particles drops the flow of fluid, simultaneously increases the flow rate (in both x and y-directions) and temperature of dust granules.
- Increase in Prandtl number reduces the temperature boundary layer of fluid and dust granules as well.
- Increase in viscous dissipation and Biot number rise the heat of system, increases the heat of fluid and dust particles as well.

Table 5.2: Numerical findings of Nusselt number.

$A$	$n$	$Pr$	$\alpha$	$\beta_T$	$C$	$\gamma$	$Ec^*$	$Ec_x$	$Ec_y$	$\zeta$	$-\theta'(0)$
0.0	-	-	-	-	-	-	-	-	-	-	0.3085
0.1	-	-	-	-	-	-	-	-	-	-	0.3194
0.2	0.1	-	-	-	-	-	-	-	-	-	0.3293
-	0.2	-	-	-	-	-	-	-	-	-	0.3088
-	0.3	0.7	-	-	-	-	-	-	-	-	0.2827
-	-	0.8	-	-	-	-	-	-	-	-	0.3211
-	-	0.9	-	-	-	-	-	-	-	-	0.3539
-	-	1.0	1.0	-	-	-	-	-	-	-	0.3825
-	-	-	2.0	-	-	-	-	-	-	-	0.3902
-	-	-	3.0	-	-	-	-	-	-	-	0.3974
-	-	-	4.0	1.0	-	-	-	-	-	-	0.4041
-	-	-	-	2.0	-	-	-	-	-	-	0.4256
-	-	-	-	3.0	-	-	-	-	-	-	0.4421
-	-	-	-	4.0	0.1	-	-	-	-	-	0.4555
-	-	-	-	-	0.2	-	-	-	-	-	0.4984
-	-	-	-	-	0.3	-	-	-	-	-	0.5310
-	-	-	-	-	0.4	0.1	-	-	-	-	0.5577
-	-	-	-	-	-	0.2	-	-	-	-	0.5474
-	-	-	-	-	-	0.3	-	-	-	-	0.5375
-	-	-	-	-	-	0.4	1.0	-	-	-	0.5280
-	-	-	-	-	-	-	2.0	-	-	-	0.5115
-	-	-	-	-	-	-	3.0	-	-	-	0.4949
-	-	-	-	-	-	-	4.0	1.0	-	-	0.4784
-	-	-	-	-	-	-	-	2.0	-	-	0.3669
-	-	-	-	-	-	-	-	3.0	-	-	0.2555
-	-	-	-	-	-	-	-	4.0	1.0	-	0.1441
-	-	-	-	-	-	-	-	-	2.0	-	0.1330
-	-	-	-	-	-	-	-	-	3.0	-	0.1220
-	-	-	-	-	-	-	-	-	4.0	1.0	0.1109
-	-	-	-	-	-	-	-	-	-	2.0	0.1798
-	-	-	-	-	-	-	-	-	-	3.0	0.2267
-	-	-	-	-	-	-	-	-	-	4.0	0.2607

## Chapter 6

# Numerical study of unsteady Williamson fluid flow and heat transfer in the presence of MHD through a permeable stretching surface

In this chapter, Williamson fluid model with unsteady flow field characteristics are discussed. In the flow system the nanosized particles are suspended having the magnetic field interaction. The flow is achieved due to permeable stretching surface. The flow model for a numerical solution is regulated by means of coupled partial differential equations via shooting method. Mathematical modeling yields physical parameters, namely the Weissenberg, Prandtl, and Lewis numbers, the unsteady, magnetic, thermophoresis and Brownian motion parameters. The Williamson fluid velocity, temperature, and concentration of nanoparticles are found to be a decreasing function towards unsteady parameter.

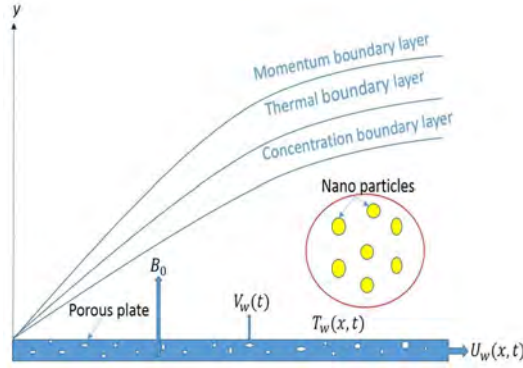


Figure 6.1: Physical model.

## 6.1 Mathematical formulation

The Constitutive equation for Williamson fluid model is defined in section 1.5.1. The component form of continuity and momentum equations can be defined as

$$\frac{\partial u}{\partial x} + \frac{\partial v}{\partial y} = 0, \quad (6.1)$$

$$\rho \left( \frac{\partial u}{\partial t} + u \frac{\partial u}{\partial x} + v \frac{\partial u}{\partial y} \right) = -\frac{\partial p}{\partial x} + \frac{\partial}{\partial x} (\tau_{xx}) + \frac{\partial}{\partial y} (\tau_{xy}), \quad (6.2)$$

$$\rho \left( \frac{\partial v}{\partial t} + u \frac{\partial v}{\partial x} + v \frac{\partial v}{\partial y} \right) = -\frac{\partial p}{\partial y} + \frac{\partial}{\partial x} (\tau_{yx}) + \frac{\partial}{\partial y} (\tau_{yy}), \quad (6.3)$$

here  $u(x, y, t)$  and  $v(x, y, t)$  are the velocity components along the flow direction and normal to the flow direction respectively. The boundary layer approximations with zero pressure gradient assumption reduces the constitutive equations as follows,

$$\frac{\partial u}{\partial x} + \frac{\partial v}{\partial y} = 0, \quad (6.4)$$

$$\frac{\partial u}{\partial t} + u \frac{\partial u}{\partial x} + v \frac{\partial u}{\partial y} = \nu \left[ \frac{\partial^2 u}{\partial y^2} + \sqrt{2} \Gamma \frac{\partial u}{\partial y} \frac{\partial^2 u}{\partial y^2} \right] - \frac{\sigma B^2(t) u}{\rho}, \quad (6.5)$$

$$\frac{\partial T}{\partial t} + u \frac{\partial T}{\partial x} + v \frac{\partial T}{\partial y} = \alpha_m \frac{\partial^2 T}{\partial y^2} + \tau \left[ D_B \frac{\partial C_n}{\partial y} \frac{\partial T}{\partial y} + \frac{D_T}{D_\infty} \left( \frac{\partial T}{\partial y} \right)^2 \right], \quad (6.6)$$

$$\frac{\partial C_n}{\partial t} + u \frac{\partial C_n}{\partial x} + v \frac{\partial C_n}{\partial y} = D_B \frac{\partial^2 C_n}{\partial y^2} + \frac{D_T}{D_\infty} \frac{\partial^2 T}{\partial y^2}, \quad (6.7)$$

there respective conditions at boundary are

$$u = U_w(x, t), \quad v = V_s(t), \quad T = T_w(x, t), \quad C_n = C_w(x, t) \quad \text{at } y = 0,$$

$$u \rightarrow 0, \quad T \rightarrow T_\infty, \quad C_n \rightarrow C_\infty \quad \text{when } y \rightarrow \infty. \quad (6.8)$$



In above equations  $\nu$  represents kinematic viscosity,  $\tau = \frac{(\rho c)_p}{(\rho c)_f}$  defines the ratio of effective heat capacity of the nanoparticles to the effective heat capacity of base fluid.  $T$  is fluid temperature and  $C_n$  is nanoparticle concentration. The assumed forms of stretching velocity, surface temperature, mass fluid velocity, surface nanoparticle concentration and magnetic field are given as follows

$$\begin{aligned} U_w(x, t) &= \frac{ax}{1-ct}, \quad V_s(t) = \frac{-V_o}{(1-ct)^{\frac{1}{2}}}, \quad B(t) = \frac{B_o}{(1-ct)^{\frac{1}{2}}}, \\ T_w(x, t) &= T_\infty + \frac{T_o U_w x}{\nu(1-ct)^{\frac{1}{2}}}, \quad C_w(x, t) = C_\infty + \frac{C_o U_w x}{\nu(1-ct)^{\frac{1}{2}}}, \end{aligned} \quad (6.9)$$

here  $B_o$  is the magnetic field intensity and  $V_o$  is uniform suction/injection velocity. One can introduce a stream function  $\psi$  which satisfy the continuity equation, such that

$$u = \frac{\partial \psi}{\partial y}, \quad v = -\frac{\partial \psi}{\partial x}. \quad (6.10)$$

The set of transformations for order reduction can be defined as

$$\begin{aligned} \eta &= y \sqrt{\frac{U_w}{\nu x}}, \quad \psi = \sqrt{U_w \nu x} f(\eta), \\ \theta &= \frac{T - T_\infty}{T_w - T_\infty}, \quad \phi = \frac{C_n - C_\infty}{C_w - C_\infty}. \end{aligned} \quad (6.11)$$

By using *Eqs.*(6.20) – (6.22) into *Eqs.*(6.16) – (6.19) one can obtain

$$f'''[1 + We f''] + f f'' - f'^2 - A[f' + \frac{\eta}{2} f''] - M^2 f' = 0, \quad (6.12)$$

$$\theta'' + Pr(f\theta' - 2f'\theta) - Pr \frac{A}{2}(\eta\theta' + 3\theta) + Pr[Nb\theta'\phi' + Nt(\theta')^2] = 0, \quad (6.13)$$

$$\phi'' + PrLe(f\phi' - 2f'\phi) - Pr \frac{A}{2}Le(\eta\phi' + 3\phi) + \frac{Nt}{Nb}\theta'' = 0, \quad (6.14)$$

along with the conditions at boundary,

$$\begin{aligned} f(0) &= s, \quad f'(0) = 1, \quad \phi(0) = 1, \quad \theta(0) = 1, \\ f' &\rightarrow 0, \quad \phi \rightarrow 0, \quad \theta \rightarrow 0, \quad \text{at } \eta \rightarrow \infty. \end{aligned} \quad (6.15)$$

The dimensionless number  $We$ ,  $A$ ,  $M$  and  $Pr$ ,  $Nb$ ,  $Nt$ ,  $Le$  and  $s$  are the Weissenberg number, unsteadiness parameter, magnetic parameter, Prandtl number, Brownian motion parameter, thermophoresis parameter, Lewis number and mass transfer parameter  $s > 0$  for suction and  $s < 0$  for injection are defined below

$$We = \sqrt{\frac{a^3 \Gamma x^2}{\nu(1-ct)^3}}, \quad A = \frac{c}{a}, \quad M = \sqrt{\frac{\sigma}{\rho a}} B_o,$$

$$Pr = \frac{\mu C_p}{k}, \quad Nb = \frac{\tau D_B (C_w - C_\infty)}{\nu},$$

$$Nt = \frac{\tau D_T (T_w - T_\infty)}{\nu T_\infty}, \quad Le = \frac{\alpha_m}{D_B}, \quad s = \frac{v_o}{\sqrt{\nu a}}. \quad (6.16)$$

### 6.1.1 Skin friction coefficient, local Nusselt number and local Sherwood number

The skin friction coefficient is defined below

$$C_f = \frac{\tau_w}{\frac{1}{2} \rho U_w^2}, \quad (6.17)$$

For the Williamson fluid surface shear stress  $\tau_w$  is defined as

$$\tau_w = \mu_o \left[ \frac{\partial u}{\partial y} + \frac{\Gamma}{\sqrt{2}} \left( \frac{\partial u}{\partial y} \right)^2 \right]_{y=0}, \quad (6.18)$$

after incorporating the Eq (6.29) into Eq (6.28), one has following expression

$$\frac{C_f Re_x^{\frac{1}{2}}}{2} = f''(0) + \frac{We}{2} f''^2(0). \quad (6.19)$$

Expression for Nusselt number,

$$Nu_x = \frac{x q_w}{k(T_w - T_\infty)}, \quad (6.20)$$

and,

$$q_w = -k \left( \frac{\partial T}{\partial r} \right)_{r=R}, \quad (6.21)$$

using Eq (6.32) into Eq (6.31) one has

$$Nu_x Re_x^{-\frac{1}{2}} = -\theta'(0). \quad (6.22)$$

The Sherwood number is defined as

$$Sh_x = \frac{x q_m}{D_B (C_w - C_\infty)}, \quad (6.23)$$

where

$$q_m = -D_B \left( \frac{\partial C_n}{\partial y} \right)_{y=0}, \quad (6.24)$$

by using Eq (6.35) into Eq (6.34) one can get

$$Re_x^{-\frac{1}{2}} Sh_x = -\phi'(0), \quad (6.25)$$

here  $Re_x = \frac{U_x}{\nu}$  denotes the Reynolds number.

## 6.2 Numerical procedure of solution

The system given by *Eqs* (6.23) – (6.25) is non-linear and it is difficult to find out the closed form solution therefore for numerical solution one can write

$$f''' = \frac{f'^2 + A(f' + \frac{\eta}{2}) - ff'' + M^2f'}{1 + We f''}, \quad (6.26)$$

$$\theta'' = Pr \frac{A}{2} (\eta \theta' + 3\theta) - Pr [f\theta' - 2f'\theta - Pr(Nb\theta'\phi' + Nt(\theta')^2)], \quad (6.27)$$

$$\phi'' = Pr \frac{A}{2} Le(\eta\phi' + 3\phi) - Pr Le(f\phi' - 2f'\phi) - \frac{Nt}{Nb} \theta''. \quad (6.28)$$

to implement shooting method we have introduced dummy variables as follows

$$\begin{aligned} f &= y_1, \quad f' = y_2, \quad f'' = y_3, \quad f''' = y_3', \\ \theta &= y_4, \quad \theta' = y_5, \quad \theta'' = y_5', \\ \phi &= y_6, \quad \phi' = y_7, \quad \phi'' = y_7', \end{aligned} \quad (6.29)$$

The equivalent form of *Eqs*(6.37) – (6.39) in terms of initial value problem can be written as:

$$y_1' = y_2, \quad (6.30)$$

$$y_2' = y_3, \quad (6.31)$$

$$y_3' = \frac{y_2^2 + A(y_2 + \frac{\eta}{2}y_3) - y_1y_3 + M^2y_2}{1 + We y_3}, \quad (6.32)$$

$$y_4' = y_5, \quad (6.33)$$

$$y_5' = -pr(y_1y_5 - 2y_2y_4) + Pr \frac{A}{2} (\eta y_5 + 3y_4) - Pr [Nb y_5 y_7 + Nt(y_5)^2], \quad (6.34)$$

$$y_6' = y_7, \quad (6.35)$$

$$y_7' = Pr \frac{A}{2} Le(\eta y_7 + 3y_6) - Pr Le(y_1y_7 - 2y_2y_6) - \frac{Nt}{Nb} y_5', \quad (6.36)$$

the reduced endpoint conditions are

$$\begin{aligned} y_1(0) &= s, \quad y_2(0) = 1, \quad y_3(0) = a_1, \quad y_4(0) = 1, \\ y_5(0) &= a_2, \quad y_6(0) = 1, \quad y_7(0) = a_3. \end{aligned} \quad (6.37)$$

where  $a_1, a_2$  and  $a_3$  are initial guessed value.

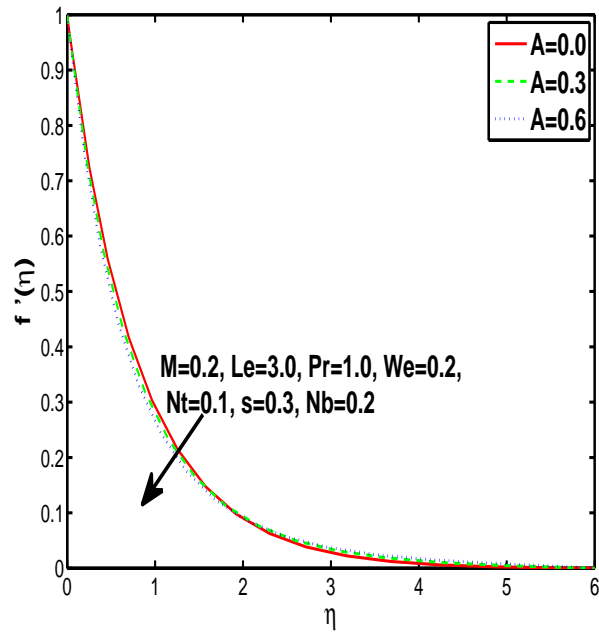


Figure 6.2: Impact of unsteadiness  $A$  on velocity.

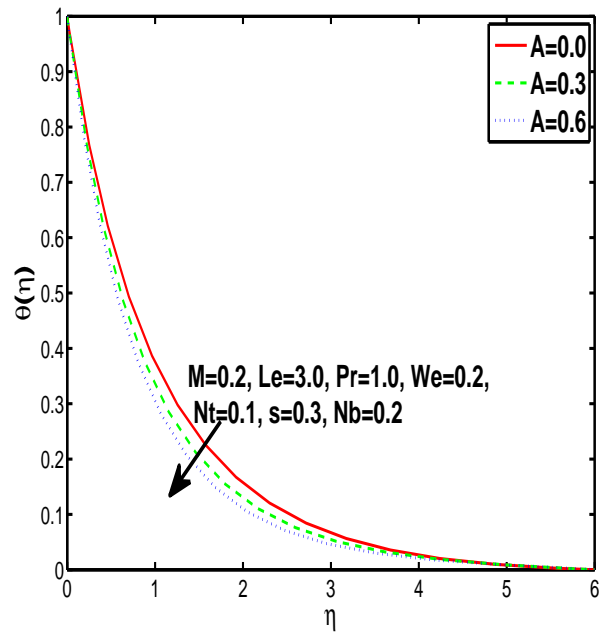


Figure 6.3: Impact of unsteadiness parameter  $A$  on temperature profile.

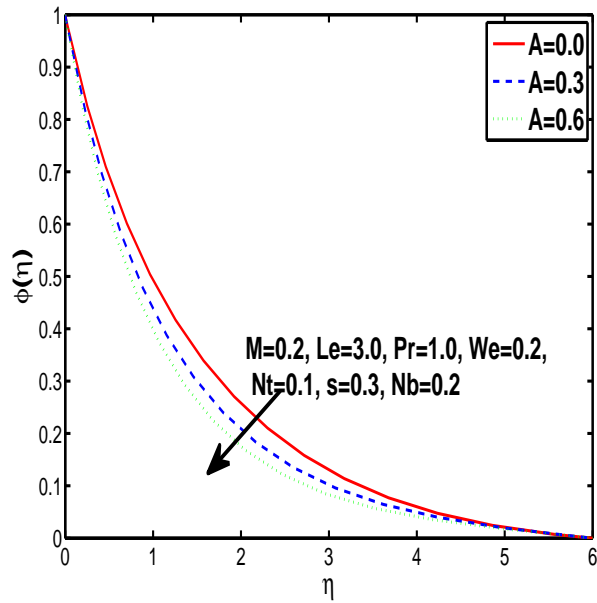


Figure 6.4: Impact of unsteadiness parameter  $A$  on nanoparticle concentration profile.

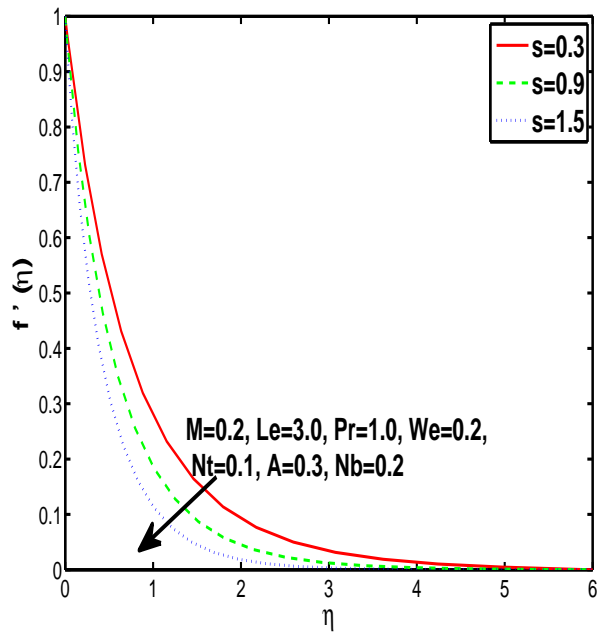


Figure 6.5: Impact of  $s$  on velocity profile.

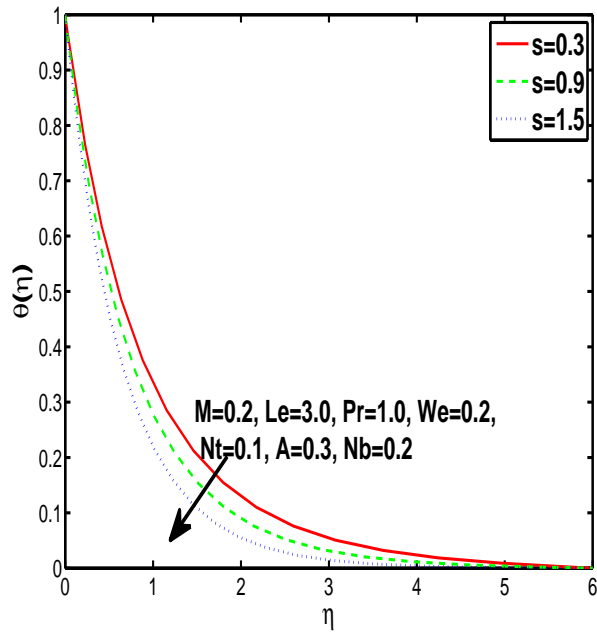


Figure 6.6: Impact of  $s$  on temperature profile.

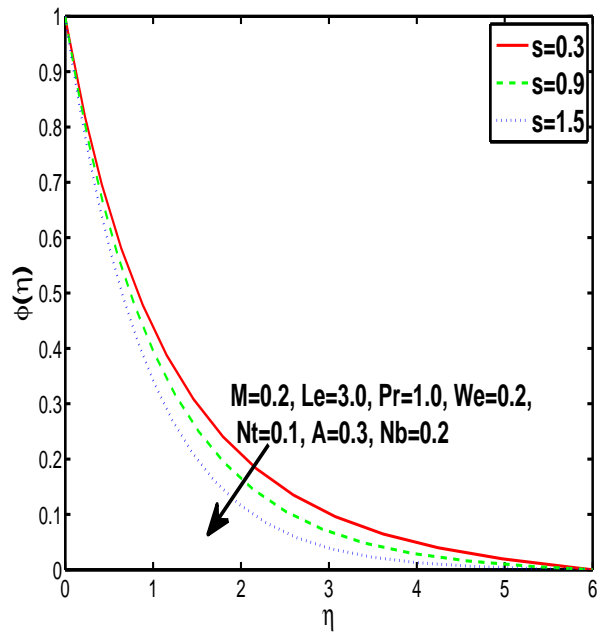


Figure 6.7: Impact of mass transfer parameter  $s$  on concentration profile.

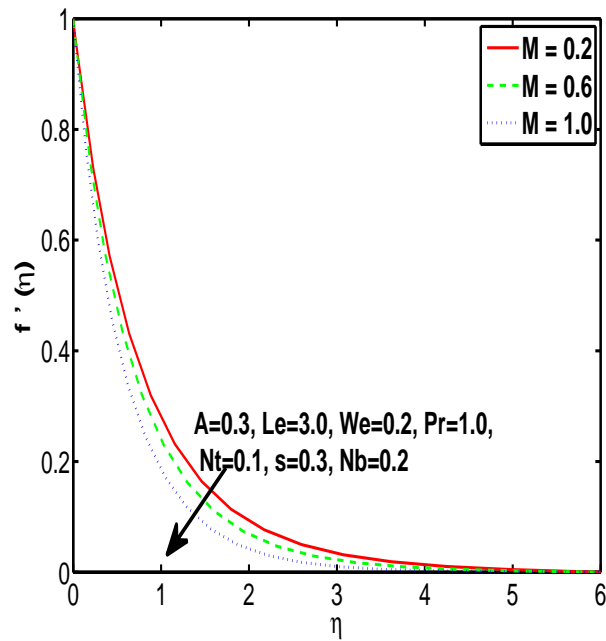


Figure 6.8: Outcome of  $M$  on velocity.

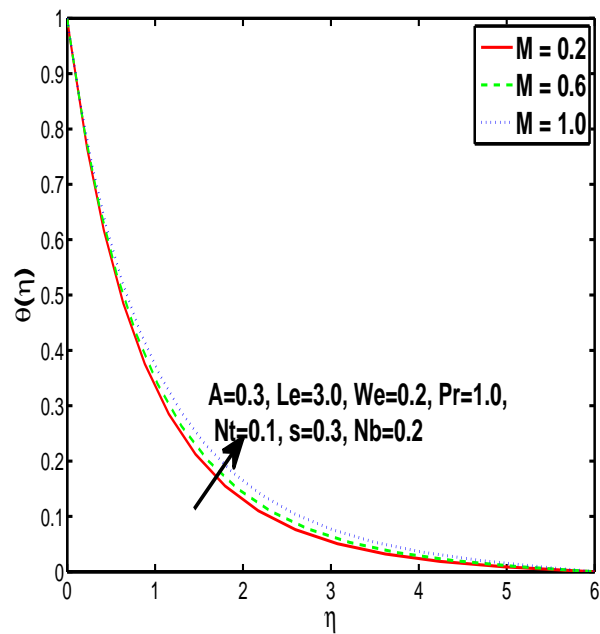


Figure 6.9: Impact of magnetic parameter  $M$  on temperature profile.

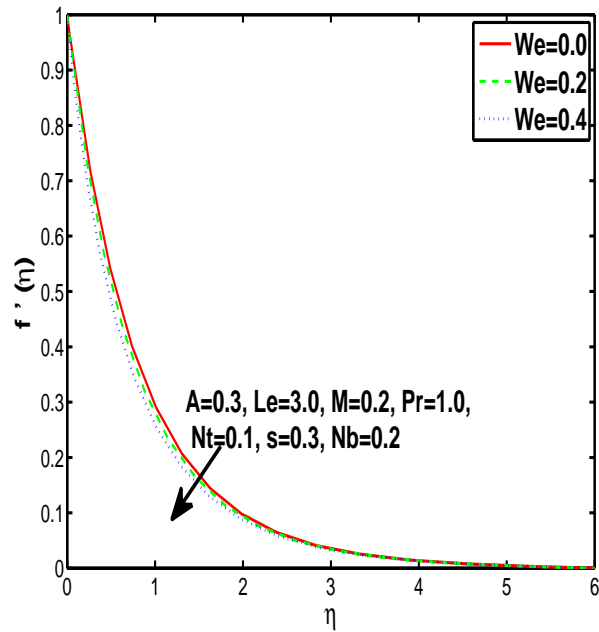


Figure 6.10: Impact of Weissenberg number  $We$  on velocity profile.

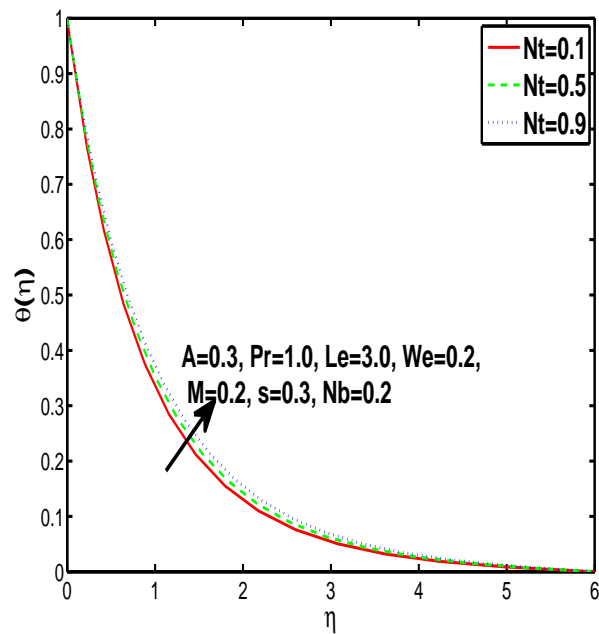


Figure 6.11: Impact of  $Nt$  on temperature profile.



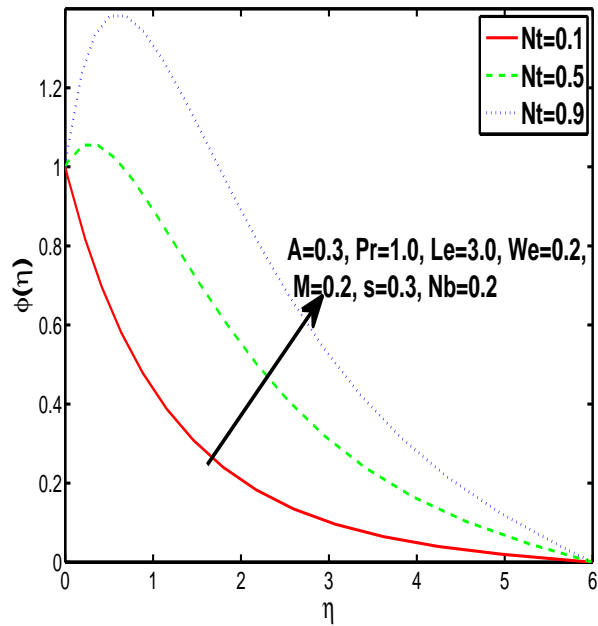


Figure 6.12: Outcome of  $Nt$  on concentration profile.

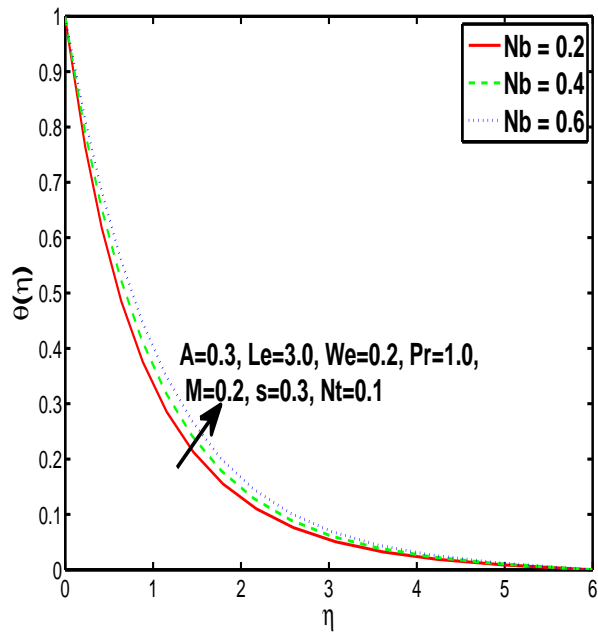


Figure 6.13: Outcome of  $Nb$  on temperature.

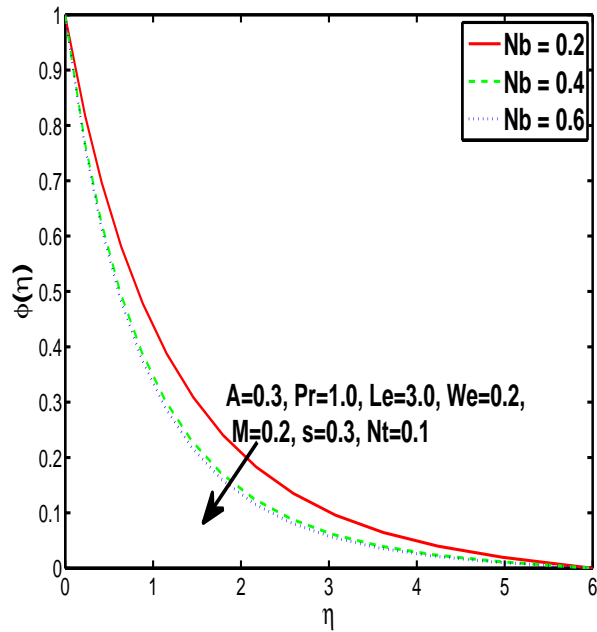


Figure 6.14: Outcome of  $Nb$  on concentration profile.

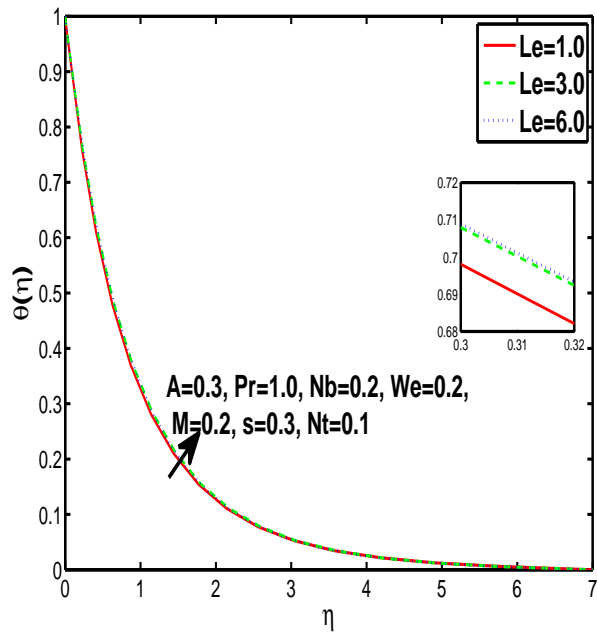


Figure 6.15: Impact of Lewis number  $Le$  on temperature profile.

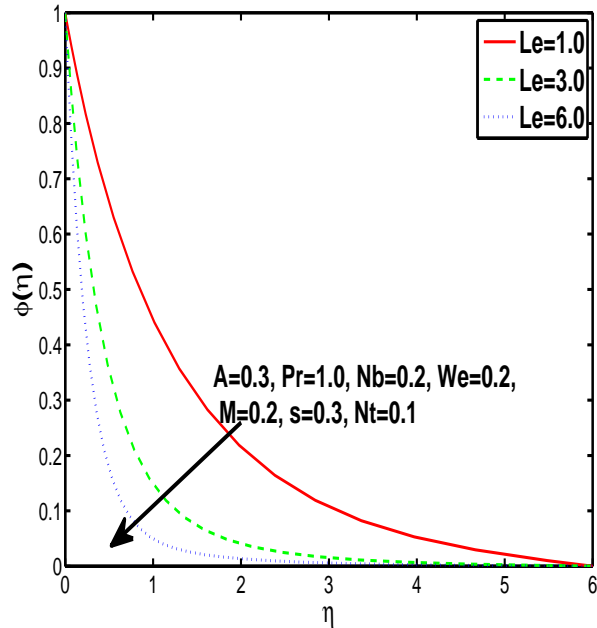


Figure 6.16: Outcome of  $Le$  on concentration profile.

### 6.3 Outcomes and discussions

The outcomes by means of shooting method are reported through both tables and figures. In detail, *Fig. 6.2 – 6.4.* exhibit that there is a decrease in velocity, temperature and concentration to be more specific in unsteadiness parameter. *Fig. 6.2.* depicts that momentum boundary layer decreases with increase in unsteadiness parameter  $A$ . *Fig. 6.3.* shows that increase in unsteadiness parameters decreases the fluid temperature due to rapid transfer of heat through the permeable sheet. Similarly noticed for nanoparticle concentration via unsteadiness parameter shown in *Fig. 6.4.* It is noticed in *Fig. 6.5.* to *6.7.* that fluid velocity, temperature and nanoparticle is decreasing function of mass transfer parameter that an increase in mass transfer parameter brings decline curves in velocity, temperature and nanoparticle concentration. *Fig. 6.8. – 6.9.* provides the impact of magnetic field parameter on both fluid velocity and temperature distributions. It is observed that velocity profile is decreasing function of magnetic field parameter  $M$ . When magnetic field parameter increases the magnitude of lorentz force increases. Hence large resistance is forced by fluid particles as a result velocity of fluid decreases. In parallel context large resistance enhances the temperature of the fluid. *Fig. 6.10.* is used to examine

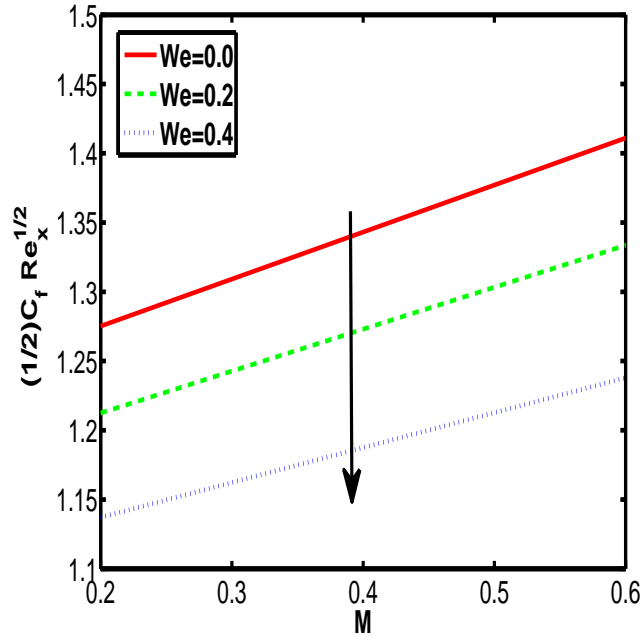


Figure 6.17: Skin friction variation due to change in magnetic parameter  $M$  and Weissenberg parameter  $We$ .

the impact of Weissenberg number on velocity profile. It is noticed that the velocity profile is decreasing function of Weissenberg number. The Weissenberg number is ratio of relaxation time to retardation time. Therefore increase in relaxation time which confirms the dominance of viscous forces as a result velocity curves shows decline values. The outcome of thermophoresis on both temperature and concentration of nano-particles are tested in *Fig. 6.11 – 6.12*. It is clear from figures by increasing the rise of thermophoresis parameter increases the temperature and nanoparticle concentration. *Fig. 6.13. – 6.14.* reveals the effect of dimensionless Brownian motion parameter on the thermal and concentration boundary layer. It is clear from definition of Brownian motion parameter that there is rise in energy of nano-particles due to which temperature of the nanofluid increases. In result of this motion the heat of system increases.

The increase in kinetic energy is the cause of dispersion of nanoparticles which declines the concentration boundary layer thickness of nanofluid. *Fig. 6.15.* shows the influence of Lewis number on heat of system minutely. The Lewis number has direct relation with thermal diffusion so increment in Lewis number enhances the heat transfer as a result temperature increases. *Fig. 6.16.* reports the outcome of Lewis number on concentra-

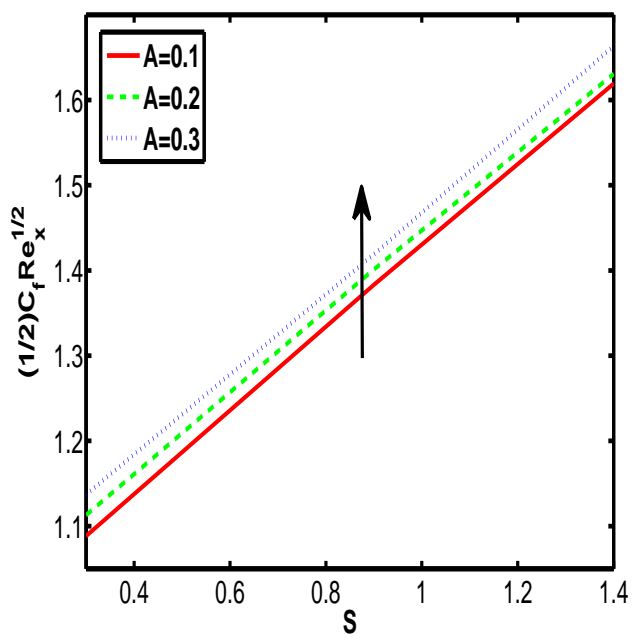


Figure 6.18: Skin friction variation due to change in  $A$  and  $s$ .

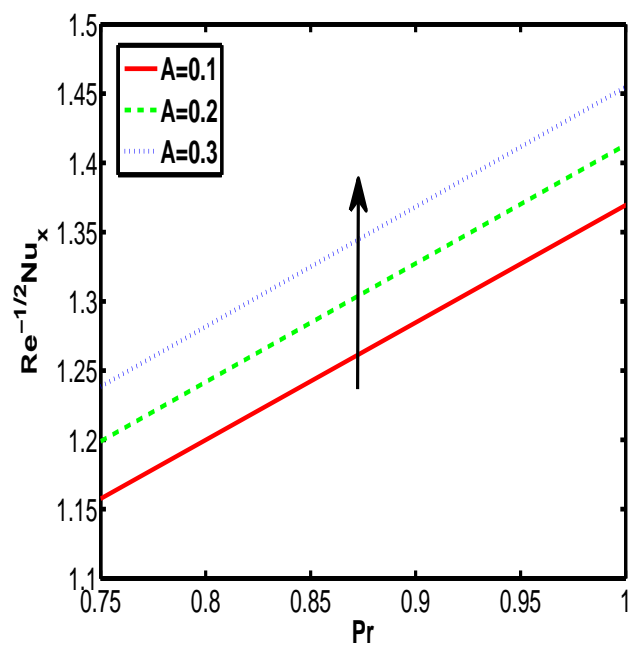


Figure 6.19: Local Nusselt number variation due to change in  $A$  and  $Pr$ .

Table 6.1: Comparison of skin friction  $-f''(0)$  with previously published data considering unsteadiness parameter variation  $A$  when  $M = s = We = 0$ .

A	Khan et al.[11]	Present results
<b>0.0</b>	1.0000	1.0005
<b>0.2</b>	1.06801	1.0685
<b>0.4</b>	1.13469	1.1349
<b>0.6</b>	1.19912	1.1992

tion profile. The concentration of nano-particles is decreasing function of Lewis number. *Fig. 6.17.* reveals the results due to friction offered by stretching permeable surface. It clarifies rise in skin friction due to increase in magnetic parameter. But there is decline in  $(1/2)Re_x^{1/2}C_f$  by increment in Weissenberg number. The influence of unsteadiness parameter on both local Nusselt number and local Sherwood number shown in *Fig. 6.19. – 6.20.* respectively. It is observed that due to increase in  $A$ , the Sherwood number and also Nusselt number increases. Moreover it is also clear from figures that the local Nusselt and Sherwood numbers reflects incitng values towards higher values of Prandtl and Lewis numbers respectively. *Table. 6.1.* is constructed to provide the comparison of our work with existing literature. It is observed that have an excellent match with Khan et al [81]. *Table. 6.2.* indicates the effect of non dimensional parameters upon skin friction coefficient  $(f''(0) + \frac{We}{\sqrt{2}}f''^2(0))$ . Values in table shows that enhancement in Local skin friction due to increase in unsteadiness parameter  $A$ , mass transfer  $s$  and magnetic parameter  $M$  but put it drops due to increment in Weissenberg number  $We$ . *Table. 6.3.* reports the effects of non dimensional parameter on Local Nusselt number  $-\theta'(0)$ . Results implies that the Nusselt number increases with the increase in unsteadiness parameter  $A$  and Prandtl number  $Pr$ . *Table. 6.4.* uncover the impact of non dimensional parameters towards the local Sherwood number  $-\phi'(0)$ . For the controlled values of  $s$ ,  $M$  and  $We$  there is an increase in the Sherwood number by the increase in  $A$ ,  $Pr$ ,  $Le$  and  $Nb$ . But enhancement of  $Nt$  reduces the local Sherwood number.

## 6.4 Concluding remarks

There are various non-dimensional parameters involved in this problem. Particularly unsteadiness parameter, Weissenberg number, mass transfer parameter, magnetic field, ther-

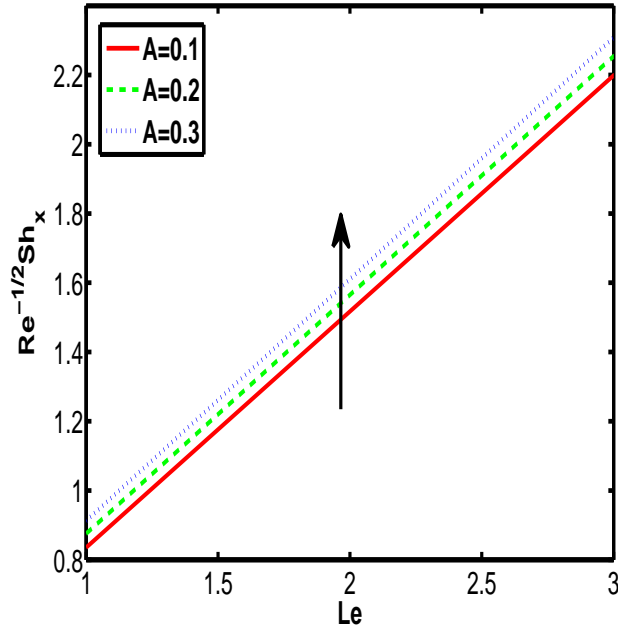


Figure 6.20: Sherwood number variation due to change in unsteadiness parameter  $A$  and Lewis number  $Le$ .

mophoresis and Brownian parameter plays distinct role in effecting flow as well as temperature and concentration flow rate through a permeable sheet.

- The Williamson fluid velocity, temperature and nanoparticles concentrations are a decreasing function of the unsteady parameter.
- The fluid velocity, temperature and nanoparticle concentration reflect declining curves for the mass transfer parameter.
- The velocity profile shows a declining nature towards the magnetic field parameter but the opposite trend is noticed for the case temperature profile.
- Both temperature and nanoparticles concentration show increasing values via thermophoresis parameter.
- The skin friction coefficient increases for the positive values of both mass transfer parameter and unsteadiness parameter.
- The Nusselt number shows higher values for the increasing values of both Prandtl number and unsteadiness parameter.

Table 6.2: Numerically computed values of Skin friction.

$A$	$M$	$s$	$We$	$\frac{1}{2}Re^{1/2}C_f$
0.0	0.2	0.3	0.2	1.0000
0.1	-	-	-	1.08854
0.2	-	-	-	1.1805
0.3	-	-	-	1.2710
-	0.6	-	-	1.3711
-	1.0	-	-	1.4829
-	0.2	0.5	-	1.4139
-	-	1.5	-	1.6679
-	-	0.3	0.6	1.2757
-	-	-	0.2	1.03711
-	-	-	0.4	0.83330

Table 6.3: Numerically computed values of Nusselt number by fixing  $s = 0.3$  and  $M = We = 0.2$ .

$A$	$Pr$	$Nt$	$Nb$	$Le$	$Re^{1/2}Nu_x$
0.0	0.72	0.1	0.2	1.0	1.0893
0.1	-	-	-	-	1.1621
0.2	-	-	-	-	1.2413
0.3	-	-	-	-	1.3225
-	1.00	-	-	-	1.4748
-	1.50	-	-	-	1.6071
-	0.72	0.5	-	-	1.2489
-	-	0.9	-	-	1.0015
-	-	0.1	0.8	-	1.0867
-	-	-	1.4	-	0.9061
-	-	-	0.2	1.0	1.1781
-	-	-	-	1.0	1.1575

Table 6.4: Numerically computed values of Sherwood number for different values of  $A, Pr, Nt, Nb$  and  $Le$  by fixing  $s = 0.3$  and  $M = We = 0.2$ .

$A$	$Pr$	$Nt$	$Nb$	$Le$	$Re^{1/2}Sh_x$
0.0	0.72	0.1	0.3	1.0	0.7915
0.1	-	-	-	-	0.8373
0.2	-	-	-	-	0.8953
0.3	-	-	-	-	0.9622
-	1.00	-	-	-	1.1455
-	1.50	-	-	-	1.3167
-	0.72	0.5	-	-	0.9744
-	-	0.9	-	-	1.0117
-	-	0.1	0.6	-	1.2146
-	-	-	1.4	-	1.2167
-	-	-	0.3	1.0	0.9083
-	-	-	-	1.0	0.8797



# Bibliography

- [1] C.E. Brennen, *Fundamentals of multiphase flows*, Cambridge University Press, (2005).
- [2] M. Ishii and T. Hibiki, *Thermo-fluid dynamics of two-phase flows*, Library of congress, (2006).
- [3] P.G. Saffmann, *On the stability of laminar flow of a dusty gas*, *Journal of Fluid Mechanics*, 13, 120-128 (1962).
- [4] S.L. Soo, *The Fluid Dynamics of Multiphase System*, Blaisdell, (1968).
- [5] F.E. Marble, *Dynamics of a gas containing small solid partials*, in: *Proceeding of the Fifth AGARD Colloquium Combustion and Propulsion*, Pergamon Press, Oxford, (1963)175-213.
- [6] J.T.C. Liu, *Flow induced by an oscillating infinite plat plate in a dusty gas*, *The Physics of Fluids*, 9(1966)1716-1720.
- [7] D.H. Michael and D.A. Miller, *Plane parallel flow of a dusty gas*, *Mathematika*, 13(1966)97-109.
- [8] F.H. Harlow, A.A. Amsden, *Numerical Calculation of Multiphase Fluid Flow*, *Journal of Computational Physics*, 17(1975)19-52.
- [9] R.F. Bishop, *Thermo-fluid Dynamic Theory of Two-Phase Flow*, *Physics Bulletin*, 26(1975)544.
- [10] R.E. Singleton, *Fluid mechanics of gas-solid particle flow in boundary layers (Ph.D. Dissertation)*, California Institute of Technology, (1964).
- [11] T. Kawaguchi, *MRI measurement of granular flows and fluid-particle flows*, *Advanced Powder Technology*, 21, (2010)235-241.

- [12] D.A. Drew, *Stability of a Stokes layer of a dusty gas*, *The Physics of Fluids*, 22(1979)2081-2086.
- [13] K.S. Mekheimer, E.F. El Shehawey and A.M. Elaw, *Peristaltic Motion of a Particle Fluid Suspension in a Planar Channel*, *International Journal of Theoretical Physics*, 37(1998)2895-2920.
- [14] R. Sivaraj and B.R. Kumar, *Unsteady MHD dusty viscoelastic fluid Couette flow in an irregular channel with varying mass diffusion*, *International Journal of Heat and Mass Transfer*, 55(2012)3076-3089.
- [15] S. Mosayebidorcheh, O.D.Makinde, D.D.Ganji and M.Abedian Chermahini, *DTM-FDM hybrid approach to unsteady MHD Couette flow and heat transfer of dusty fluid with variable properties*, *Thermal Science and Engineering Progress*, 2(2017)57-63.
- [16] N. Ijaz, A. Zeeshan, M.M. Bhatti and Rahmat Ellahi, *Analytical study on liquid-solid particles interaction in the presence of heat and mass transfer through a wavy channel*, *Journal of Molecular Liquids*, 250(2018)80-87.
- [17] S.K. Kumar and L.V.K.V. Sarma, *Fluid-particle suspension flow past a stretching sheet*, *International Journal of Engineering Sciences*, 29(1991)123-132.
- [18] E. Valentini and M. Maiellaro, *Nonlinear stability for dusty fluids*, *Architectural Mechanics*, 41(1990)759-768.
- [19] S. Naramgari and C. Sulochana, *MHD flow of dusty nanofluid over a stretching surface with volume fraction of dust particles*, *Ain Shams Engineering Journal*, 7(2016)709-716.
- [20] N. Sandeep, C. Sulochana and B.R. Kumar *Unsteady MHD radiative flow and heat transfer of a dusty nanofluid over an exponentially stretching surface*, *International Journal Engineering Science and Technology*, 19(2016)227-240.
- [21] K.G. Kumar, N.G. Rudraswamy, B.J. Gireesha and S. Manjunatha, *Non linear thermal radiation effect on Williamson fluid with particle-liquid suspension past a stretching surface*, *Results in Physics*, 7(2017)3196-3202.
- [22] K. Stewarston, *The Theory of unsteady Laminar Boundary Layers*, *Advances in Applied Mechanics*, 6(1960)1-37.

- [23] B.V. Perepelitza, *Investigation of temperature statistic characteristics in turbulent water flow with unsteady heat transfer*, *Experimental Thermal and Fluid Sciences*, 6(1993)348-352.
- [24] N. Bachok, A. Ishak and I. Pop, *Unsteady boundary-layer flow and heat transfer of a nanofluid over a permeable stretching/shrinking sheet*, *International Journal of Heat and Mass Transfer*, 55(2012)2102-2109.
- [25] D. Andrew S.Rees, and Andrew P. Bassom, *Unsteady thermal boundary layer flows of a Bingham fluid in a porous medium following a sudden change in surface heat flux*, *International Journal of Heat and Mass Transfer*, 93(2016)1100-1106.
- [26] R.V. Williamson, *The flow of pseudoplastic materials*, *Industrial and Engineering Chemistry Research*, 11(1929)1108-1111.
- [27] Madiha Bibi, Khalil-Ur-Rehman<sup>1</sup>, M.Y. Malik and M. Tahir *Numerical study of unsteady Williamson fluid flow and heat transfer in the presence of MHD through a permeable stretching surface*, *The European Physics Journal Plus*, 133(2016)154.
- [28] M.Y. Malik, S. Bilal, T. Salahuddin and Khalil Ur Rehman, *Three-Dimensional Williamson Fluid Flow over a Linear Stretching Surface*, *Mathematical Sciences letters, An International Journal* 1(2017)53-61.
- [29] T. Hayat, M.Z. Kiyani, A. Alsaedi, M. Ijaz Khan and I. Ahmad, *Mixed convective three-dimensional flow of Williamson nanofluid subject to chemical reaction*, *International Journal of Heat and Mass Transfer*, 127(2018)422-429.
- [30] I. Zehra, M.M. Yousaf and S. Nadeem, *Numerical solutions of Williamson fluid with pressure dependent viscosity*, *Results in Physics*, 5(2015)20-25.
- [31] S. Bilal, K.U. Rehman M.Y. Malik and M. Khan *Effects of temperature dependent conductivity and absorptive/generative heat transfer on MHD three dimensional flow of Williamson fluid due to bidirectional non-linear stretching surface*, *Results in Physics*, 7(2017)204-212.
- [32] M.Y. Malik, M. Bibi, F. Khan, and T. Salahuddin, *Numerical solution of Williamson fluid flow past a stretching cylinder and heat transfer with variable thermal conductivity and heat generation/absorption*, *AIP Advances*, 6(2016)035101.

- [33] T. Hayat, S. Ahmad, M.I. Khan and A. Alsaedi, *Exploring magnetic dipole contribution on radiative flow of ferromagnetic Williamson fluid*, *Results in Physics*, 8(2018)545-551.
- [34] N.S. Akbar, S. Nadeem, R.U. Haq and Z.H. Khan (2013). *Numerical solutions of magneto hydrodynamic boundary layer flow of tangent hyperbolic fluid flow towards a stretching sheet with magnetic field*, *Indian Journal of Physics*, 87(2013)1121-1124.
- [35] M. Fathizadeh, M. Madani, Yasir Khan, Naeem Faraz, Ahmet Yildirim, and Serap Tutkun, *An effective modification of the homotopy perturbation method for MHD viscous flow over a stretching sheet*, *Journal of King Saud University- Science*, 25(2017)107-113.
- [36] A.M Siddiqui, S. Bhatti, M.A. Rana and M. Zahid, *Blade coating analysis of a Williamson fluid*, *Results in Physics*, 7(2017)2845-2850.
- [37] K.U. Rehman, A.A. Khan, M.Y. Malik and U. Ali, *Mutual effects of stratification and mixed convection on Williamson fluid flow under stagnation region towards an inclined cylindrical surface*, *MethodsX*, 4(2017)429-444.
- [38] M. Ramzan, M. Bilal and J.D. Chung, *MHD stagnation point Cattaneo-Christov heat flux in Williamson fluid flow with homogeneous heterogeneous reactions and convective boundary condition A numerical approach*, *Journal of Molecular Liquids*, 225(2017)856-862.
- [39] S. Bilal, K.U. Rehman and M.Y. Malik, *Numerical investigation of thermally stratified Williamson fluid flow over a cylindrical surface via Keller box method*, *Results in Physics*, 7(2017)690-696.
- [40] S. G. Kumar, S.V.K. Varma, R.V.M.S S. Kiran Kumar, C.S.K. Raju, S.A. Shehzad and M.N. Bashir, *Three-Dimensional Hydromagnetic Convective Flow of Chemically Reactive Williamson Fluid with Non-Uniform Heat Absorption and Generation*, *International Journal Chemical Reactor Engineering*, 17(2018)doi.org/10.1515/ijcre-2018-0118.
- [41] M. Khan, T. Salahuddin, M.Y. Malik, Farzana Khan and Arif Hussain, *Variable diffusion and conductivity change in 3D rotating Williamson fluid flow along with magnetic field and activation energy*, *International Journal of Numerical Methods Heat and Fluid Flow*, (2019)DOI 10.1108/HFF-02-2019-0145.

- [42] S.U.S. Choi and J.A. Eastman, *Enhancing thermal conductivities of fluids with nanoparticles, Proceedings of the 1995 ASME International Mechanical Engineering Congress and Exposition (San Francisco)*, (1995).
- [43] S.K. Nandy, and T.R. Mahapatra. *Effects of slip and heat generation/absorption on MHD stagnation flow of nanofluid past a stretching/shrinking surface with convective boundary conditions, International Journal of Heat and Mass Transfer*, 64(2013)1091-1100.
- [44] H. Shabgard, S. Kheradmand, H. Farzaneh and C. Bae, *Numerical simulation of cooling performance of an exhaust gas recirculation (EGR) cooler using nano-fluids, Applied Thermal Engineering*, 110(2017)244-252.
- [45] M.Y. Malik, T. Salahuddin, A. Hussain, S. Bilal, *MHD flow of tangent hyperbolic fluid over a stretching cylinder: using Keller box method, Journal of Magnetism and Magnetic Materials*, 395(2015)271-276.
- [46] Madiha Bibi, A. Zeeshan, M.Y. Malik and K.U. Rehman, *Numerical investigation of the unsteady solid-particle flow of a tangent hyperbolic fluid with variable thermal conductivity and convective boundary, The European Physics Journal Plus*, 134(2019)298.
- [47] T. Salahuddin, M.Y. Malik, Arif Hussain, M. Awais, Imad Khan and Mair Khan, *Analysis of tangent hyperbolic nanofluid impinging on a stretching cylinder near the stagnation point, Results in Physics*, 7(2017)426-434.
- [48] T. Salahuddin, Imad Khan, M.Y. Malik, Mair Khan, Arif Hussain and M. Awais, *The European Physical Journal Plus*, 132(2017)205.
- [49] K.U. Rehman, A.S. Alshomrani, M.Y. Malik, I. Zehra and M. Naseer, *Thermophysical aspects in tangent hyperbolic fluid flow regime: A short communication, Case Studies in Thermal Engineering* 12(2018)203-212.
- [50] K.G. Kumar, B.J. Gireesha, M.R. Krishnamurthy and N.G.Rudraswamy, *An unsteady squeezed flow of a tangent hyperbolic fluid over a sensor surface in the presence of variable thermal conductivity, Results in Physics*, 7(2017)3031-3036.
- [51] M.Ali Abbas, Y.Q. Bai, M.M. Bhatti and M.M. Rashidi, *Three dimensional peristaltic flow of hyperbolic tangent fluid in non-uniform channel having flexible walls, Alexandria Engineering Journal*, 55(2016)653-662.

- [52] Sara I. Abdelsalam and M. M. Bhatti, *The study of non-Newtonian nanofluid with hall and ion slip effects on peristaltically induced motion in a non-uniform channel*, *RCS Advances* 8(2018)7904.
- [53] A. Shahid, M.M. Bhatti, O.A. Beg and A. Kadir, *Numerical study of radiative Maxwell viscoelastic magnetized flow from a stretching permeable sheet with the Cattaneo-Christov heat flux model*, *Neural Computing and Applications*, 30(2017)3467-3478.
- [54] B.C. Sakiadis, *Boundary-layer behaviour on continuous solid surface. I. Boundary layer equations for two dimensional and axisymmetric flow*, *American Institute of Chemical Engineering Journal*, 7(1961)26-28.
- [55] L.J. Crane, *Flow past a stretching sheet*, *Journal of Applied Mathematics and Physics ZAMP*, 21(1970)645-647.
- [56] L.J. Grubka, and K.M. Bobba, *Heat transfer characteristics of a continuous stretching surface with variable temperature*, *Journal of Heat Transfer*, 107(1985)248-250.
- [57] C.Y. Wang, *The three-dimensional flow due to a stretching flat surface*, *The Physics of Fluids*, 27(1984)1915-1917.
- [58] A. Hussain, M.Y. Malik, M. Khan, T. Salahuddin, *Application of generalized Fourier heat conduction law on MHD viscoelastic fluid flow over stretching surface*, *International Journal of Numerical Methods Heat and Fluid Flow*, 29(2019) doi.org/10.1108/HFF-02-2019-0161.
- [59] C.D. Surma Devi, H.S. Takhar and G. Nath *Unsteady, three-dimensional, boundary-layer flow due to a stretching surface*, *International Journal of Heat and Mass Transfer*, 29(1986)1996-1999.
- [60] B. Mahanthesh, B.J. Giresha and Rama Subba Reddy Gorla, *Unsteady three-dimensional MHD flow of a nano Eyring-Powell fluid past a convectively heated stretching sheet in the presence of thermal radiation, viscous dissipation and Joule heating*, *Journal of the Association of Arab Universities for Basic and Applied Sciences*, 23(2016)75-84.
- [61] P.D. Ariel, *Generalized three-dimensional flow due to a stretching sheet*, *Journal of Applied Mathematics and Mechanics ZAMM*, 12(2003)844-852.

- [62] P.D. Ariel, *On computation of the three-dimensional flow past a stretching sheet*, *Applied Mathematics and Computation*, 188(2007)1244-1250.
- [63] P.D. Ariel, *The three-dimensional flow past a stretching sheet and the homotopy perturbation method*, *Computers and Mathematics with Applications*, 54(2007)920-925.
- [64] Prashu and R. Nandkeolyar, *A numerical treatment of unsteady three-dimensional hydromagnetic flow of a Casson fluid with Hall and radiation effects*, *Results in Physics* 11(2018)966-974.
- [65] T. Hayat, M. Bilal Ashraf and Elbaz, *Three-dimensional flow of Eyring Powell nanofluid over an exponentially stretching sheet*, *International Journal of Numerical Methods Heat and Fluid Flow*. 25(2015)593-616.
- [66] K.G. Kumar, S. Manjunatha, B.J. Gireesha, F.M. Abbasi and S.A. Shehzad, *Numerical illustrations of 3D tangent hyperbolic liquid flow past a bidirectional moving sheet with convective heat transfer at the boundary*, *Heat transfer-Asian Research* 48(2019)1899-1912.
- [67] M.E.H. Hafidzuddin, R. Nazar, N.M. Arifin and I. Pop, *Unsteady three-dimensional flow and heat transfer past a permeable stretching/shrinking surface*, *AIP Conference Proceedings*. (2015)1660.
- [68] A. Ishak, L. Yian, and I. Pop, *Stagnation-point flow over a shrinking sheet in a micropolar fluid*, *Chemical Engineering Communications*, 197(2010)1417-1427.
- [69] B.J. Gireesha, B. Mahanthesh, P.T. Manjunatha, and R.S.R. Gorla, *Numerical solution for hydromagnetic boundary layer flow and heat transfer past a stretching surface embedded in non-Darcy porous medium with fluid-particle suspension*, *Journal of the Nigerian Mathematical Society*, 34(2015)267-285.
- [70] M.H.M. Yasin, A. Ishak, and I. Pop, *Boundary layer flow and heat transfer past a permeable shrinking surface embedded in a porous medium with a second-order slip: A stability analysis*, *Applied Thermal Engineering*.115(2017)1407-1411.
- [71] X. Sia, L. Lia, L. Zhenga, X. Zhangb and B. Liua, *The exterior unsteady viscous flow and heat transfer due to a porous expanding stretching cylinder*, *Computers and Fluids*, 105(2014)280-284.

- [72] V.R. Malghan, *History of MHD power plant development, Energy Conversion and Management*, 37(1996)569-590.
- [73] J.S. Chiou and H. N. Kao, *Heat transfer characteristics of a MHD laminar jet flowing over a convex surface, Applied Mathematical Modelling*, 18(1994)679-684.
- [74] E.H. Aly and K. Vajravelu, *Exact and numerical solutions of MHD nano boundary-layer flows over stretching surfaces in a porous medium, Applied Mathematics and Computation*, 232(2014)191-204.
- [75] K.Vajravelu and J.Nayfeh, *Hydromagnetic flow of a dusty fluid over a stretching sheet, International Journal of Non-Linear Mechanics*, 27(1992)937-945.
- [76] L. Debnath and A.K. Ghosh, *On unsteady hydromagnetic flows of a dusty fluid between two oscillating plates, Applied Scientific Research*, 45(1988)353-365.
- [77] A. Hussain, M.Y. Malik, T. Salahuddin, S. Bilal and M. Awais, *Combined effects of viscous dissipation and Joule heating on MHD Sisko nanofluid over a stretching cylinder, Journal of Molecular Liquids*, 231(2017)341-352.
- [78] T. Hayat, M. Waqas, A. Alsaedi, G. Bashir, and F. Alzahrani, *Magnetohydrodynamic (MHD) stretched flow of tangent hyperbolic nanoliquid with variable thickness, Journal of Molecular Liquids*, 229(2017)178-184.
- [79] G. Jithender Reddy, R. Srinivasa Raju, and J. Anand Rao, *Influence of viscous dissipation on unsteady MHD natural convective flow of Casson fluid over an oscillating vertical plate via FEM, Ain Shams Engineering Journal* (2017).
- [80] T. Salahuddin, M.Y. Malik, A. Hussain, S. Bilal, M. Awais, I. Khan, *MHD squeezed flow of Carreau-Yasuda fluid over a sensor surface, Alexandria Engineering Journal*, 56(2017)27-34.
- [81] M. Khan, and M. Azam, *Unsteady heat and mass transfer mechanisms in MHD Carreau nanofluid flow, Journal of Molecular Liquids*, 225(2017)554-562.
- [82] G.B. Rybchinskaya and S.A. Kovalev, *Prediction of the stability of pool boiling heat transfer to finite disturbances, International Journal of Heat Mass Transfer*, 21(1978)694-700.



- [83] H.C. Unal, *Temperature distributions in fins with uniform and non-uniform heat generation and non-uniform heat transfer coefficient*, *International Journal of Heat Mass Transfer*, 30(1987)1467-1477.
- [84] H.C. Unal, *The effect of the boundary conditions at a fin tip on the performance of the fin with and without heat generation*, *International Journal Heat Mass Transfer*, 31(1988)1483-1496.
- [85] T.R. Mahapatraa, D. Pala and S. Mondalb, *Mixed convection flow in an inclined enclosure under magnetic field with thermal radiation and heat generation*, *International Communications in Heat and Mass Transfer*, 41(2013)47-56.
- [86] M. Torabi and K. Zhang, *Heat transfer and thermodynamic performance of convective–radiative cooling double layer walls with temperature-dependent thermal conductivity and internal heat generation*, *Energy Conversion and Management*, 89(2014)12-23.
- [87] T.C. Chiam, *Heat transfer in a fluid with variable thermal conductivity over a linearly stretching sheet*, *Acta Mechanica*, 129(1998)63-72.
- [88] S. Yao, T. Fang and Y. Zhong, *Heat transfer of a generalized stretching/shrinking wall problem with convective boundary conditions*, *Communications in Non-linear Science and Numerical Simulation*, 16(2011)752-760.
- [89] B.J. Gireeshaa, G.K. Ramesh, M.S. Abel and C.S. Bagewadi, *Boundary layer flow and heat transfer of a dusty fluid flow over a stretching sheet with non-uniform heat source/sink*, *International Journal of Multiphase Flow*, 37(2011)977-982.
- [90] A. Hussain, M.Y. Malik, T. Salahuddin, A. Rubab and M. Khan, *Effects of viscous dissipation on MHD tangent hyperbolic fluid over a nonlinear stretching sheet with convective boundary conditions*, *Results in Physics*, 7(2017)3502-3509.
- [91] J. Ahmed, A. Begum, A. Shahzad and R. Ali, *MHD axisymmetric flow of power-law fluid over an unsteady stretching sheet with convective boundary conditions*, *Results in Physics*, 6(2016)973-981.
- [92] S. Manjunatha and B.J. Gireesha, *Effects of variable viscosity and thermal conductivity on MHD flow and heat transfer of a dusty fluid*, *Ain Shams Engineering Journal*, 7(2016)505-515.

- [93] M.Y. Malik, M. Bibi, F. Khan and T. Salahuddin, *Numerical solution of Williamson fluid flow past a stretching cylinder and heat transfer with variable thermal conductivity and heat generation/absorption*, *AIP Advances*, 6(2016)035101-13.
- [94] B.J. Gireesha, K. Ganesh, Kumar, G.K. Ramesh, and B.C. Prasannakumara, *Non-linear convective heat and mass transfer of Oldroyd-B nanofluid over a stretching sheet in the presence of uniform heat source/sink*, *Results in Physics*, 9(2018)1555-1563.
- [95] G.K. Ramesh, B.J. Gireesha and C.S. Bagewadi, *MHD flow of a dusty fluid near the stagnation point over a permeable stretching sheet with non-uniform source/sink*, *International Journal of Heat Mass Transfer*, 55(2012)4900-4907.
- [96] D. Pal and G. Mandal, *Thermal radiation and MHD effects on boundary layer flow of micropolar nanofluid past a stretching sheet with non-uniform heat source/sink*, *International Journal of Mechanical Sciences* 126(2017)308-318.
- [97] B. Mahanthesh and B.J. Gireesha, *Thermal Marangoni convection in two-phase flow of dusty Casson fluid*, *Results in Physics* 8(2018)537-544.
- [98] H. Zbib, M.R. Ebrahimi, F.E. Mozaffari and A. Lohi, *Comprehensive analysis of fluid-particle and particle-particle interactions in a liquid-solid fluidized bed via CFD-DEM coupling and tomography*, *Powder Technology*, 340(2018)116-130.
- [99] K. Ganesh Kumar, B.J. Gireesha and R.S.R. Gorla, *Flow and heat transfer of dusty hyperbolic tangent fluid over a stretching sheet in the presence of thermal radiation and magnetic field*, *International Journal of Mechanical and Materials Engineering*, 13(2018)DOI 10.1186/s40712-018-0088-8.
- [100] B.J. Gireesha, B. Mahanthesh and K.L. Krupalakshmi, *Hall effect on two-phase radiated flow of magneto-dusty-nanoliquid with irregular heat generation/consumption*, *Results in Phys*, 7(2017)4340-4348.
- [101] G. Kalpana, K.R. Madhura, and Ramesh B. Kudenatti, *Impact of temperature-dependant viscosity and thermal conductivity on MHD boundary layer flow of two-phase dusty fluid through permeable medium*, *Engineering Science and Technology, an International Journal* 22(2019)416-427.
- [102] T.Hayat, M. Awais, S. Asghar, *Radiative effects in a three-dimensional flow of MHD Eyring-Powell fluid*, *Journal of the Egyptian Mathematical Society*, 21(2013)379-384.

- [103] R. Gayathri, A. Govindarajan and R. Sasikala, *Three-dimensional couette flow of dusty fluid with heat transfer in the presence of magnetic field*, (NCMTA 18), doi :10.1088/1742-6596/1000/1/012147(2018).
- [104] M.M. Bhatti, A. Zeeshan, and R. Ellahi, *Study of heat transfer with nonlinear thermal radiation on sinusoidal motion of magnetic solid particles in a dusty fluid*, *Journal of Theoretical and Applied Mechanics*, 46(2016)75-94.
- [105] B. Gebhart, *Effects of viscous dissipation in natural convection*, *Journal of Fluid Mechanics* 14(1962)225-232.
- [106] M.I. Khan, T. Hayat, M.I. Khan and A. Alsaedi, *A modified homogeneous-heterogeneous reactions for MHD stagnation flow with viscous dissipation and Joule heating*, *International Journal of Heat and Mass Transfer*, 113(2017)310-317.
- [107] K.G. Kumar, B.J. Gireesha and S. Manjunatha, *Scrutinization of joule heating and viscous dissipation on MHD flow and melting heat transfer over a stretching sheet*, *International Journal of Applied Mechanics and Engineering*, 23(2018)429-443.
- [108] S.A. Shehzadi, T. Hayat and A. Alsaedi, *Influence of convective heat and mass conditions in MHD flow of nanofluid*, *Bulletin of Polish Academy of Sciences: Technology Sciences*, 63(2015)doi:10.1515/bpasts-2015-0053.
- [109] A. Guha and K. Pradhan, *Natural convection of non-Newtonian power-law fluids on a horizontal plate*, *International Journal of Heat and Mass Transfer*, 70(2014)930-938.
- [110] S. Geethan Kumar, S.V.K. Varma, R.V.M.S S. Kiran Kumar, C.S.K. Raju, S.A. Shehzad and M.N. Bashir, *Three- dimensional hydromagnetic convective flow of chemically reactive Williamson fluid with non-uniform heat absorption and generation*, *International Journal of Chemical Reactor Engineering*, 17(2018)doi.org/10.1515/ijcre-2018-0118 .
- [111] J. Buongiorno and W. Hu, *Nanofluid coolants for advanced nuclear power plants*, *Proceedings of ICAPP-05, Seoul*, (2005)15-19.
- [112] R.K. Tiwari and M.K. Das *Heat transfer augmentation in a two-sided lid-driven differentially heated square cavity utilizing nanofluids*, *International Journal of Heat and Mass Transfer*, 50(2007)2002-2018.

- [113] L.M. Srivastawa and V.P. Srivastawa, *On two-phase model of pulsatile blood flow with entrance effects*, 20(1983)761-777.
- [114] R.P. Chhabra, *Bubbles, Drops, and Particles in Non-Newtonian Fluids*, CRC Press, (2006).
- [115] S. Manjunatha, B.J. Gireesha and C.S. Bagewadi, *Effect of thermal radiation on boundary layer flow and heat transfer of dusty fluid over an unsteady stretching sheet*, *International Journal of Engineering, Science and Technology*, 4(2012)36-48.
- [116] S.E. Charm and G.S. Kurland, *Blood Flow and Microcirculation*, Wiley, New York, (1974).
- [117] Christopher K. W. Tam, *The drag on a cloud of spherical particles in low Reynolds number flow*, *Journal of Fluid Mechanics*, 38(1969)537-546.

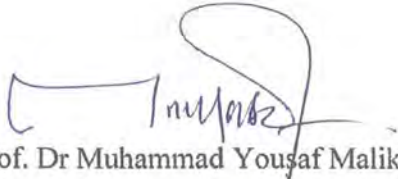
Turnitin Originality Report

Numerical investigations of unsteady solid-liquid Non-Newtonian flows over stretching surfaces by Madiha Bibi .



From DRSM (DRSM L)

- Processed on 22-Apr-2021 09:24 PKT
- ID: 1566308777
- Word Count: 29967

  
Prof. Dr Muhammad Youşaf Malik

Attested  
(Supervisor)

Similarity Index

17%

Similarity by Source

Internet Sources:

13%


Publications:

8%

Student Papers:

5%

  
Focal Person (Turnitin)  
Quaid-i-Azam University  
Islamabad

  
Madiha Bibi  
(Ph.D Scholar)

**sources:**

1

1% match (publications)

["Advances in Fluid Dynamics". Springer Science and Business Media LLC, 2021](#)

2

1% match (publications)

["Applied Mathematics and Scientific Computing". Springer Nature, 2019](#)

3

1% match (publications)

[G. K. Ramesh, B. J. Gireesha, C. S. Bagewadi, "Heat Transfer in MHD Dusty Boundary Layer Flow over an Inclined Stretching Sheet with Non-Uniform Heat Source/Sink". Advances in Mathematical Physics, 2012](#)

4

< 1% match (student papers from 02-Jan-2015)

[Submitted to Higher Education Commission Pakistan on 2015-01-02](#)

5

< 1% match (student papers from 03-Sep-2015)

[Submitted to Higher Education Commission Pakistan on 2015-09-03](#)

6

< 1% match (student papers from 21-Jan-2016)

[Submitted to Higher Education Commission Pakistan on 2016-01-21](#)

7

< 1% match (student papers from 02-Jan-2017)

[Submitted to Higher Education Commission Pakistan on 2017-01-02](#)

8

< 1% match (student papers from 06-Jun-2018)

[Submitted to Higher Education Commission Pakistan on 2018-06-06](#)